Technische Universität München

Max-Planck-Institut für Quantenoptik

Quantum Information Processing and Cavity QED

Christian Schön

Vollständiger Abdruck der von der Fakultät für Physik
der Technischen Universität München
zur Erlangung des akademischen Grades eines

Doktors der Naturwissenschaften (Dr. rer. nat.)

genehmigten Dissertation.

Vorsitzender :		Univ.-Prof. Dr. Dr. h.c. A. Laubereau
Prüfer der Dissertation :	1.	Hon.-Prof. I. Cirac, Ph. D.
	2.	Univ.-Prof. Dr. M. Kleber

Die Dissertation wurde am 16.06.05 bei der
Technischen Universität München eingereicht und
durch die Fakultät für Physik am 27.07.05 angenommen.

Abstract

This work is about the implementation of quantum information processing in the realm of cavity QED. The first part deals with trapping an atom in a cavity, the second part discusses the utilization of an atom as a source of entangled flying qubits and the third part turns to multi-atom effects.

The aim of the first part is to find ways to trap an atom in a cavity. In contrast to other approaches we propose a method where the cavity is basically in the vacuum state and the atom in the ground state. The idea is to induce a spatial dependent ac-Stark shift by irradiating the atom with a weak laser field, so that the atom experiences a trapping force. The main feature of our set-up is that dissipation can be strongly suppressed. We present analytic expressions for the lifetime of the atom as well as for the trapping potential parameters and compare our estimations with numerical simulations.

In the second part we consider the deterministic generation of entangled multi-qubit states by the sequential coupling of an ancillary system to initially uncorrelated qubits. We characterize all achievable states in terms of classes of matrix-product states and give a recipe for the generation on demand of any multi-qubit state. The proposed methods are suitable for any sequential generation-scheme, though we focus on streams of single photon time-bin qubits emitted by an atom coupled to an optical cavity. We show, in particular, how to generate familiar quantum information states such as W, GHZ, and cluster states, within such a framework.

Finally we investigate an ensemble of atoms coupled to a single cavity mode via a Raman transition between two ground states. In the bad cavity regime we identify traces of interference effects in the output-field of the cavity. Within a conditional scheme they can be employed to prepare the atoms in entangled states. We introduce an appropriate model and show that current experimental set-ups are in principle suitable for the implementation of such a scheme.

Contents

Chapter 1

Introduction

Quantum information theory is based on ideas from quantum physics, classical information theory and computer science. It employs coherent quantum effects to accomplish tasks which are untractable by classical means. Its most intriguing applications are quantum computing and quantum cryptography.

A quantum computer [1–5] employs two-level quantum systems (qubits) to store information. In contrast to classical bits an n-qubit register can be prepared in a state representing a superposition of 2^n different numbers. For certain tasks, processing this information by unitary transformations on the corresponding 2^n-dimensional complex Hilbert space leads to an exponential speedup compared to classical computers [5–7]. Most remarkable are Shor's algorithm for factorizing numbers [8] and Grover's algorithm for unstructured search [9]. A quantum computer would allow to break all classical cryptosystems which are based on the impossibility of factorizing large numbers in relatively short times.

The most mature field in quantum information is quantum cryptography [10]. In fact, first commercial equipment is already offered [11]. Quantum cryptography protocols (see, for instance [12]) employ the laws of quantum mechanics to establish a secret random key between spatially separated parties via a quantum channel in a provable secure way. The basic idea is simple: since every measurement perturbs the system and one cannot duplicate an unknown quantum state, any eavesdropper can be detected and, in this case, the transmitted key is discarded. Using photonic degrees of freedom as qubits, say, polarization states or time-bins of energy eigenstates, has the advantage that photons propagate safely over long distances. Therefore photonic devices are the most promising systems for quantum communication tasks. However, the distance for direct quantum communication is bound by the absorption length of the fiber used to transmit the photonic quantum state. To overcome this limitation, the concept of quantum repeaters has

been introduced [13, 14].

The basic building block for such a device is provided by cavity QED, which constitutes a natural interface between atoms as quantum memory and photons. Consequently, in quantum networks, atoms coupled to a cavity mode represent the nodes [15–17]. In those cases the idea is to store the quantum information in two internal ground levels of each atom and to entangle them by using real or virtual photon exchange through the cavity mode. In this context, a coherent and controllable evolution of the system is essential since a single spontaneous emission or cavity loss may have dramatic effects for all quantum information tasks (see, however [18]). Moreover, all proposals for quantum computation using atoms interacting via a common cavity mode [19] require that the atoms are trapped in the cavity in a fixed position. In this work, we address the prospects of cavity QED with respect to system control and coherent effects.

During the last years, a significant experimental progress has taken place, allowing to observe quantum phenomena in the interaction of a single atom with a single mode of the electromagnetic field, both in the optical [20–30] and the microwave [31, 32] regime. Some of these experiments are currently limited by the fact that (neutral) atoms typically move almost freely in the cavity and eventually leave it, which restricts the duration of the experiment as well as its controllability. For example, in the optical regime, the coupling between the atoms and the cavity mode strongly depends on the position of the atom, and thus when it moves this can strongly affect the interaction.

In order to overcome these problems, several strategies to trap an atom in a cavity have been put forward [33–45]. Some of them involve using some external laser fields, which exert a confining force to the atom, something that has been successfully realized in recent experiments [42–45]. In a far-off resonant trap this is achieved by employing a far-off resonant trapping beam along the cavity axis. A more intriguing approach consists of using the cavity mode itself to confine the atom [33–37]. In remarkable experiments [38–41] it has been possible to keep an atom in a cavity just using the force provided by a single photon. In this work we will show that it is in principle possible to trap an atom in its ground state in a cavity, which is basically in the vacuum state. This is accomplished by irradiating the atom with a weak laser field, which induces a spatial dependent ac-Stark shift, so that the atom experiences a trapping force. Compared to other strategies, our method may have some practical advantages for the implementation of quantum information processing since decoherence processes are appreciable reduced.

A single atom interacting coherently with a single mode of an optical cavity can be employed as a deterministic source of single photons [46]. Compared to the widely used parametric down-conversion scheme, which

is a reliable source of entangled twin-photons, it has the advantage that the pulse shape and the time of the emission are in principle well-controlled. Therefore a lot of effort has been made in recent years to develop efficient and deterministic single photon sources [28–30]. Photonic multi-qubit states can be generated by letting a source emit photonic qubits in a sequential manner [47,48]. If we do not initialize the source after each step, the created qubits will in general be entangled. Moreover, if we allow for specific operations inside the source before each photon emission, we will be able to create different multi-qubit states at the output.

Entangled multi-qubit states are a valuable resource for the implementation of quantum computation and quantum communication protocols, like distributed quantum computing [49,50], quantum cryptography [51] or quantum secret sharing [52]. The question arises, which multi-qubit photon states can be generated with certain resources, i.e. the number of accessible atomic levels and the allowed operations on the atom-cavity system. We will solve this problem within a more general framework, realizing that the cavity QED approach is only a particular instance of a general sequential generation scheme, where an ancillary system is coupled in turn to a number of initially uncorrelated qubits.

It is the purpose of this work to provide a complete characterization of all multipartite quantum states achievable within a sequential generation scheme. It turns out that the classes of states attainable with increasing resources are exactly given by the hierarchy of so-called matrix-product states (MPS) [53,54]. These states typically appear in the theory of one-dimensional spin systems [55], as they are the variational set over which density matrix renormalization group techniques are carried out [56]. Thus, our analysis stresses the importance of MPS, since we show that they naturally appear in a completely different and relevant physical context. Moreover, particular instances of low-dimensional MPS, like cluster states [57] or GHZ states [58], are a valuable resource in quantum information [59]. Conversely, we will provide a recipe for the generation on demand of any multi-qubit state within a sequential generation scheme. Due to the general validity of these results, we will first state and prove them without referring to any particular physical system. This will be then applicable to all sequential set-ups, like streams of photonic qubits emitted either by a cavity QED source [28–30,46] or by a quantum dot coupled to a microcavity [60,61].

Leaving the realm of the single atom in a cavity, we finally turn to a system of many atoms coupled to the same cavity mode. We will consider a situation which resembles recent cavity QED experiments [62] and investigate traces of collective effects in the output-field of the cavity mode.

In particular, we consider an ensemble of atoms coupled to a single cavity

mode via a Raman transition between two internal ground levels. In the bad cavity regime we observe an enhanced transfer of excitation into the cavity output-field compared to the case of independent atoms. This so-called superradiance effect was predicted by Dicke [63] for atoms in a completely symmetric state decaying via a symmetric interaction. States belonging to other families of Dicke states [64], i.e. with a different symmetry type, evolve into subradiant states, which span a decoherence free subspace [65–67]. These states raised considerable interest recently since they are in general entangled and stable. In order to break the symmetry of the initial atomic state, usually individual addressing of the atoms by a laser field is required [68–70]. Albeit this is not feasible in the scenario considered here, subradiant states appear naturally with a certain probability due to inhomogeneous atom-cavity coupling. Therefore the set-up is in principle suitable for the generation of entangled multi-atom states employing a scheme, which relies on the concept of conditional dynamics due to continuous monitoring of photons leaking out of the cavity [69, 70].

The work is structured as follows. In the first chapter we introduce the theoretical model for an atom coupled to a single cavity mode. We also summarize the most important concepts used throughout this work. In the second chapter we introduce a scheme for trapping an atom in the vacuum-field of a cavity. In the third chapter we characterize all sequentially generated multi-qubit states in terms of classes of matrix product states. In particular we refer to a cavity-QED single-photon source, which generates multi-qubit photon states. In the final chapter we investigate collective effects for an ensemble of atoms in a cavity and point out that the system can be employed for the probabilistic generation of entangled atomic states.

If not explicitly stated otherwise, we use $\hbar = 1$.

Chapter 2

Basic concepts

Throughout this work we will consider systems of one or many atoms interacting with a single cavity mode. In this chapter we derive the theoretical model for such a system and consider the case of one two-level atom as a representative example. The coupling between the atomic transition and the quantized cavity field is described by the Jaynes-Cummings model introduced in section 2.1.1. Both, the atom and the cavity mode couple also to the free radiation field. In section 2.1.2 we consider the resulting losses and derive the master equation for cavity and atomic decay. The complete model for a driven two-level atom, coupling to a single cavity mode will be presented in section 2.1.3. An efficient simulation technique for solving the master equation is provided by the quantum-jump approach, which will be discussed in section 2.2. In section 2.3. we derive the quantum regression theorem. It enables us to determine two-time expectation values for a dissipative system described by a master equation. Finally we define input and output modes and derive a relation between the corresponding operators and the system operators in section 2.4. Therefore we employ the quantum Langevin equation.

2.1 Atom-cavity interaction including dissipation

2.1.1 Jaynes-Cummings model

The interaction between a single cavity mode and a two-level atom is described by the Jaynes-Cummings model [71]. In the following we will introduce it in a similar way as in [72]. We denote the frequency of the transition between the ground state $|g\rangle$ and the excited state $|e\rangle$ of the atom by ω_a.

This transition couples to a cavity mode with frequency ω_c. The Hamiltonian of the system in the dipole approximation is

$$H = \frac{\omega_a}{2}\,\sigma_z + \omega_c\, a^\dagger a - ig\big(\sigma_+ + \sigma_-\big)\big(a - a^\dagger\big), \tag{2.1}$$

with the atomic operators $\sigma_+ = |e\rangle\langle g|$, $\sigma_- = |g\rangle\langle e|$ and $\sigma_z = |e\rangle\langle e| - |g\rangle\langle g|$. $a^\dagger$ and a are the creation and annihilation operator of the cavity mode. In an interaction picture rotating with ω_c we obtain the Jaynes-Cummings Hamiltonian [71]

$$H_{JC} = \frac{\Delta_{ac}}{2}\sigma_z - ig\big(\sigma_+ a - \sigma_- a^\dagger\big), \tag{2.2}$$

where we introduced the detuning $\Delta_{ac} = \omega_a - \omega_c$. In (2.2) we neglected the fast oscillating terms of the form $\sigma_- a$ and $\sigma_+ a^\dagger$. They do not preserve the number of quanta and are strongly suppressed. This is the so-called rotating-wave approximation. We also neglected the coupling of the system to the environment. This is justified if the spontaneous emission rate of the atom γ and the cavity decay rate κ obey

$$\begin{aligned} \gamma &\ll g\sqrt{\bar{n}}, \\ \kappa &\ll g/\sqrt{\bar{n}}, \end{aligned} \tag{2.3}$$

with $\bar{n}$ being the average photon number in the cavity.

We will now calculate the time evolution of the system for an initial state

$$|\Psi_I(0)\rangle = \sum_{n=0}^{\infty} a_n |g, n\rangle, \tag{2.4}$$

where $|g, n\rangle$ is the product state with the atom in $|g\rangle$ and n photons in the cavity mode. H_{JC} is block-diagonal in the basis $\{|e, n\rangle, |g, n+1\rangle\}$ with n being the number of photons in the cavity. In other words, the total number of quanta is conserved and $|e, n\rangle$ only couples to $|g, n+1\rangle$ while $|g, 0\rangle$ is uncoupled. Substituting the ansatz

$$|\Psi_I(t)\rangle = \sum_{n=0}^{\infty} \big(c_{g,n}(t)|g, n\rangle + c_{e,n}(t)|e, n\rangle\big) \tag{2.5}$$

into the Schrödinger equation with the Hamiltonian from Eq. (2.2) leads to the equations of motion

$$\begin{aligned} \frac{dc_{g,n}(t)}{dt} &= \frac{i\Delta}{2}\, c_{g,n}(t) + g\sqrt{n}\, c_{e,n-1}(t), \\ \frac{dc_{e,n-1}(t)}{dt} &= -\frac{i\Delta}{2}\, c_{e,n-1}(t) - g\sqrt{n}\, c_{g,n}(t) \end{aligned} \tag{2.6}$$

for the probability amplitudes with initial conditions $c_{g,n}(0) = a_n$ and $c_{e,n-1}(0) = 0$. The solution of Eqs. (2.6) is given by

$$\begin{aligned} c_{g,n}(t) &= a_n \left[\cos\left(\sqrt{\Delta_{ac}^2 + 4g^2 n}\; t/2\right) + \frac{i\Delta_{ac} \sin\left(\sqrt{\Delta_{ac}^2 + 4g^2 n}\; t/2\right)}{\sqrt{\Delta_{ac}^2 + 4g^2 n}} \right] \\ c_{e,n-1}(t) &= -a_n \frac{2g\sqrt{n} \sin\left(\sqrt{\Delta_{ac}^2 + 4g^2 n}\; t/2\right)}{\sqrt{\Delta_{ac}^2 + 4g^2 n}}. \end{aligned} \tag{2.7}$$

For the resonant case, we set $\Delta_{ac} = 0$ and obtain for the probability to find the system in the atomic ground state

$$P_g(t) = \sum_{n=0}^{\infty} |c_{g,n}(t)|^2 = \frac{1}{2} \sum_{n=0}^{\infty} |a_n|^2 \left(1 + \cos(2g\sqrt{n}\; t)\right). \tag{2.8}$$

To illustrate this result, we assume the field being initially prepared in a coherent state with mean photon number $\bar{n}$, i.e.

$$|a_n|^2 = \frac{\bar{n}^n e^{-\bar{n}}}{n!} \tag{2.9}$$

and plot $P_g(t)$ in Fig. 2.1 for $\bar{n} = 10$. It oscillates at a frequency approx-

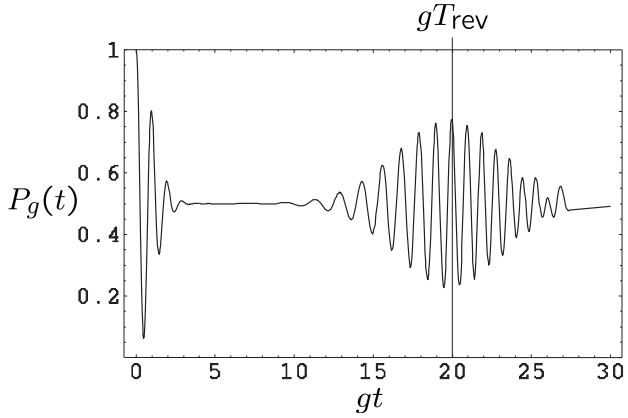

Figure 2.1: The plot shows the probability P_g to find the atom in its ground state $|g\rangle$. Initially we assumed a coherent state with mean photon number $\bar{n} = 10$. One observes Rabi oscillations at a frequency of approximately $2g\sqrt{\bar{n}}$ under an envelope that periodically collapses and revives. The first revival appears at approximately $T_{\mathrm{rev}} \simeq 2\pi\sqrt{\bar{n}}/g$.

imately equal to $2g\sqrt{\bar{n}}$ under an envelope that periodically collapses and

revives. The reason for this behavior is the interference between the individual oscillatory terms with different frequencies $2g\sqrt{n}$. So the collapse is a consequence of the initial spread of different photon numbers in the field. The peak of the revival appears at time $T_{\rm rev}$ when a significant number of oscillating terms are in phase. For the first revival we find

$$2g\sqrt{\bar{n}}\;T_{\rm rev} - 2g\sqrt{\bar{n}-1}\;T_{\rm rev} = 2\pi \tag{2.10}$$

with the approximate solution

$$T_{\rm rev} \approx 2\pi\sqrt{\bar{n}}/g. \tag{2.11}$$

Also other initial field states lead to the phenomenon of collapses and revivals. Their form depends on the initial probability distribution of the photon numbers.

A different behavior of the system arises if the cavity mode is initially prepared in a Fock state. Then the initial state is

$$|\Psi_I(0)\rangle = |g,n\rangle. \tag{2.12}$$

It couples only to $|e,n-1\rangle$ and the system remains in the corresponding subspace. The time evolution is then governed by the Hamiltonian

$$H_n = -\frac{\Delta_{ac}}{2}\sigma_z - ig\sqrt{n}\big(|e,n-1\rangle\langle g,n| - |g,n\rangle\langle e,n-1|\big), \tag{2.13}$$

which is diagonal in the basis of the so-called dressed states

$$\begin{pmatrix} |+,n\rangle \\ |-,n\rangle \end{pmatrix} = \begin{pmatrix} \sin\theta_n & \cos\theta_n \\ \cos\theta_n & -\sin\theta_n \end{pmatrix} \begin{pmatrix} |g,n\rangle \\ |e,n-1\rangle \end{pmatrix}. \tag{2.14}$$

Here, $\tan 2\theta_n = -2g\sqrt{n}/\Delta_{ac}$ and $0 \le 2\theta_n \le \pi$. Together with $|g,0\rangle$ the dressed states form the eigen subspaces of H_I. The corresponding eigen values are

$$\begin{aligned} E_0 &= \Delta_{ac}/2, \\ E_\pm^n &= \pm\sqrt{(\Delta_{ac}/2)^2 + g^2 n}. \end{aligned} \tag{2.15}$$

This result shows that the permanent exchange of excitation between the atom and the cavity mode due to the Jaynes-Cummings interaction leads to a shift of the original eigenvalues of the system. In the resonant case ($\Delta_{ac} = 0$) the original eigen frequencies are shifted by $\pm\sqrt{n}\,g$. For $n = 1$ one speaks of "vacuum Rabi oscillations" and in the Schrödinger picture for $n = 1$ the original resonance frequency $\omega_a = \omega_c$ is then shifted by $\pm g$. The effect can be verified experimentally by measuring the transmission spectrum of the cavity and identifying the shifted resonance peaks. Since dissipation (due to atom and cavity decay) suppresses the effect, observing it, as reported in [27], is a clear evidence for the strong-coupling regime ($g \gg \kappa, \gamma$).

2.1.2 Dissipation

If (2.3) is not fulfilled, one has to consider the coupling of the atom and the cavity mode to the free radiation field. The time-evolution of the system is then described by the master equation. First we introduce a general recipe for its derivation. Then we apply it on the one hand to the case of a harmonic oscillator, which is a suitable model for a cavity mode, and on the other hand to a two-level atom. Similar derivations of the master equation can be found in [73–75].

System-reservoir approach

We consider a system S which couples to a reservoir of modes R. The Hamiltonian is then of the form

$$H = H_S + H_R + H_{SR}. \tag{2.16}$$

Here, H_R and H_S describe the free evolution of S and R. The coupling is given by H_{SR}. The reduced density operator of the system is deduced from the system-reservoir density operator $\chi(t)$ by tracing over the reservoir modes, i.e. $\rho(t) = \mathrm{tr}_R(\chi(t))$. The time evolution of $\chi(t)$ is governed by the Schrödinger equation

$$\frac{d\chi}{dt} = -i[H, \chi]. \tag{2.17}$$

In an interaction picture with respect to the free Hamiltonian $H_S + H_R$ we obtain

$$\frac{d\widetilde{\chi}(t)}{dt} = -i[\widetilde{H}_{SR}(t), \widetilde{\chi}(t)], \tag{2.18}$$

with

$$\begin{aligned} \widetilde{\chi}(t) &= e^{i(H_S+H_R)t}\ \chi(t)\ e^{-i(H_S+H_R)t}, \\ \widetilde{H}_{SR}(t) &= e^{i(H_S+H_R)t}\ H_{SR}\ e^{-i(H_S+H_R)t}. \end{aligned} \tag{2.19}$$

We formally integrate (2.18), substitute the result for $\widetilde{\chi}(t)$ on the right hand side of (2.18) and obtain the exact equation

$$\frac{d\widetilde{\chi}(t)}{dt} = -i[\widetilde{H}_{SR}(t), \chi(0)] - \int_0^t dt'[\widetilde{H}_{SR}(t), [\widetilde{H}_{SR}(t'), \widetilde{\chi}(t')]]. \tag{2.20}$$

If the system-reservoir coupling is turned on at $t = 0$ and there are no correlations between S and R initially, the initial state factorizes in

$$\widetilde{\chi}(0) = \chi(0) = \rho(0) \otimes R_0, \tag{2.21}$$

where R_0 is the density operator of the reservoir at $t = 0$. For the system density operator in the interaction picture

$$\widetilde{\rho}(t) = e^{iH_S t}\ \rho(t)\ e^{-iH_S t} \tag{2.22}$$

the master equation is then given by

$$\frac{d\widetilde{\rho}(t)}{dt} = -\int_0^t dt'\ \mathrm{tr}_R\left(\left[\widetilde{H}_{SR}(t), [\widetilde{H}_{SR}(t'), \widetilde{\chi}(t')]\right]\right). \tag{2.23}$$

The assumption of weak system-reservoir coupling and the fact, that the reservoir is, due to its size, basically not affected by the coupling to the system, leads to the relation

$$\widetilde{\chi}(t) = \widetilde{\rho}(t) \otimes R_0 + \mathcal{O}(H_{SR}). \tag{2.24}$$

Substituting this into (2.23) and neglecting terms of higher than second order in H_{SR} amounts to making the Born approximation. The master equation reads then

$$\frac{d\widetilde{\rho}(t)}{dt} = -\int_0^t dt'\ \mathrm{tr}_R\left(\left[\widetilde{H}_{SR}(t), [\widetilde{H}_{SR}(t'), \widetilde{\rho}(t') \otimes R_0]\right]\right). \tag{2.25}$$

This implies that the future evolution of the system depends on its history. This is in principle a reasonable assumption since an earlier state of the system changed the reservoir state in the past and the latter interacts with the system again in the future. On the other hand the reservoir is a large system in thermal equilibrium and we can assume that the changes due to the interaction with the system are not preserved for a long time. The question is whether this time is long enough to affect the future evolution of the system. To figure this out one has to compare the reservoir correlation time with the time scale for significant changes in the system, as is done in the next section. For a Markovian process the future depends only on the present state. In the Markov approximation we replace $\widetilde{\rho}(t')$ therefore by $\widetilde{\rho}(t)$ and obtain the master equation in the Born-Markov approximation

$$\frac{d\widetilde{\rho}(t)}{dt} = -\int_0^t dt'\ \mathrm{tr}_R\left(\left[\widetilde{H}_{SR}(t), [\widetilde{H}_{SR}(t'), \widetilde{\rho}(t) \otimes R_0]\right]\right). \tag{2.26}$$

Master equation for the harmonic oscillator

We will now consider an harmonic oscillator with frequency ω_0 and creation and annihilation operators $a^\dagger$ and a. The reservoir R is modelled as a collection of harmonic oscillators with frequency ω_j and creation and annihilation

operators $r_j^\dagger$ and r_j. The coupling strength between the system oscillator and the jth reservoir mode is given by κ_j. In the rotating-wave approximation the Hamiltonian of the composite system (2.16) is

$$\begin{aligned} H_S &= \omega_0 a^\dagger a, \\ H_R &= \sum_i \omega_i r_i^\dagger r_i, \\ H_{SR} &= \sum_i \left(\kappa_i^* a r_i^\dagger + \kappa_i a^\dagger r_i\right) = a\Gamma^\dagger + a^\dagger \Gamma. \end{aligned} \tag{2.27}$$

We introduced a collective reservoir operator Γ. Assuming that the reservoir is in thermal equilibrium at temperature T we have the initial state

$$R_0 = \prod_j e^{-\omega_j r_j^\dagger r_j / k_B T} \left(1 - e^{-\omega_j / k_B T}\right), \tag{2.28}$$

where k_B is the Boltzmann constant. In an interaction picture with respect to $H_S + H_R$ the Hamiltonian is given by

$$\begin{aligned} \widetilde{H}_{SR} &= \sum_i \left(\kappa_i^*\, a\, r_i^\dagger e^{i(\omega_i - \omega_0)t} + \kappa_i\, a^\dagger r_i e^{-i(\omega_i - \omega_0)t}\right) \\ &= a\widetilde{\Gamma}^\dagger e^{-i\omega_0 t} + a^\dagger \widetilde{\Gamma} e^{i\omega_0 t}, \end{aligned} \tag{2.29}$$

where $\widetilde{\Gamma}$ is introduced as the collective reservoir operator in the interaction picture.

Substituting this into the master equation in the Born approximation (2.25) leads to

$$\begin{aligned} \frac{d\widetilde{\rho}(t)}{dt} &= -\int_0^t d\tau \Big[\big(aa^\dagger \widetilde{\rho}(t-\tau) - a^\dagger \widetilde{\rho}(t-\tau) a\big) e^{-i\omega_0 \tau} \langle \widetilde{\Gamma}^\dagger(t) \widetilde{\Gamma}(t-\tau)\rangle_R + h.c. \\ &\quad + \big(a^\dagger a\, \widetilde{\rho}(t-\tau) - a\, \widetilde{\rho}(t-\tau) a^\dagger\big) e^{i\omega_0 \tau} \langle \widetilde{\Gamma}(t) \widetilde{\Gamma}^\dagger(t-\tau)\rangle_R + h.c.\Big], \end{aligned} \tag{2.30}$$

where we defined $\tau = t - t'$. The reservoir correlation functions are given by

$$\begin{aligned} \langle \widetilde{\Gamma}^\dagger(t) \widetilde{\Gamma}(t-\tau)\rangle_R &= \int_0^\infty d\omega\, e^{i\omega\tau} f(\omega) |\kappa(\omega)|^2\, \bar{n}(\omega, T) \\ \langle \widetilde{\Gamma}(t) \widetilde{\Gamma}^\dagger(t-\tau)\rangle_R &= \int_0^\infty d\omega\, e^{-i\omega\tau} f(\omega) |\kappa(\omega)|^2 \big(\bar{n}(\omega, T) + 1\big). \end{aligned} \tag{2.31}$$

We introduced a density of states $f(\omega)$ such that $f(\omega)d\omega$ is the number of oscillators with frequencies in the interval $[\omega, \omega + d\omega]$ and

$$\bar{n}(\omega, T) = \frac{e^{-\omega/k_B T}}{1 - e^{-\omega/k_B T}} \tag{2.32}$$

is the mean number of photons for an oscillator with frequency ω in thermal equilibrium at temperature T. If the reservoir correlation time is short on the time scale of significant changes in the system, the reservoir correlation functions can be approximated by $\delta(\tau)$ and $\widetilde{\rho}(t-\tau) \to \widetilde{\rho}(t)$ (Markov approximation). An analysis of the reservoir correlation functions [75] reveals that they are peaked at $\tau = 0$. The width of the peak is given by the reservoir correlation time $t_R = 1/k_B T$. At room temperature we have $t_R \approx 0.25\ 10^{-13} s$ while, if the oscillator a represents an optical cavity mode, the typical timescale on which $\widetilde{\rho}(t-\tau)$ varies is given by $t_S \sim 10^{-8} s$. This clearly justifies the Markov approximation. For the master equation of the harmonic oscillator in the Born-Markov approximation we obtain

$$\begin{aligned}\frac{d\widetilde{\rho}}{dt} &= \left(a\widetilde{\rho}a^\dagger - a^\dagger a\widetilde{\rho}\right)\int_0^t d\tau \int_0^\infty d\omega e^{-i(\omega-\omega_0)\tau} f(\omega)|\kappa(\omega)|^2 \\ &\quad + \left(a\widetilde{\rho}a^\dagger + a^\dagger\widetilde{\rho}a - a^\dagger a\widetilde{\rho} - \widetilde{\rho}aa^\dagger\right) \times \\ &\quad \int_0^t d\tau \int_0^\infty d\omega e^{-i(\omega-\omega_0)\tau} f(\omega)|\kappa(\omega)|^2 \bar{n}(\omega, T) + h.c.. \end{aligned} \tag{2.33}$$

The upper limit of the τ integration is given by $t \sim t_S$ while the integration is dominated by much shorter times $\sim t_R$. Therefore we can extend the integration to infinity and obtain

$$\lim_{t\to\infty} \int_0^t d\tau\ e^{-i(\omega-\omega_0)\tau} = \pi\delta(\omega-\omega_0) + \frac{iP}{\omega_0-\omega}, \tag{2.34}$$

where P is the Cauchy principal value. With the definitions

$$\begin{aligned}\Delta &= P\int_0^\infty d\omega\ \frac{f(\omega)|\kappa(\omega)|^2}{\omega_0-\omega}, \\ \Delta' &= P\int_0^\infty d\omega\ \frac{f(\omega)|\kappa(\omega)|^2}{\omega_0-\omega}\ \bar{n}(\omega, T), \\ \kappa &= \pi f(\omega_0)|\kappa(\omega_0)|^2, \\ \bar{n}_0 &= \bar{n}(\omega_0, T) \end{aligned} \tag{2.35}$$

we obtain for the master equation in the interaction picture

$$\begin{aligned}\frac{d\widetilde{\rho}}{dt} &= -i\Delta[a^\dagger a, \widetilde{\rho}] + \kappa\left(2a\widetilde{\rho}a^\dagger - a^\dagger a\widetilde{\rho} - \widetilde{\rho}a^\dagger a\right) \\ &\quad + 2\kappa\bar{n}_0\left(a\widetilde{\rho}a^\dagger + a^\dagger\widetilde{\rho}a - a^\dagger a\widetilde{\rho} - \widetilde{\rho}aa^\dagger\right). \end{aligned} \tag{2.36}$$

Transforming back to the Schrödinger picture and grouping the terms such that they appear in the Lindblad form leads to the master equation for the

damped harmonic oscillator

$$\begin{aligned}\frac{d\rho}{dt} &= -i\omega_0'[a^\dagger a,\rho] + \kappa(\bar{n}_0+1)\left(2a\rho a^\dagger - a^\dagger a\rho - \rho a^\dagger a\right) \\ &\quad +\kappa\bar{n}_0\left(2a^\dagger\rho a - aa^\dagger\rho - \rho aa^\dagger\right), \end{aligned} \tag{2.37}$$

where

$$\omega_0' = \omega_0 + \Delta. \tag{2.38}$$

The decaying harmonic oscillator is a suitable model for a single cavity mode coupled to the environment through lossy cavity mirrors.

Spontaneous decay of a two-level atom

We will now employ the formalism developed above to describe a two-level atom with ground state $|g\rangle$ and excited state $|e\rangle$ coupled to the modes of the radiation field in thermal equilibrium at temperature T. The Hamiltonian (2.16) is given in the rotating-wave and dipole approximation by

$$\begin{aligned} H_S &= \frac{\omega_a}{2}\sigma_z, \\ H_R &= \sum_{\mathbf{k},\lambda}\omega_k\, r^\dagger_{\mathbf{k},\lambda} r_{\mathbf{k},\lambda}, \\ H_{SR} &= \sum_{\mathbf{k},\lambda}\left(\kappa^*_{\mathbf{k},\lambda} r^\dagger_{\mathbf{k},\lambda}\sigma_- + \kappa_{\mathbf{k},\lambda} r_{\mathbf{k},\lambda}\sigma_+\right), \end{aligned} \tag{2.39}$$

where ω_a is the atomic transition frequency and

$$\kappa_{\mathbf{k},\lambda} = -ie^{i\mathbf{k}\cdot\mathbf{r}_A}\sqrt{\frac{\omega_k}{2\epsilon_0 V}}\;\hat{e}_{\mathbf{k},\lambda}\cdot\mathbf{d}_{eg}. \tag{2.40}$$

Here, the summation over the reservoir modes involves a summation over the wavevector $\mathbf{k}$ and the polarization λ. They correspond to the reservoir mode $r_{\mathbf{k},\lambda}$ with frequency ω_k and unit polarization vector $\hat{e}_{\mathbf{k},\lambda}$. The position of the atom is given by $\mathbf{r}_A$ and V is the quantization volume. The dipole matrix element of the atomic transition is given by

$$\begin{aligned} \mathbf{d}_{eg} &= e\langle e|\hat{q}|g\rangle, \\ \mathbf{d}_{ge} &= (\mathbf{d}_{eg})^*, \end{aligned} \tag{2.41}$$

where e is the electronic charge and $\hat{q}$ is the coordinate operator for the bound electron. $\kappa_{\mathbf{k},\lambda}$ is then the dipole coupling constant for the reservoir

mode with wavevector $\mathbf{k}$ and polarization λ. The collective reservoir operator is given by

$$\Gamma = \sum_{\mathbf{k},\lambda} \kappa_{\mathbf{k},\lambda} r_{\mathbf{k},\lambda} \tag{2.42}$$

in the Schrödinger picture and transforms to

$$\widetilde{\Gamma} = \sum_{\mathbf{k},\lambda} \kappa_{\mathbf{k},\lambda} r_{\mathbf{k},\lambda} e^{-i\omega_k t} \tag{2.43}$$

in the interaction picture with respect to $H_S + H_R$.

The derivation of the master equation for the two-level atom is analogous to the case of the harmonic oscillator. Substitution of the operators a and $a^\dagger$ by the atomic lowering and raising operators σ_- and σ_+ in Eq. (2.33) leads to

$$\begin{aligned} \frac{d\widetilde{\rho}}{dt} &= \left[\gamma(\bar{n}_a + 1) + i(\Delta' + \Delta)\right]\left(\sigma_- \widetilde{\rho} \sigma_+ - \sigma_+ \sigma_- \widetilde{\rho}\right) \\ &\quad + \left(\gamma \bar{n}_a + i\Delta'\right)\left(\sigma_+ \widetilde{\rho} \sigma_- - \widetilde{\rho} \sigma_- \sigma_+\right) + h.c., \end{aligned} \tag{2.44}$$

with

$$\begin{aligned} \Delta &= \sum_\lambda P \int d^3k \; \frac{f(\mathbf{k})|\kappa(\mathbf{k},\lambda)|^2}{\omega_a - kc}, \\ \Delta' &= \sum_\lambda P \int d^3k \; \frac{f(\mathbf{k})|\kappa(\mathbf{k},\lambda)|^2}{\omega_a - kc} \, \bar{n}(kc, T), \\ \gamma &= \pi \sum_\lambda \int d^3k \; f(\mathbf{k})|\kappa(\mathbf{k},\lambda)|^2 \; \delta(kc - \omega_A), \\ \bar{n}_a &= \bar{n}(\omega_a, T). \end{aligned} \tag{2.45}$$

After the transformation back to the Schrödinger picture the master equation for the radiatively damped two-level atom turns out to be

$$\begin{aligned} \frac{d\rho}{dt} &= -i\frac{\omega_a'}{2}[\sigma_z, \rho] + \gamma(\bar{n}_a + 1)\left(2\sigma_- \rho \sigma_+ - \sigma_+ \sigma_- \rho - \rho \sigma_+ \sigma_-\right) \\ &\quad + \gamma \bar{n}_a \left(2\sigma_+ \rho \sigma_- - \sigma_- \sigma_+ \rho - \rho \sigma_- \sigma_+\right), \end{aligned} \tag{2.46}$$

with

$$\omega_a' = \omega_a + 2\Delta' + \Delta. \tag{2.47}$$

The difference $\omega_a' - \omega_a$ is called Lamb shift and contains a temperature dependent contribution Δ' which did not appear for the harmonic oscillator. This follows from the commutator $[\sigma_-, \sigma_+] = -\sigma_z$ which replaces $[a, a^\dagger] = 1$

for the harmonic oscillator. Note that this result does not provide an accurate calculation of the Lamb shift, which for example includes relativistic effects. The Lindblad term proportional to $\gamma(\bar{n}_a + 1)$ describes the transition rate from $|e\rangle$ to $|g\rangle$. It contains the spontaneous emission rate which is independent of $\bar{n}_a$ and the stimulated emissions induced by thermal photons from the reservoir. The Lindblad term proportional to $\gamma\bar{n}_a$ describes the transition rate from $|g\rangle$ to $|e\rangle$, where a thermal photon from the reservoir is absorbed.

2.1.3 A driven two-level atom in a cavity

In this section we combine the results of the preceding sections and present the master equation for a two-level atom driven directly by a laser and coupled to a single cavity mode taking into account cavity losses through imperfect mirrors and spontaneous emissions of the atom into the background modes.

In the absence of dissipation the time-evolution of the system is described by the Jaynes-Cummings model. In general the dynamical behavior of the atom depends on the statistical properties of its environment. The cavity restricts the mode structure of the free radiation field for a certain space angle. If the cavity is far off-resonant the coupling of the atom to the environment is suppressed and an inhibition of spontaneous emission is predicted [76]. On the other hand, a resonant cavity can cause an enhancement of atomic decay via a lossy cavity mode [77]. In principle an accurate description of an atom in a cavity therefore involves the quantization of the electromagnetic field with the cavity mirrors as boundary conditions. Fortunately this is not necessary since in the optical regime the inhibition of spontaneous decay in the off-resonant case is negligible. The enhancement in the resonant case is a consequence of the coupling between atom and cavity mode (described by the Jaynes-Cummings model) and a strong coupling of the latter to the free radiation field ($\kappa \gg g$). The combination of the presented methods is therefore appropriate to describe the system and leads to the master equation

$$\frac{d\rho}{dt} = -i[H, \rho] + \big(\mathcal{L}_a + \mathcal{L}_c\big)\rho. \tag{2.48}$$

Here, $\mathcal{L}_a\rho$ and $\mathcal{L}_c\rho$ are the Linblad terms from Eq. (2.46) and Eq. (2.37) and account for the coupling to the free radiation field of the atom and the cavity mode, respectively. The mean number of photons in a reservoir-mode with an optical frequency is negligible at room temperature. Therefore we set

$$\bar{n}_a = \bar{n}_0 = 0 \tag{2.49}$$

in Eqs. (2.46) and (2.37). Terms which describe induced emissions and absorptions vanish. The Lindblad terms are then given by

$$\begin{aligned} \mathcal{L}_a\rho &= \gamma\left(2\sigma_-\rho\sigma_+ - \sigma_+\sigma_-\rho - \rho\sigma_+\sigma_-\right), \\ \mathcal{L}_c\rho &= \kappa\left(2a\rho a^\dagger - a^\dagger a\rho - \rho a^\dagger a\right), \end{aligned} \tag{2.50}$$

where we neglected the effect of the interaction between the atom and the laser with Rabi frequency Ω on the atomic damping. Therefore we need $\omega_a \gg \Omega$ [75], which is justified for atomic transitions in the optical regime.

The Hamiltonian of the system is given by Eq. (2.1) and a term which accounts for the laser field with frequency ω_l. In the rotating-wave approximation we obtain

$$H = \omega_c a^\dagger a + \frac{\omega_a}{2}\sigma_z + \frac{\Omega}{2}\left(e^{-i\omega_l t}\sigma_+ + e^{i\omega_l t}\sigma_-\right) + g\left(\sigma_+ a + a^\dagger\sigma_-\right), \tag{2.51}$$

where we applied the unitary transformation $a \mapsto ia$. The coupling-strength between the cavity mode and the atom is given by g. The "new" free energies of the cavity mode and the atomic transition

$$\begin{aligned} \omega_c &\equiv \omega_0', \\ \omega_a &\equiv \omega_a' \end{aligned} \tag{2.52}$$

absorb the corrections from Eqs. (2.38) and (2.47). It is desirable to transform H into a time-independent form. In an interaction picture rotating with the frequency of the laser ω_l we obtain

$$H_I = -\Delta_{cl}\; a^\dagger a - \frac{\Delta_{al}}{2}\;\sigma_z + \frac{\Omega}{2}\left(\sigma_+ + \sigma_-\right) + g\left(\sigma_+ a + a^\dagger\sigma_-\right), \tag{2.53}$$

where

$$\begin{aligned} \Delta_{cl} &= \omega_l - \omega_c, \\ \Delta_{al} &= \omega_l - \omega_a. \end{aligned} \tag{2.54}$$

This model contains already the most important ingredients we will use throughout this work.

2.2 Quantum-jump approach

In order to solve master equations of the form (2.48) for more than one atom or strong driving it is favorable to employ a numerical method. The quantum-jump approach [78–81] yields a very efficient simulation technique.

As long as we consider a closed system it can be described by a pure state. Its time evolution is given by the Schrödinger equation. For the derivation of the master equation we traced out the reservoir modes and therefore have to deal with mixed states described by density operators. The master equation can be understood as the time-evolution equation of an ensemble average. The idea of the quantum-jump approach is to simulate only a single trajectory. From the master equation one can derive an effective Hamiltonian which describes the time evolution according to the Schrödinger equation as long as no quanta of excitation is transferred to the reservoir modes. This has the advantage that one has to deal only with pure states. The emission of a photon is described as a sudden change of the system wavefunction and is therefore called jump. Finally one averages over the single trajectories to obtain the solution of the master equation.

We will now introduce the quantum-jump method by applying it to the master equation

$$\frac{d\rho}{dt} = -i[H,\rho] + \mathcal{L}\rho. \tag{2.55}$$

The Hamiltonian H describes the coherent evolution of the system while $\mathcal{L}$ describes the decay and is given in the Lindblad form by

$$\mathcal{L}\rho = \sum_i \kappa_i \big(2a_i\rho a_i^\dagger - a_i^\dagger a_i\rho - \rho a_i^\dagger a_i\big), \tag{2.56}$$

where we consider the optical regime, i.e. we assume the vacuum state for the reservoir. $a_i^\dagger$ and a_i are the system operators which couple to the reservoir. In the system discussed in 1.3 they are given by the annihilation operator of the cavity mode ($a_1 \equiv a$) and the lowering operator of the atomic transition ($a_2 \equiv \sigma_-$). Equation (2.55) can be rewritten as

$$\frac{d\rho}{dt} = -i\big(H_{\text{eff}}\rho - \rho H_{\text{eff}}^\dagger\big) + \mathcal{L}\rho \tag{2.57}$$

employing a non-Hermitian effective Hamiltonian

$$H_{\text{eff}} = H - i\sum_i \kappa_i a_i^\dagger a_i. \tag{2.58}$$

It describes the time-evolution of the system according to the Schrödinger equation

$$\frac{d|\Psi\rangle}{dt} = -iH_{\text{eff}}|\Psi\rangle \tag{2.59}$$

under the condition that no photon has been emitted yet. The effective time evolution causes the norm of the state to decrease. The probability for "no

jump" in the time interval $[t, t+\Delta t]$ is given by

$$P_0 = \langle \Psi_{\text{eff}} | \Psi_{\text{eff}} \rangle \tag{2.60}$$

with

$$\begin{aligned} |\Psi_{\text{eff}}\rangle &= e^{-iH_{\text{eff}}\Delta t} |\Psi(t)\rangle \\ &\approx |\Psi\rangle - iH\Delta t|\Psi(t)\rangle - \Delta t \sum_i \kappa_i \, a_i^\dagger a_i |\Psi(t)\rangle. \end{aligned} \tag{2.61}$$

We have chosen Δt such that terms of the order Δt^2 are negligible and the probability of the emission of two photons within Δt vanishes. A jump is described by the reset operators

$$\sqrt{2\kappa_i} \; a_i. \tag{2.62}$$

In the following we give a recipe for the simulation of the system using the quantum-jump technique:

- determine the probability of no emission in the time-interval $[t, t+\Delta t]$:

$$\begin{aligned} P_0 &= \langle \Psi_{\text{eff}} | \Psi_{\text{eff}} \rangle \\ &\approx 1 - 2\Delta t \sum_i \kappa_i \langle \Psi | a_i^\dagger a_i | \Psi \rangle \end{aligned} \tag{2.63}$$

- choose a random number in $[0, 1]$: r

- if $r > P_0$ a jump occurred and the particular choice is determined randomly according to the probabilities:

$$p_i = \frac{\kappa_i \langle \Psi | a_i^\dagger a_i | \Psi \rangle}{\sum_j \kappa_j \langle \Psi | a_j^\dagger a_j | \Psi \rangle} \tag{2.64}$$

  the renormalized reset state after the jump is then given by:

$$\frac{a_i |\Psi\rangle}{\sqrt{\langle \Psi | a_i^\dagger a_i | \Psi \rangle}} \tag{2.65}$$

- if $r < P_0$ no jump occurred and the system evolves according to the effective Hamiltonian into:

$$\frac{|\Psi_{\text{eff}}\rangle}{\sqrt{\langle \Psi_{\text{eff}} | \Psi_{\text{eff}} \rangle}} \tag{2.66}$$

- repeat the procedure for the following time-steps to obtain a complete single trajectory of the system;
- average over many trajectories to obtain the solution for $\rho(t)$.

We will now convince ourselves that this procedure simulates the master equation (2.55). After each time-step Δt the system ends up either in in one of the reset states (2.65) with probability $p_i(1-P_0)$ or performs a conditional time evolution and ends up in the normalized conditional state (2.66) with probability P_0. In terms of a density matrix, the state of the system after a time Δt is given by the sum over the two possible outcomes weighted with the corresponding probabilities. For the sake of simplicity we use $|\Psi(t+\Delta t)\rangle = |\Psi(\Delta t)\rangle$ and $|\Psi(t)\rangle = |\Psi\rangle$ and write

$$|\Psi(\Delta t)\rangle\langle\Psi(\Delta t)| = P_0 \frac{|\Psi_{\text{eff}}\rangle\langle\Psi_{\text{eff}}|}{\langle\Psi_{\text{eff}}|\Psi_{\text{eff}}\rangle} + (1-P_0)\sum_i p_i \frac{a_i|\Psi\rangle\langle\Psi|a_i^\dagger}{\langle\Psi|a_i^\dagger a_i|\Psi\rangle}. \tag{2.67}$$

Substituting P_0 from Eq. (2.63) and p_i from Eq. (2.64) leads to

$$|\Psi(\Delta t)\rangle\langle\Psi(\Delta t)| = |\Psi_{\text{eff}}\rangle\langle\Psi_{\text{eff}}| + 2\Delta t\sum_i \kappa_i a_i|\Psi\rangle\langle\Psi|a_i^\dagger. \tag{2.68}$$

With the conditional density operator

$$|\Psi_{\text{eff}}\rangle\langle\Psi_{\text{eff}}| \approx |\Psi\rangle\langle\Psi| - i\big[H, |\Psi\rangle\langle\Psi|\big]\Delta t - \sum_j \kappa_j a_j^\dagger a_j, |\Psi\rangle\langle\Psi|\Delta t \tag{2.69}$$

and $\rho = |\Psi\rangle\langle\Psi|$ we end up with

$$\frac{\rho(t+\Delta t)-\rho(t)}{\Delta t} = -i[H,\rho(t)] + \mathcal{L}\rho(t). \tag{2.70}$$

In the limit $\Delta t \to 0$ we recover the master equation (2.55).

2.3 Quantum regression theorem

Two-time expectation values provide valuable information about the properties of quantum systems. In the case of a single-mode $a(t)$ of a cavity, which couples to the free radiation field, the first order correlation function

$$G_1(t, t+\tau) \propto \langle a^\dagger(t) a(t+\tau)\rangle \tag{2.71}$$

is employed to calculate the spectrum of the field and the second order correlation function

$$G_2(t, t+\tau) \propto \langle a^\dagger(t) a^\dagger(t+\tau) a(t+\tau) a(t)\rangle \tag{2.72}$$

reveals information about the photon statistics. Solving the master equation for the system density operator $\rho(t)$ allows us to calculate time-dependent expectation values only at one instance of time. In the following we will derive the quantum regression theorem [82,83] which enables us to evaluate products of operators at different times. Therefore we use the method presented in [75].

In the Heisenberg picture the expectation value for a product of arbitrary system operators O_1 and O_2 evaluated at two different times is given by

$$\langle O_1(t)O_2(t')\rangle = \mathrm{tr}\left[\chi(0)O_1(t)O_2(t')\right], \tag{2.73}$$

where $\chi(0)$ denotes the initial state of system S and reservoir R. The evolution of O_1 and O_2 is given, according to the Heisenberg equation of motion, by

$$\begin{aligned} O_1(t) &= e^{iHt}O_1(0)e^{-iHt}, \\ O_2(t') &= e^{iHt'}O_2(0)e^{-iHt'}, \end{aligned} \tag{2.74}$$

where H is the Hamiltonian acting on $S \otimes R$. From the Schrödinger equation we obtain for the system-reservoir density operator $\chi(t)$

$$\chi(t) = e^{-iHt}\chi(0)e^{iHt}. \tag{2.75}$$

Substituting (2.74) and (2.75) in (2.73) leads to

$$\langle O_1(t)O_2(t')\rangle = \mathrm{tr}_S\left[O_2(0)\mathrm{tr}_R\left(e^{-iH(t'-t)}\chi(t)O_1(0)e^{iH(t'-t)}\right)\right], \tag{2.76}$$

where we used the cyclic property of the trace and the fact that O_2 acts only on the system S. With $\tau = t' - t$ $(t' \geq t)$ we define

$$\chi_1(\tau) = e^{-iH\tau}\chi(t)O_1(0)e^{iH\tau}. \tag{2.77}$$

The time evolution of $\chi_1(\tau)$ is given by

$$\frac{d\chi_1(\tau)}{d\tau} = -i[H, \chi_1(\tau)] \tag{2.78}$$

with the initial condition $\chi_1(0) = \chi(t)O_1(0)$. Since we are looking for an expression independent of the reservoir, we define the reduced density operator

$$\rho_1(\tau) = \mathrm{tr}_R\left(\chi_1(\tau)\right). \tag{2.79}$$

Under the assumption, that $\chi(t) = \rho(t) \otimes R_0$, i.e. the reservoir is described by its initial state R_0, we can write

$$\chi_1(0) = \rho_1(0) \otimes R_0. \tag{2.80}$$

In analogy to the derivation of the master equation in section 2.1.2, we apply the Born-Markov approximation and since $\chi_1(\tau)$ in Eq. (2.78) and $\chi(t)$ in Eq. (2.17) obey the same Hamiltonian, we find

$$\frac{d\rho_1(\tau)}{d\tau} = \mathcal{L}\rho_1(\tau), \tag{2.81}$$

where $\mathcal{L}$ is the Lindblad operator in the system master equation for $\rho(t)$. The formal solution is given by

$$\rho_1(\tau) = e^{\mathcal{L}\tau}\rho_1(0) = e^{\mathcal{L}\tau}\rho(0)O_1(0) \tag{2.82}$$

and with this result we obtain from Eq. (2.76)

$$\langle O_1(t)O_2(t+\tau)\rangle = \mathrm{tr}_S\Big(O_2(0)e^{\mathcal{L}\tau}[\rho(t)O_1(0)]\Big). \tag{2.83}$$

Similar analysis leads to

$$\langle O_1(t)O_2(t+\tau)O_3(t)\rangle = \mathrm{tr}_S\Big(O_2(0)e^{\mathcal{L}\tau}[O_3(0)\rho(t)O_1(0)]\Big). \tag{2.84}$$

In the following we will show that the equations of motion for the expectation values of system operators are also the equations of motion for the two-time expectation values. Therefore we assume that there exists a complete set of system operators A_i, such that for an arbitrary operator O and for each A_i

$$\mathrm{tr}_S\big(A_i[\mathcal{L}O]\big) = \sum_j M_{ij}\mathrm{tr}_S\big(A_jO\big), \tag{2.85}$$

where the M_{ij} are time-independent. The time evolution equation for each of them is then given by

$$\begin{aligned}\frac{d\langle A_i(t)\rangle}{dt} = \mathrm{tr}_S\big(A_i\dot{\rho}(t)\big) &= \mathrm{tr}_S\big(A_i[\mathcal{L}\rho(t)]\big)\\ &= \sum_j M_{ij}\mathrm{tr}_S\big(A_j\rho(t)\big)\\ &= \sum_j M_{ij}\langle A_j(t)\rangle.\end{aligned} \tag{2.86}$$

In vector notation this set of coupled linear equations for the expectation values $\langle A_i\rangle$ reads

$$\frac{d\langle\mathbf{A}(t)\rangle}{dt} = \mathbf{M}\langle\mathbf{A}(t)\rangle, \tag{2.87}$$

where $\mathbf{M}$ is the evolution matrix defined by the M_{ij} and $\mathbf{A}$ is the column vector of the operators A_i. With Eq. (2.83) we find for an arbitrary system operator O_1

$$\begin{aligned}\frac{d}{d\tau}\langle O_1(t)A_i(t+\tau)\rangle &= \mathrm{tr}_S\Big[A_i(0)\big(\mathcal{L}e^{\mathcal{L}\tau}[\rho(t)O_1(0)]\big)\Big] \\ &= \sum_j M_{ij}\mathrm{tr}_S\big(A_j(0)e^{\mathcal{L}\tau}[\rho(t)O_1(0)]\big) \\ &= \sum_j M_{ij}\langle O_1(t)A_j(t+\tau)\rangle \end{aligned} \tag{2.88}$$

and in vector notation

$$\frac{d}{d\tau}\langle O_1(t)\mathbf{A}(t+\tau)\rangle = \mathbf{M}\langle O_1(t)\mathbf{A}(t+\tau)\rangle. \tag{2.89}$$

The statement, that the set of correlation functions $\langle O_1(t)A_i(t+\tau)\rangle$ satisfies the same system of linear equations as the set expectation values $\langle A_i(t+\tau)\rangle$ is called quantum regression theorem. Analogously

$$\frac{d}{d\tau}\langle O_1(t)\mathbf{A}(t+\tau)O_2(t)\rangle = \mathbf{M}\langle O_1(t)\mathbf{A}(t+\tau)O_2(t)\rangle. \tag{2.90}$$

holds for two arbitrary system operators O_1 and O_2.

2.4 Input and output in damped quantum systems

The decay of a quantum system leads to an excitation of the reservoir modes. Measuring this output-field reveals information about the dynamics of the system. On the other hand, if excitation from the reservoir modes is transferred to the system, one is interested in the effect of this input-field on the system. In the following we derive a relation between input and output field and system operators by establishing the quantum Langevin equation. This method was originally proposed in [84, 85].

The Hamiltonian of a system coupling to the environment is of the form (2.16). The reservoir modes are described by creation and annihilation operators $r(\omega)$ and $r^\dagger(\omega)$ with

$$[r(\omega), r^\dagger(\omega)] = \delta(\omega - \omega'). \tag{2.91}$$

The free evolution of the continuum of reservoir modes is given by

$$H_R = \int_{-\infty}^{\infty} \omega\, r^\dagger(\omega)\, r(\omega) d\omega \tag{2.92}$$

and the system-reservoir coupling is described by

$$H_{SR} = i\int_{-\infty}^{\infty} \kappa(\omega)\big(r^\dagger(\omega)a - a^\dagger r(\omega)\big)d\omega. \tag{2.93}$$

Here, a is the system operator which couples linearly to the reservoir modes with coupling strength $\kappa(\omega)$. Note that the lower limit of the integration is extended to "$-\infty$" since we consider a frame rotating with some system frequency, which is typically much larger than the obtained bandwidths.

The Heisenberg equations of motion for $r(\omega)$ and an arbitrary system operator s are given by

$$\begin{aligned} \frac{dr(\omega)}{dt} &= -i\omega\ r(\omega) + \kappa(\omega)a, \\ \frac{ds}{dt} &= -i[s, H_S] + \int \kappa(\omega)\left(r^\dagger[s,a] - [s,a^\dagger]r(\omega)\right)d\omega, \end{aligned} \tag{2.94}$$

with H_S being an arbitrary system Hamiltonian. The solution of the differential equation for $r(\omega)$ is given by

$$r(\omega) = e^{-i\omega(t-t_0)}r_0(\omega) + \kappa(\omega)\int_{t_0}^{t} e^{-i\omega(t-t')}a(t')dt', \tag{2.95}$$

where $r_0(\omega)$ is the value of $r(\omega)$ at $t = t_0$. We substitute this result into Eq. (2.94) and apply the first Markov approximation

$$\kappa(\omega) = \sqrt{\kappa/2\pi}, \tag{2.96}$$

i.e. the system-reservoir coupling strength is independent of frequency. Introducing the input field

$$r_{\rm in} = \frac{1}{\sqrt{2\pi}}\int e^{-i\omega(t-t_0)}r_0(\omega)d\omega, \tag{2.97}$$

which satisfies the commutation relation

$$[r_{\rm in}(t), r_{\rm in}^\dagger(t')] = \delta(t-t'), \tag{2.98}$$

we finally obtain the quantum Langevin equation

$$\frac{ds}{dt} = -i[s,H_S] - \Big([s,a^\dagger]\big(\frac{\kappa}{2}\,a + \sqrt{\kappa}\ r_{\rm in}(t)\big) - \big(\frac{\kappa}{2}\,a^\dagger + \sqrt{\kappa}\ r_{\rm in}^\dagger(t)\big)[s,a]\Big) \tag{2.99}$$

for the system operator s. With (2.96) we derive from Eq. (2.95) as well

$$\int r(\omega)d\omega = r_{\rm in}(t) + \frac{\sqrt{\kappa}}{2}\,a(t). \tag{2.100}$$

We consider now $t_1 > t$ and define $r_1(\omega)$ as the value of $r(\omega)$ at $t = t_1$. Instead of Eq. (2.95) we obtain

$$r(\omega) = e^{-i\omega(t-t_1)}r_1(\omega) - \kappa(\omega)\int_t^{t_1} e^{-i\omega(t-t')}a(t')dt' \tag{2.101}$$

and define the output mode as

$$r_{\rm out}(t) = \frac{1}{\sqrt{2\pi}}\int e^{-i\omega(t-t')}r_1(\omega)d\omega. \tag{2.102}$$

Using this definition leads to the time-reversed quantum Langevin equation

$$\frac{ds}{dt} = -i[s,H_S] - \Big([s,a^\dagger]\big(-\frac{\kappa}{2}\,a + \sqrt{\kappa}\;r_{\rm out}(t)\big) - \big(-\frac{\kappa}{2}\,a^\dagger + \sqrt{\kappa}\;r^\dagger_{\rm out}(t)\big)[s,a]\Big). \tag{2.103}$$

As above, we obtain

$$\int r(\omega)d\omega = r_{\rm out}(t) - \frac{\sqrt{\kappa}}{2}\,a(t). \tag{2.104}$$

Substracting this from Eq. (2.100) leads to the desired input-output relation

$$r_{\rm out}(t) - r_{\rm in}(t) = \sqrt{\kappa}\;a(t), \tag{2.105}$$

which can also be used to transform between the Langevin equation (2.99) and its time-reversed version (2.103).

The formalism presented here is suitable for a complete description of a system with input and output. The quantum Langevin equation (2.99) enables us to determine the time-evolution of an arbitrary system operator $s(t)$ for a given input. The output-field can then be calculated employing the boundary condition (2.105). For a detailed discussion of these results we refer to [86, 87].

Chapter 3

Trapping atoms in the vacuum field of a cavity

In this chapter we propose a new scheme for trapping an atom in a cavity by employing the cavity mode itself. Compared to others our approach has the advantage that spontaneous decay is strongly suppressed because the atom is in its ground state and the cavity is in the vacuum state.

The plan of this chapter is as follows. In Section 3.1 we give a qualitative description of our scheme and estimate its operating conditions such as the depth of the trapping potential and the lifetime of the state. In section 3.2 we give a full description of the method including dissipative processes. The analytical results and estimations are checked numerically in section 3.3.

3.1 Description

We consider an atom with two internal ground levels $|g\rangle$ and $|g'\rangle$, which can be employed to store quantum information. They are resonantly coupled by two cavity modes to two excited levels $|e\rangle$ and $|e'\rangle$, respectively. Additionally, an external plane-wave laser field detuned by Δ excites the same transition (see Fig. 3.1). In the following we will consider only the levels $|g\rangle$ and $|e\rangle$, since for the other two levels the same description applies (they are independent).

3.1.1 Trapping an atom with a single photon

In order to understand the mechanism that we propose, it is convenient first to revise the method used in previous experiments [38–41] to keep an atom in a cavity. The interaction between the atom and the cavity mode is

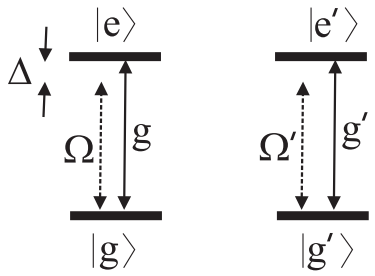

Figure 3.1: Level scheme of the atom. The two ground levels $|g\rangle$ and $|g'\rangle$ are resonantly coupled by two cavity modes to two excited levels $|e\rangle$ and $|e'\rangle$. The coupling strength is given by g and g'. There is an additional external laser field which couples to the atomic transitions with the Rabi frequencies Ω and Ω'.

characterized by a coupling constant

$$g(z) = g_0 \exp\big(-z^2/2\sigma^2\big), \tag{3.1}$$

which depends on the distance z of the atom from the cavity axis. σ denotes the width of the Gaussian profile of the cavity mode. In Fig. 3.2 we show the set-up, as well as the instantaneous energy levels of an atom as a function of its position (in one dimension). The ground state of the composed atom-cavity system is $|g,0\rangle$, where $|n\rangle$ is the cavity state with n photons (in this case $n=0$). The corresponding energy, E_0 is position independent. The first two excited levels are the dressed states of the Jaynes-Cummings Hamiltonian (2.2)

$$H_{JC} = g(x)\big(\sigma_+ a + \sigma_- a^\dagger\big), \tag{3.2}$$

where we assumed that cavity mode and atomic transition are resonant ($\Delta_{ac}=0$). They are given by (2.14)

$$|\pm\rangle = \frac{1}{\sqrt{2}}(|g,1\rangle \pm |e,0\rangle), \tag{3.3}$$

with corresponding energies $E_\pm(z) = \pm g(z)$ in an interaction picture rotating with the cavity resonance frequency. As Fig. 3.2 shows, the position-dependence of $E_-(z)$ provides the atom with a confining potential at the center of the cavity. Thus, if the atom can be prepared in the state $|-\rangle$ with a kinetic energy smaller than $g_0 = g(0)$, it will remain trapped [33–41]. As the state $|-\rangle$ contains a linear combination involving one photon, one can state that the atom is trapped by a single photon. On the other hand, the state $|-\rangle$ can be efficiently prepared by starting in the state $|g,0\rangle$ and tuning

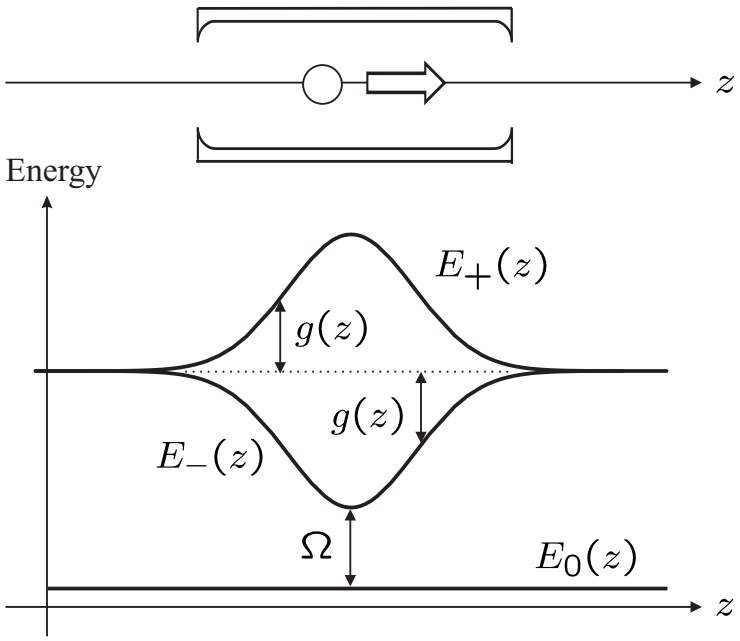

Figure 3.2: Set-up and instantaneous energy levels of the atom as a function of its position. $E_\pm(z)$ and E_0 are the energies for the upper and lower dressed state and the ground state. The external laser field is on resonance with the transition $|g,0\rangle \rightarrow |-\rangle$ near $z = 0$ and its Rabi frequency is denoted by Ω.

the external laser field to be resonant with the transition $|g,0\rangle \rightarrow |-\rangle$ near $z = 0$, as indicated in Fig. 3.2 [88].

The above discussion has omitted an important element which is present in all experiments, namely the dissipation mechanism. On the one hand, excited atoms may decay very fast (as long as the state $|e\rangle$ does not correspond to some Zeeman level, which is coupled to the cavity mode by some Raman transition [89]). More importantly, cavities have usually losses, so that the photons will leave the cavity after some time $t \simeq 1/\kappa$, where κ is the cavity damping rate. Any of these mechanisms will induce the spontaneous transition $|-\rangle \rightarrow |g,0\rangle$, and therefore the atom will no longer experience the trapping force. The typical time scale of this processes is of the order of γ^{-1} and κ^{-1}, where γ and κ are the spontaneous emission and the cavity damping rate, respectively. In practice [38–41] the atom can be promoted several times to the state $|-\rangle$ by the external laser, so that the trapping time inside the cavity can be several hundreds of κ^{-1}. Note, however, that these spontaneous transitions will break the atomic coherence if we are using more internal levels to store, for example, some quantum information in the atom

(see Fig. 3.1).

3.1.2 Position-dependent ac-Stark shift for the ground state

Our idea is to detune the external laser slightly below the transition $|g,0\rangle \rightarrow |-\rangle$ at $z = 0$. If the laser intensity is low enough, its only effect will be to produce an ac-Stark shift for the level $|g,0\rangle$, whose energy $E_0(z)$ will now depend on the position, as shown in Fig. 3.3. Thus, if the atom is in the level

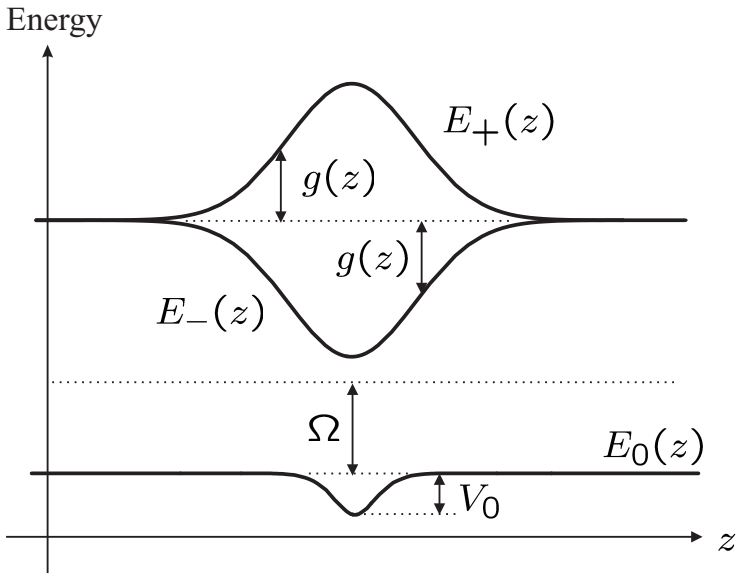

Figure 3.3: The detuned external laser with Rabi frequency Ω leads to a position dependent ac-Stark shift of $|g,0\rangle$. If the system is in the level $|g,0\rangle$ its energy $E_0(z)$ depends on the position of the atom. Therefore there exists a trapping force towards the center of the cavity.

$|g,0\rangle$, it will experience a trapping force towards $z = 0$, and therefore, it can be trapped (as long as the corresponding potential supports bound states). Note also, that since the atom is basically in the ground state and no photon is present, all the dissipative mechanisms may be drastically reduced.

In the following sections we will compute the performance of our scheme. In the rest of this section we will use very simple estimates to characterize the trapping potential and the corresponding time scales.

Denoting by Ω the Rabi frequency of the external laser, and by Δ its corresponding detuning with respect to the $|g\rangle \rightarrow |e\rangle$ transition ($\Delta < 0$), we

have that the regime of validity of our analysis will be

$$\Omega \ll |\Delta + g_0| \ll g_0, \tag{3.4}$$

where g_0 is the maximal coupling-strength in the center of the cavity. In this case, the depth of the trapping potential V_0 will be approximately equal to the ac-Stark shift of the level $|g,0\rangle$ due to its coupling to $|-\rangle$ at $z=0$, i.e.

$$V_0 \simeq \frac{\Omega^2}{8\,|\Delta + g_0|}. \tag{3.5}$$

On the other hand, losses will be due to the small contamination of level $|g,0\rangle$ with level $|-\rangle$ given by the off-resonant coupling. The population of this level will be of the order of $\Omega^2/4|\Delta+g_0|^2$, and therefore the lifetime of the state will be

$$\tau \simeq \frac{4|\Delta+g_0|^2}{\Omega^2}\min(\gamma^{-1},\kappa^{-1}). \tag{3.6}$$

Equations (3.5) and (3.6) indicate that the lifetime can be made arbitrarily big at the expense of reducing the potential depth.

In three dimensions, one can easily estimate the condition for a potential to possess a bound state. It is given by [90] $2mV_0\sigma^2/\hbar^2 \gtrsim \pi^2/4$, where σ is the cavity width, m is the atomic mass, and we have included $\hbar$ to make the dimensions more explicit. We can rewrite this as $16V_0(\sigma/\lambda)^2 \gtrsim E_R$, where λ is an optical transition wavelength and E_R the corresponding energy of one photon recoil. Since $\sigma \gtrsim \lambda$ in all cases we see that by taking $V_0 > E_R$ we will always have an atomic bound state. Note that in a one dimensional set-up there is always a bound state for any value of V_0 [90].

So far, we have shown that it is possible to have atoms trapped in the cavity with basically zero photons and in the atomic ground state. However, the trapping potential may become very weak. Thus, in order to trap atoms it will be required that they move very slowly in the cavity in the state $|g,0\rangle$ and then, when they are close to $z=0$, the external field is turned on. Let us estimate what will be, in this case, the lifetime of the trapped state. We will assume that we have Rb atoms and the kinetic energy is of the order of one optical recoil ($E_R = \hbar^2k^2/2m$, where k is the optical wavevector). Thus, we take $E_R = 4\text{kHz} < V_0 = 10\text{kHZ}$. Let us analyze separately the optical and microwave regimes.

For the optical regime we take the parameters from [40]. There the $5^2S_{1/2}F=3 \rightarrow 5^2P_{3/2}F=4$ transition of ^{85}Rb with a frequency of 3.8×10^{14}Hz was used. The maximal coupling between cavity and atom is $g_0 \approx 16\times 2\pi\,\text{MHz}$, the cavity loss rate is $\kappa \approx 1.4\times 2\pi\,\text{MHz}$ and the spontaneous decay rate is $\gamma \approx 3\times 2\pi\,\text{MHz}$. Employing Eq. (3.6) we estimate a decay time

of 2.1×10^{-5} s. For the microwave regime we consider circular Rydberg states, so we have [33, 91] $g_0 \approx 67 \times 2\pi\,\mathrm{kHz}$, $\kappa \approx 1.6 \times 2\pi\,\mathrm{Hz}$ and $\gamma \approx 1.6 \times 2\pi\,\mathrm{Hz}$, where γ is the spontaneous decay rate of the Rydberg transition. We reach a life time of 40 s (3.6).

These estimates look very promising. They will be optimized and compared with numerical calculations in the following sections. On the other hand, let us stress that we have calculated here the time for a single loss event, since it will destroy the coherence present in the atomic state. For the reference [34–41], in the optical experiments in which the atom is trapped in a cavity both the effective decay rate and the potential depth seen by the atom scale proportionally to the population of the excited level. However, in our case the potential depth (3.5) scales in a different way. Thus we expect that our scheme will be useful under appropriate conditions (small initial velocities). In the following sections we will also analyze the trapping time if several loss events are allowed.

3.2 Model

In this section we will introduce in detail the model that describes the situation we have in mind. In the first subsection we will start with the full Hamiltonian characterizing the atom-cavity interaction and perform some approximations in order to derive the estimates given in the previous section. Then we will introduce the decay mechanisms in this picture.

3.2.1 Hamiltonian dynamics

The Hamiltonian describing the dynamics of the atom and the cavity mode is given by Eq. (2.51). Here we consider also the kinetic energy $p^2/2m$ of the atom and, since it couples resonantly to the cavity mode, we define $\omega_0 \equiv \omega_a = \omega_c$ and write

$$\begin{aligned} H &= \frac{p^2}{2m} + \omega_0(a^\dagger a + \frac{1}{2}\sigma_z) + g(z)(\sigma^+ a + a^\dagger \sigma^-) \\ &\quad + \frac{\Omega}{2}(\sigma^+ e^{-i\omega_l t} + \sigma^- e^{i\omega_l t}). \end{aligned} \tag{3.7}$$

Here, ω_l and Ω are the frequency and the Rabi frequency of the laser and $g(z)$ the position dependent coupling constant between the cavity mode and the atom.

In order to make the analysis simpler, we will project our system in the subspace spanned by the states $\{|g,0\rangle, |e,0\rangle, |g,1\rangle\}$. In any case, the reader

can easily verify that the population of all other levels will be much smaller than the last two, which will be scarcely populated. The Hamiltonian (3.7) in this subspace can be rewritten as $H = p^2/2m + H'(z)$ with

$$\begin{aligned} H'(z) &= g(z)\left(|e,0\rangle\langle g,1| + |g,1\rangle\langle e,0|\right) + \frac{\Omega}{2}\left(|g,0\rangle\langle e,0| + |e,0\rangle\langle g,0|\right) \\ &\quad - \frac{\Delta}{2}\left(|g,1\rangle\langle g,1| + |e,0\rangle\langle e,0| - |g,0\rangle\langle g,0|\right) \end{aligned} \tag{3.8}$$

in a frame rotating with the laser frequency ω_l. $H'(z)$ can be diagonalized exactly but instead of doing that, we calculate its eigenstates and eigenvalues in lowest order perturbation theory with respect to Ω, which is assumed to be small with respect to $|\Delta + g(z)|$ for all values of z (see Fig. 3.3), where $\Delta = \omega_l - \omega_0$. We obtain

$$\begin{aligned} |\Psi_0(z)\rangle &= |g,0\rangle + \frac{\Omega/2}{\Delta^2 - g(z)^2}\big(g(z)|g,1\rangle + \Delta|e,0\rangle\big), \\ |\Psi_1(z)\rangle &= \frac{1}{\sqrt{2}}\Big(|g,1\rangle - |e,0\rangle - \frac{\Omega/2}{\Delta + g(z)}|g,0\rangle\Big), \\ |\Psi_2(z)\rangle &= \frac{1}{\sqrt{2}}\Big(|g,1\rangle + |e,0\rangle - \frac{\Omega/2}{\Delta - g(z)}|g,0\rangle\Big), \end{aligned} \tag{3.9}$$

and the corresponding eigenvalues

$$\begin{aligned} \lambda_0(z) &= \frac{\Delta}{2} + \frac{\Omega^2}{8}\Big(\frac{1}{\Delta + g(z)} + \frac{1}{\Delta - g(z)}\Big), \\ \lambda_1(z) &= -\frac{\Delta}{2} - g(z) - \frac{\Omega^2/8}{\Delta + g(z)}, \\ \lambda_2(z) &= -\frac{\Delta}{2} + g(z) - \frac{\Omega^2/8}{\Delta + g(z)}. \end{aligned} \tag{3.10}$$

As we see, the ground state is basically $|g,0\rangle$ with a vanishing contribution of levels $|g,1\rangle$ and $|e,0\rangle$ in the limit $\Omega \ll |\Delta + g(z)|$. However, it acquires a position-dependent shift in its energy. The two terms in the shift come from the ac-Stark shifts due to $|-\rangle$ and $|+\rangle$, respectively, which, with the chosen detuning, do not compensate each other. The shift is maximal at $z = 0$. To obtain the potential depth V_0 we have to subtract the shift at $g(z) = 0$. This gives

$$V_0 = -\frac{\Omega^2 g_0^2}{4\Delta\,(\Delta^2 - g_0^2)}. \tag{3.11}$$

In the limit (3.4) we have $\Delta \approx -g_0$. If we plug this into (3.11) we obtain (3.5).

Starting out with $\Omega = 0$, if the atom is initially in $|g, 0\rangle$ and has a small velocity near $z = 0$, and we turn the laser on, it will basically remain in the eigenstate $|\Psi_0(z)\rangle$, and therefore will experience the potential $\lambda_0(z)$. For this picture to be valid, we need the kinetic energy of the atom to be smaller than $|\Delta + g_0|$ since in this case we can adiabatically eliminate the levels $|g, 1\rangle$ and $|e, 0\rangle$ and obtain the effective Hamiltonian

$$H_{ad} = \frac{p^2}{2m} + \lambda_0(z)|g, 0\rangle\langle g, 0|. \tag{3.12}$$

3.2.2 Dissipation

We introduce a cavity decay rate κ and a spontaneous decay rate γ for the atom. To take both into account we use the master equation (2.48) that describes the time evolution of this open quantum systems. The state of the system, which is now in general a mixed one, is given by a density matrix ρ. For our system we obtain

$$\frac{d\rho}{dt} = -i[H, \rho] + (\mathcal{L}_c + \mathcal{L}_a)\rho. \tag{3.13}$$

Here,

$$\mathcal{L}_c\rho = \kappa \left(2\, a\, \rho\, a^\dagger - a^\dagger a\, \rho - \rho\, a^\dagger a\right) \tag{3.14}$$

describes the cavity damping, whereas

$$\mathcal{L}_a\rho \;=\; \gamma\Big(2 \int_{-1}^{1} N(u)\, \sigma^-\, e^{-iuz}\, \rho\, e^{iuz}\, \sigma^+ \mathrm{d}u - \sigma^+\sigma^-\, \rho - \rho\, \sigma^+\sigma^-\Big) \tag{3.15}$$

describes spontaneous emission. In the first term of this expression we take into account the photon recoil experienced by the atom after a photon emission (u is the momentum shift). The angular factor $N(u)$ accounts for the pattern of the dipole radiation. Since we consider here a one dimensional version, we have $N(u) = 1$.

To simulate a single trajectory we use the quantum-jump approach introduced in section 2.2. Therefore one defines an effective non-Hermitian Hamiltonian

$$H_{\text{eff}} = H - i\kappa a^\dagger a - i\gamma\sigma_+\sigma_-, \tag{3.16}$$

which describes the time evolution of the system under the condition that no emission takes place. The master equation can than be written in the form

$$\begin{aligned} \frac{d\rho}{dt} \;&=\; 2\,\kappa\, a\, \rho\, a^\dagger + 2\,\gamma \int_{-1}^{1} N(u)\, \sigma^-\, e^{-iuz}\, \rho\, e^{iuz}\, \sigma^+ \mathrm{d}u \\ &\quad - i\left[\left(H_{\text{eff}} + \frac{p^2}{2m}\right)\rho - \rho\left(H_{\text{eff}}^\dagger + \frac{p^2}{2m}\right)\right]. \end{aligned} \tag{3.17}$$

The decay rates contribute to the effective time evolution as damping terms. Therefore the norm of the state decreases. This means that the probability to find no photon in the time interval $(0, t)$ decreases with time "t".

Dissipation occurs in our model due to the small contamination of level $|\Psi_0\rangle$ with the states $|g, 1\rangle$ and $|e, 0\rangle$, which in turn decay due to cavity damping and spontaneous emission, respectively. In order to determine the effective decay rate (or jump time) we take the sum over the probabilities for the excited states $|g, 1\rangle$ and $|e, 0\rangle$ in $|\Psi_0\rangle$ weighted with the cavity decay rate κ and the spontaneous emission rate γ. For the coupling constant we assume that the atom is in the center of the cavity ($g(z) = g_0$). We obtain

$$\begin{aligned} \gamma_{\text{eff}} &= \kappa \cdot |\langle g, 1|\Psi_0\rangle|^2 + \gamma \cdot |\langle e, 0|\Psi_0\rangle|^2 \\ &= \kappa \cdot \left| \frac{g_0\Omega/2}{\Delta^2 - g_0^2} \right|^2 + \gamma \cdot \left| \frac{\Delta\Omega/2}{\Delta^2 - g_0^2} \right|^2 \\ &= \frac{\Omega^2 \left(\kappa\ g_0^2 + \gamma\ \Delta^2\right)}{4\left(\Delta^2 - g_0^2\right)^2}. \end{aligned} \tag{3.18}$$

This gives an effective decay time of

$$\tau_{\text{eff}} = \frac{1}{\gamma_{\text{eff}}} = \frac{4\left(\Delta^2 - g_0^2\right)^2}{\Omega^2 \left(\kappa\ g_0^2 + \gamma\ \Delta^2\right)}. \tag{3.19}$$

For the estimation of the life time in Eq. (3.6) we neglected the contribution of the upper dressed level $|+\rangle$ to the disturbed eigenstate $|\Psi_0\rangle$. If we consider this and the approximation $\Delta \approx -g_0$ and plug it with $\kappa = \gamma = max(\kappa, \gamma)$ into (3.19) we end up with the expression (3.6).

3.2.3 Potential depth and effective life time

In Fig. 3.4 and Fig. 3.5 we have plotted the potential depths V_0 and the effective life time τ_{eff} versus Δ and Ω. From Fig. 3.4(A) we see that in order to get a long decay time it would be desirable to have $|\Delta| \gg |g_0|$. In Fig. 3.4(B) the region $-g_0 < \Delta < 0$ is not of interest since there one obtains no attractive potential ($V_0 < 0$). One has to find a compromise between Δ close to $-g_0$ in order to get a deep potential and $|\Delta| \gg |g_0|$ in order to obtain a long decay time. This behavior is not surprising because if the detuning is close to $-g_0$ the population in $|-\rangle$ increases. This leads to a short decay time and a deep potential. The same reasoning explains the plots in Fig. 3.5 since the Rabi frequency Ω is a measure for the coupling strength between the atomic transition and the laser.

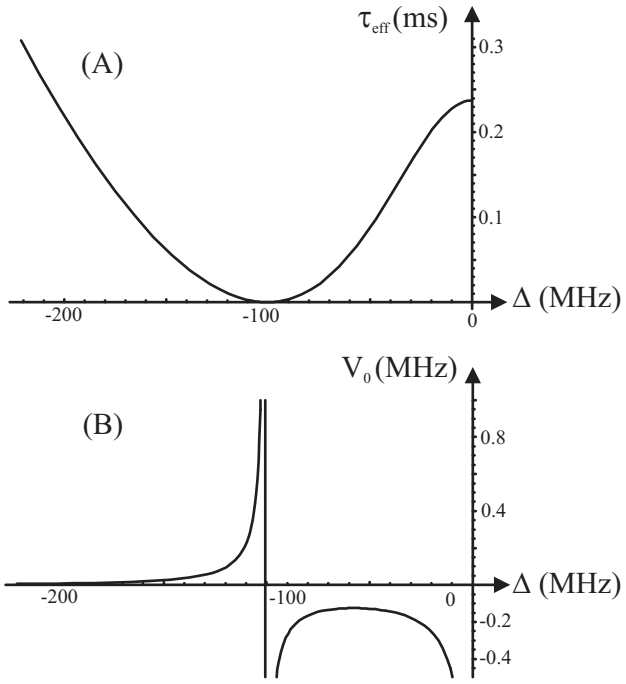

Figure 3.4: Effective decay time τ_{eff} (A) and potential depth V_0 (B) versus laser detuning $\Delta = \omega_l - \omega_0$. For the Rabi frequency of the laser we took $\Omega = 0.70 \times 2\pi$MHz. The coupling strength between cavity and atom is $g_0 = 16 \times 2\pi$ MHz, the cavity loss rate $\kappa = 1.4 \times 2\pi$ MHz and the spontaneous decay rate $\gamma = 3 \times 2\pi$ MHz.

For the parameters from [40] and a potential depth of $V_0 = 10\,\text{kHz}$ the longest effective life time we can achieve in the optical regime is $\tau_{\text{eff}} = 0.18\,\text{ms}$. The corresponding values for the laser parameters are

$$\begin{aligned} \Omega &= 0.70 \times 2\pi\,\text{MHz}, \\ |\Delta| &= 1.90\, g_0 = 30 \times 2\pi\,\text{MHz}. \end{aligned} \tag{3.20}$$

In the microwave regime [33, 91] we get $\tau_{\text{eff}} = 1.26\,\text{sec}$ with

$$\begin{aligned} \Omega &= 54 \times 2\pi\,\text{kHz}, \\ |\Delta| &= 2.06\, g_0 = 0.14 \times 2\pi\,\text{MHz}. \end{aligned} \tag{3.21}$$

It is remarkable that since we used the expressions from (3.11) and (3.19) we are not in the limit $\Delta \approx -g_0$ (3.4). This inreases the life time in the optical regime considerably.

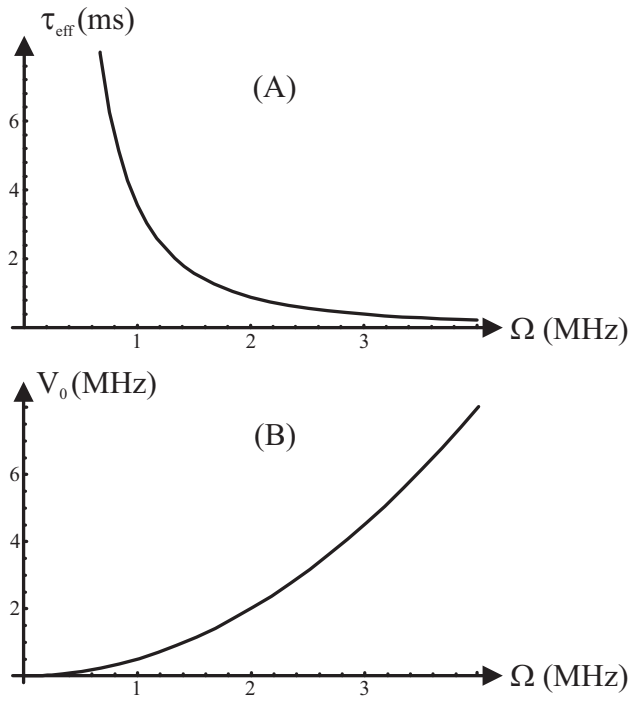

Figure 3.5: Effective decay time τ_{eff} (A) and potential depth V_0 (B) versus Rabi frequency Ω of the laser. For the laser detuning we took $|\Delta| = 1.90\, g_0 = 30 \times 2\pi\,\text{MHz}$. The other parameters are the same as in Fig. 3.4.

3.3 Numerical results

Here we investigate the behavior of the system numerically. For the analytic results we made certain approximations. The comparison with the numerical results will show if these assumption are justified for realistic parameters. Furthermore we will include spontaneous emission and photon recoil.

We denote the state of the system by $|\Phi\rangle$. For the simulation we write it as

$$|\Phi\rangle = |\varphi_{g0}\rangle + |\varphi_{g1}\rangle + |\varphi_{e0}\rangle, \tag{3.22}$$

where $|\varphi_i\rangle = |i\rangle\langle i|\Phi\rangle$. We consider only the contributions of $|g,0\rangle$, $|g,1\rangle$ and $|e,0\rangle$ since the population of the levels with two and more excitations is negligible. As for the analytic estimations we restrict the investigations to one dimension. The probability amplitudes for the system being in the states $|g,0\rangle$, $|g,1\rangle$ and $|e,0\rangle$ at position "z" are given by $\varphi_{g0}(z) = \langle z|\varphi_{g0}\rangle$, $\varphi_{g1}(z) = \langle z|\varphi_{g1}\rangle$ and $\varphi_{e0}(z) = \langle z|\varphi_{e0}\rangle$.

In the first subsection we calculate the ground state of the system with

and without the assumptions made above. In the following we include dissipation and compare the decay time with the effective decay time τ_{eff} we estimated in the last section. Finally we consider spontaneous emissions and recoil and investigate how long the atom remains in the cavity for different parameters. Apart from one simulation with the parameters from the analytic estimation we will only consider the optical regime in this section.

3.3.1 The ground state

To obtain the ground state we apply the imaginary time evolution [92] to an arbitrary initial state until it remains unchanged. Instead of the time evolution operator $e^{-\mathrm{i}H\Delta t}$ one uses a modified operator $e^{-H\Delta t}$. Denoting the eigenvectors of H with $|\Phi_i\rangle$ and the corresponding eigenvalues with μ_i we obtain in each time-step

$$\begin{aligned} e^{-H\Delta t}|\Phi\rangle &= \sum_i e^{-\mu_i \Delta t}|\Phi_i\rangle\langle\Phi_i|\Phi\rangle \\ &= e^{-\mu_0\Delta t}\sum_i e^{-(\mu_i-\mu_0)\Delta t}|\Phi_i\rangle\langle\Phi_i|\Phi\rangle, \end{aligned} \tag{3.23}$$

where μ_0 is the lowest eigenvalue. Since we normalize the state after each step the corresponding eigenvector $|\Phi_0\rangle$ is not damped. After a sufficient number of iterations this damps away all states orthogonal to $|\Phi_0\rangle$, which is the ground state of the system.

The Hamiltonian of the system is given in Eq. (3.7). For Ω and Δ we took the values from (3.20). According to the analytic approximation they should give the maximal decay time which is achievable for a potential depth of 10 kHz. The numerical simulation of the ground state leads to the probability distribution shown in Fig. 3.6. The three plots show the population distribution of the three internal states separately. The excited states are only very weakly populated. The probability to find an atom in the center of the cavity with the system being in state $|g,1\rangle$ or $|e,0\rangle$ is three to four orders of magnitude smaller than to find it there with the state $|g,0\rangle$. We also found that the atom is well localized in the center of the cavity. At $0.1\,\sigma$, where σ is the width of the cavity, the probability to find the atom is already reduced by more than 1/2.

In order to valuate the approximations made for the analytic estimation we calculated the ground state also using the Hamiltonian from Eq. (3.12). We denote its ground state solution by $|\xi_0\rangle$. We find

$$|\Phi_0\rangle \approx |g,0\rangle \otimes |\xi_0\rangle. \tag{3.24}$$

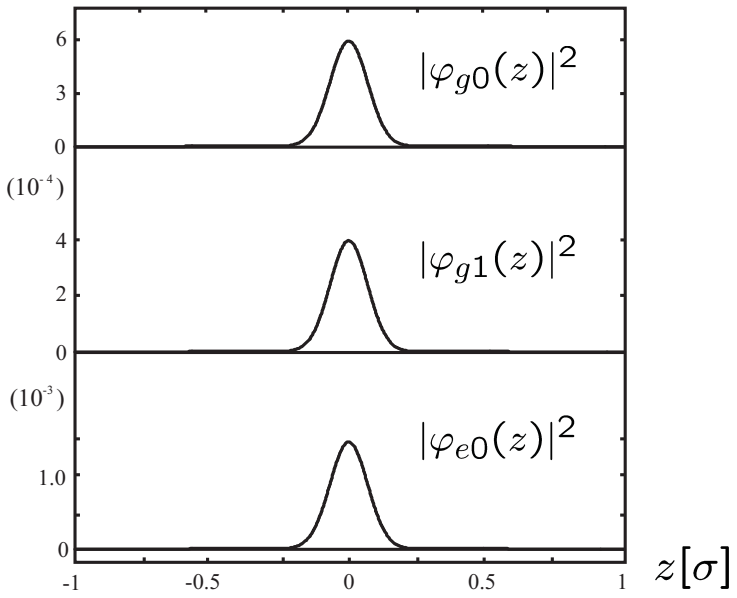

Figure 3.6: Numerical simulation of the ground state. The plots show $|\varphi_{g0}(z)|^2$, $|\varphi_{g1}(z)|^2$ and $|\varphi_{e0}(z)|^2$ versus z. They satisfy the normalization condition $\int (|\varphi_{g0}(z)|^2 + |\varphi_{g1}(z)|^2 + |\varphi_{e0}(z)|^2)\, dz = 1$. The plots are in units of σ, which is the cavity width. For the laser detuning we took $\Delta = 1.90\, g_0 = 30 \times 2\pi\,\mathrm{MHz}$ and for the Rabi frequency of the laser $\Omega = 0.70 \times 2\pi\mathrm{MHz}$. The coupling strength between cavity and atom is $g_0 = 16 \times 2\pi\,\mathrm{MHz}$, the cavity loss rate $\kappa = 1.4 \times 2\pi\,\mathrm{MHz}$ and the spontaneous decay rate $\gamma = 3 \times 2\pi\,\mathrm{MHz}$.

This means that nearly all the population is in $|g, 0\rangle$. So the approximations in the analytical approach are justified and one can trap an atom in a basically empty cavity.

3.3.2 Dissipation and photon emissions

In this subsection we include the coupling of the system to the environment and as a consequence the spontaneous emission of photons. First we will only consider the time evolution of the system under the condition that no photon is emitted and compare the decay time with the analytic estimation. Then we include also spontaneous emissions and the recoil kick the atom experiences.

In the quantum-jump approach one describes the time evolution of the system with an effective Hamiltonian as long as no photon is emitted. The

emissions which cause the system to jump in a different state are described by reset operators. The effective Hamiltonian is given by

$$\begin{aligned} H_{\text{eff}} &= \frac{p^2}{2m} - \frac{\Delta}{2}\left(|g,1\rangle\langle g,1| + |e,0\rangle\langle e,0| - |g,0\rangle\langle g,0|\right) \\ &\quad + g(z)\big(|e,0\rangle\langle g,1| + |g,1\rangle\langle e,0|\big) + \frac{\Omega}{2}\big(|g,0\rangle\langle e,0| + |e,0\rangle\langle g,0|\big) \\ &\quad - i\kappa|g,1\rangle\langle g,1| - i\gamma|e,0\rangle\langle e,0|, \end{aligned} \tag{3.25}$$

where we used an interaction picture rotating with the laser frequency ω_l and assumed that there is at most one excitation in the system.

After preparing the system in the ground state $|\Phi_0\rangle$ using the imaginary time evolution we simulated the time evolution with the effective Hamiltonian H_{eff}. This leads to a damping of the state of the system. So the probability $\langle\Phi|\Phi\rangle$ that no photon has been emitted also decreases. We compare the time after which this probability has reached $1/e$ with the effective life time τ_{eff} we estimated analytically. For the parameters from (3.20) we obtained $\tau_{\text{eff}} = 0.18\,\text{ms}$, which is reasonably close to the decay time from the numerical simulation of 0.14 ms.

In the quantum-jump approach the jumps are described by reset operators. We obtain them from the master equation (3.17). For the spontaneous emission of the atom we get

$$e^{-iuz}\sqrt{2\gamma}|g,0\rangle\langle e,0|, \tag{3.26}$$

where e^{-iuz} describes the momentum shift "u" due to the photon recoil. If the cavity emits a photon one has to apply

$$\sqrt{2\kappa}\,|g,0\rangle\langle g,1|. \tag{3.27}$$

In both cases the population of the excited level gets shifted to the ground state. After that one has to normalize the wave function.

In the following we will discuss the trapping time τ_{trap} of the atom. We define it as the time when the probability to find the atom in the cavity ($|z| < \sigma$) is reduced to 0.5. The atom has an initial kinetic energy and gains a momentum kick when it spontaneously emits a photon. When the motional energy is bigger than the trapping potential the atom leaves the cavity. So it is desirable to achieve a long decay time in order to get a low photon emission rate. On the other hand a deeper potential provides the possibility of a bound state for an atom which experienced more recoil kicks. From our analytic estimations we know that these requirements contradict each other. For the simulation we took the parameters from (3.20) for a

potential depth of $V_0 = 10\text{kHz}$ and the longest corresponding effective decay time $\tau_{\text{eff}} = 0.18\,\text{ms}$. We applied the operator e^{-iuz} to the ground state which we got from the imaginary time evolution in order to take into account an initial kinetic energy. The momentum shift "u" corresponds to the energy of one photon recoil $E_R = 4\,\text{kHz}$. After a couple of spontaneous emissions the atom leaves the cavity at time $\tau_{\text{trap}} = 0.73\,\text{ms}$.

In order to achieve a longer trapping time we first varied the detuning Δ and left the Rabi frequency $\Omega = 0.70 \times 2\pi\text{MHz}$ unchanged. The result is shown in Fig. 3.7. A larger detuning of the laser leads to a smaller potential

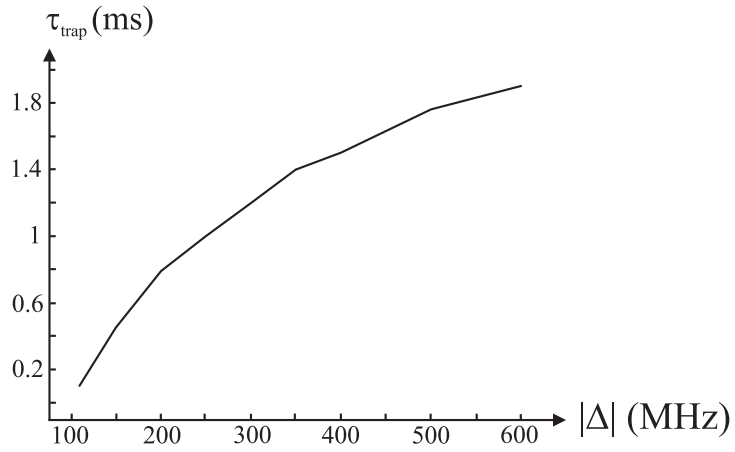

Figure 3.7: Numerical results for the trapping time τ_{trap} versus detuning Δ for a Rabi frequency $\Omega = 0.70 \times 2\pi\text{MHz}$. The coupling strength between cavity and atom is $g_0 = 16 \times 2\pi\,\text{MHz}$, the cavity loss rate $\kappa = 1.4 \times 2\pi\,\text{MHz}$ and the spontaneous decay rate $\gamma = 3 \times 2\pi\,\text{MHz}$.

depth V_0 and a longer effective life time τ_{eff}. From Fig. 3.7 we see that the longer life time has a bigger influence on the trapping time since τ_{trap} increases with growing detuning. It is not surprising that the effective life time has a crucial influence on the trapping time since it determines how fast the motional energy of the atom grows.

A larger Rabi frequency causes a smaller effective life time and a deeper potential. Consequently, we expect a decreasing trapping time when we enlarge the Rabi frequency. This is confirmed by Fig. 3.8, where we plotted τ_{trap} versus Ω for a fixed detuning $|\Delta| = 1.90\,g_0 = 30 \times 2\pi\,\text{MHz}$. Comparing this plot with the plot in Fig. 3.5(A) we ascertain a qualitative agreement. This is not surprising if we assume that the decisive variable for the trapping time τ_{trap} is the effective decay time τ_{eff}.

The longest trapping times we can achieve in the optical regime are of

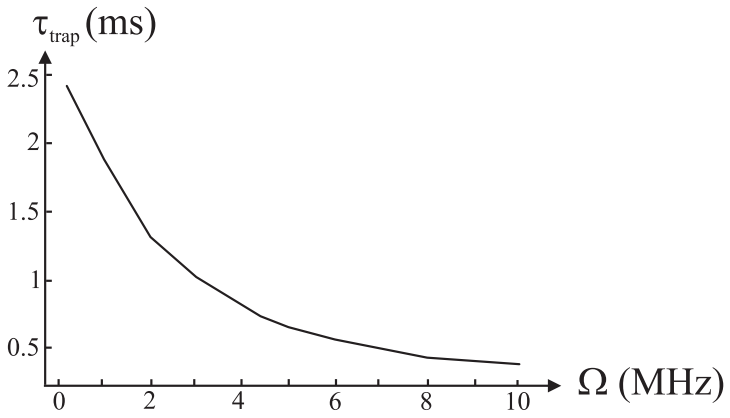

Figure 3.8: Numerical results for the trapping time τ_{trap} versus Rabi frequency Ω for a detuning $|\Delta| = 1.90\, g_0 = 30 \times 2\pi\,\text{MHz}$. The coupling strength between cavity and atom is $g_0 = 16 \times 2\pi\,\text{MHz}$, the cavity loss rate $\kappa = 1.4 \times 2\pi\,\text{MHz}$ and the spontaneous decay rate $\gamma = 3 \times 2\pi\,\text{MHz}$.

the order of 1 ms. For the microwave regime we took $g_0 = 67 \times 2\pi\,\text{kHz}$, $\kappa = 1.6 \times 2\pi\,\text{Hz}$ and $\gamma = 1.6 \times 2\pi\,\text{Hz}$. The trapping time we obtained for the laser parameters from (3.21) was $\tau_{\text{trap}} \approx 10\,\text{s}$. The reason for the good result are the very small decay rates for the Rydberg state and the micro-cavity. Another important advantage over the optical regime is that the recoil due to spontaneous emissions is practically zero.

Chapter 4

Sequential generation of entangled multi-qubit states

In this chapter we consider the deterministic generation of entangled multi-qubit states by the sequential coupling of an ancillary system to initially uncorrelated qubits. In section 4.1 we give a short introduction to the concept of matrix-product states (MPS). In section 4.2 we characterize all achievable states in terms of classes of MPS and give a recipe for the generation on demand of any multi-qubit state. The results are valid for any sequential generation-scheme.

In section 4.3 we will focus on the physical implementation of these ideas within the realm of cavity QED. The role of the ancillary system will be performed by a D-level atom coupled to a single mode of an optical cavity. The sequentially generated qubits will be time-bin qubits $|0\rangle$ and $|1\rangle$, describing the absence and presence of a photon emitted from the cavity in a certain time interval (see Fig. 4.1). We show how this set-up can be employed for

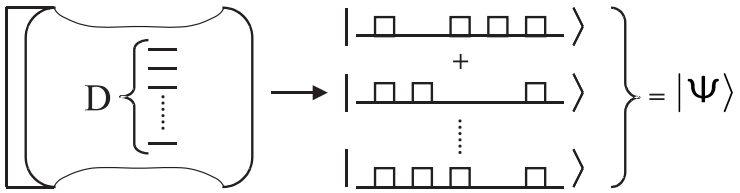

Figure 4.1: A trapped D-level atom is coupled to a cavity qubit, determined by the energy eigenstates $|0\rangle$ and $|1\rangle$. After arbitrary bipartite source-qubit operations, photonic time-bins are sequentially and coherently emitted at the cavity output, creating a desired entangled multi-qubit stream.

the generation of arbitrary multi-qubit states. Considering the limitations of

current experimental set-ups [28–30] we also show how to generate familiar multi-qubit states like W [93], GHZ [58], and cluster states [57]. Finally we use so-called matrix-product density operators (MPDO) to take into account imperfections of the scheme and to calculate the fidelity of the cluster state.

4.1 Matrix-product states

In this section we define the matrix-product states [53,54] using a picture introduced in [94–96]. In Fig. 4.2 a collection of n virtual D-level systems paired

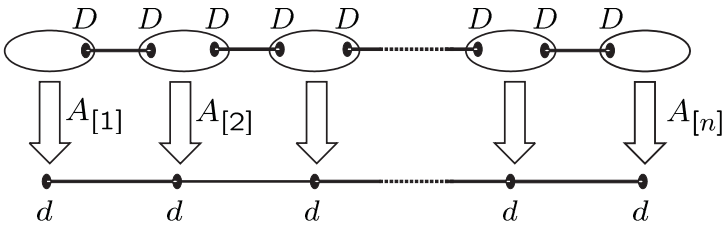

Figure 4.2: A matrix product state with D-dimensional bonds is obtained by applying linear maps $A_{[i]}$ to a collection of virtual D-level systems paired in maximally entangled states. They transform the D^2-dimensional Hilbert space of pairs of virtual systems into the local Hilbert spaces associated with the physical systems of dimension d.

in maximally entangled states $\sum_{\gamma=1}^{D}|\gamma,\gamma\rangle$ is projected onto local Hilbert spaces associated with physical systems of dimension d by linear maps

$$A=\sum_{i=1}^{d}\sum_{\alpha,\beta=1}^{D}A^{i}_{\alpha\beta}|i\rangle\langle\alpha,\beta|, \tag{4.1}$$

where $\{\alpha,\beta\}$ are any of the D levels of the virtual systems. Applying the n maps to the virtual systems leads to the n-qudit MPS

$$\begin{aligned}|\psi\rangle &= A_{[n]}\otimes\ldots\otimes A_{[i]}\Big(\sum_{\gamma=1}^{D}|\gamma,\gamma\rangle\Big)^{\otimes n}\\ &= \sum_{i_1,\ldots,i_n=1}^{d}\mathrm{tr}\big(A^{i_1}_{[1]}\ldots A^{i_n}_{[n]}B\big)|i_1,\ldots,i_n\rangle.\end{aligned} \tag{4.2}$$

The coefficients are given by products of D-dimensional matrices A^i defined as

$$A^i = \sum_{\alpha,\beta=1}^{D} A^i_{\alpha\beta} |\alpha\rangle\langle\beta|. \tag{4.3}$$

Therefore the MPS are completely defined by the linear maps $A_{[i]}$ and the matrix B, which contains the boundary conditions. For translational invariant states we have identical maps $A = A_{[1]} = \ldots = A_{[n]}$. Periodic boundary conditions correspond to $B = \mathbb{1}$.

In [97] the MPS formalism has been extended to mixed states. The basic idea is to replace the linear maps A by a general completely positive map. The states obtained from this procedure define the class of matrix product density operators. A n-qudit MPDO with D-dimensional bonds is given by

$$\rho = \sum_{i_1,i'_1\ldots,i_n,i'_n=1}^{d} \mathrm{tr}\big(M^{i_1,i'_1}_{[1]} \ldots M^{i_n,i'_n}_{[n]} \widetilde{B}\big) |i_1,\ldots,i_n\rangle\langle i'_1 \ldots i'_n|, \tag{4.4}$$

where $M^{i,i'}$ are $D^2 \times D^2$ matrices that can be decomposed as

$$M^{i,i'} = \sum_{e=1}^{d_e} A^{i,e} \otimes \bar{A}^{i',e}, \tag{4.5}$$

with D-dimensional matrices $A^{i,e}$ and $d_e \leq dD^2$. Condition (4.5) ensures that the maps are completely positive. For $M^{i,i'} = \delta_{i,i'}\mathbb{1}$ we obtain the maximally mixed state while $M^{i,i'} = A^i \otimes \bar{A}^{i'}$ gives a pure state.

Any MPDO can be expressed by a MPS applying the concept of purification [5], i.e. choosing a larger Hilbert space for the latter. Therefore we associate with each physical system an auxiliary system of dimension d_e and choose an orthonormal basis $|i,e\rangle$. The corresponding MPS is then given by

$$|\psi_e\rangle = \sum_{i_1,\ldots,i_n=1}^{d} \sum_{e_1,\ldots,e_n=1}^{d_e} \mathrm{tr}\big(A^{i_1,e_1}_{[1]} \ldots A^{i_n,e_n}_{[n]} B\big) |i_1 e_1,\ldots,i_n e_n\rangle. \tag{4.6}$$

Tracing over the ancillas re-establishes the MPDO $\rho = \mathrm{tr}(|\psi_e\rangle\langle\psi_e|)$ with the boundary condition $\widetilde{B} = B \otimes \bar{B}$.

4.2 Sequential generation of MPS with D-dimensional bonds

In the following we investigate the sequential generation of entangled multiqubit states. We will proof the following statements:

- Entangled multi-qubit states, sequentially generated by a D-dimensional source, belong to the class of D-dimensional MPS;

- Any D-dimensional MPS can be generated by a D-dimensional source such that the source decouples in the last step.

The proof of the latter implicates a recipe for the generation of any D-dimensional MPS. In appendix A we demonstrate that any state has an MPS representation. Together the two statements imply that the set of states sequentially generated by a D-dimensional source and the D-dimensional MPS are equivalent. In the second part of this section we consider a $2D$-dimensional, not completely controllable source and show that the accessible set of states is also equivalent.

4.2.1 D-dimensional source

Here, we will concentrate on set-ups where all intermediate operations are arbitrary unitaries and the ancilla decouples in the last step. The latter enables us to generate pure entangled states in a deterministic manner without the need of measurements. Let $\mathcal{H}_\mathcal{A} \simeq \mathbb{C}^D$ and $\mathcal{H}_\mathcal{B} \simeq \mathbb{C}^2$ be the Hilbert spaces characterizing a D-dimensional ancillary system and a single qubit (e.g. a time-bin qubit) respectively. In every step of the sequential generation of a multi-qubit state, we consider a unitary time evolution of the joint system $\mathcal{H}_\mathcal{A} \otimes \mathcal{H}_\mathcal{B}$. Assuming that each qubit is initially in the state $|0\rangle$ (i.e., the time-bin is empty), we disregard the qubit at the input and write the evolution in the form of an isometry $V : \mathcal{H}_\mathcal{A} \to \mathcal{H}_\mathcal{A} \otimes \mathcal{H}_\mathcal{B}$. Expressing V in terms of a basis

$$V = \sum_{i=0}^{1} \sum_{\alpha,\beta} V^i_{\alpha,\beta} |\alpha, i\rangle\langle\beta| \ , \tag{4.7}$$

the isometry condition reads

$$\sum_{i=0}^{1} V^{i\dagger} V^i = \mathbb{1}, \tag{4.8}$$

where each V^i is a $D \times D$ matrix. We choose a basis where $\{|\alpha\rangle, |\beta\rangle\}$ are any of the D ancillary levels.

If we now apply successively n, not necessarily identical, operations of

this form to an initial state $|\varphi_I\rangle \in \mathcal{H}_\mathcal{A}$, we obtain the state

$$\begin{aligned}|\Psi\rangle &= V_{[n]} \dots V_{[2]} V_{[1]} |\varphi_I\rangle \\ &= \sum_{i_1 \dots i_n = 0}^{1} \left(\sum_{\alpha_n, \beta_n} V^{i_n}_{\alpha_n, \beta_n} |\alpha_n\rangle\langle\beta_n| \right) \dots \left(\sum_{\alpha_1, \beta_1} V^{i_1}_{\alpha_1, \beta_1} |\alpha_1\rangle\langle\beta_1| \right) |\varphi_I\rangle \; |i_n, \dots, i_1\rangle \\ &= \sum_{i_1 \dots i_n = 0}^{1} V^{i_n}_{[n]} \dots V^{i_1}_{[1]} |\varphi_I\rangle \; |i_n, \dots, i_1\rangle. \end{aligned} \tag{4.9}$$

Here, and in the following, indices in squared brackets represent the steps in the generation sequence. The n generated qubits are in general entangled with the ancilla as well as among themselves. Assuming that in the last step the ancilla decouples from the system, such that $|\Psi\rangle = |\varphi_F\rangle \otimes |\psi\rangle$, we are left with the n-qubit state

$$|\psi\rangle = \sum_{i_1 \dots i_n = 0}^{1} \langle\varphi_F| V^{i_n}_{[n]} \dots V^{i_1}_{[1]} |\varphi_I\rangle \; |i_n, \dots, i_1\rangle. \tag{4.10}$$

Comparing this result with the MPS definition in Eq. (4.2) for $d = 2$, we identify $A^i = V^i$ and the boundary condition $B = |\varphi_I\rangle\langle\varphi_F|$. The scheme is illustrated in Fig. 4.3. The analogy to the MPS presentation in Fig. 4.2 is

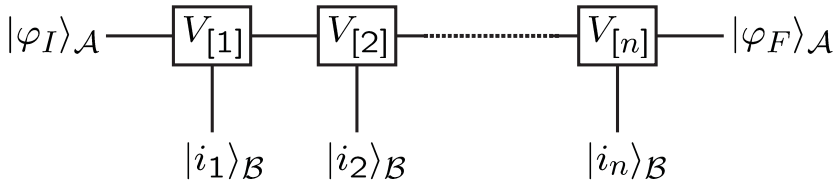

Figure 4.3: The ancillary system $\mathcal{A}$ is sequentially manipulated by isometric operations $V_{[i]}$. In each step a qubit $|i\rangle_\mathcal{B}$ is generated. Comparing this illustration with the depiction of MPS in Fig. 4.2, it becomes evident that the sequentially generated multi-qubit states are MPS, where the dimension of the ancilla corresponds to the dimension of the maximally entangled virtual systems.

evident.

Equation (4.10) shows that all sequentially generated multi-qubit states, arising from a D-dimensional ancillary system $\mathcal{H}_\mathcal{A}$, are instances of MPS with $D \times D$ matrices V^i and open boundary conditions specified by $|\varphi_I\rangle$ and $|\varphi_F\rangle$. We will now prove that the converse is also true, i.e. that every MPS of the form

$$|\tilde{\psi}\rangle = \langle\tilde{\varphi}_F| \tilde{V}_{[n]} \dots \tilde{V}_{[1]} |\tilde{\varphi}_I\rangle, \tag{4.11}$$

with arbitrary maps $\tilde{V}_{[k]} : \mathcal{H}_\mathcal{A} \to \mathcal{H}_\mathcal{A} \otimes \mathcal{H}_\mathcal{B}$, can be generated by isometries of the same dimension, and such that the ancillary system decouples in the last step. Since every state has a MPS representation, this is at the same time a general recipe for its sequential generation. The idea of the proof is an explicit construction of all involved isometries by subsequent application of singular value decompositions (SVD). We start by writing

$$\langle\tilde{\varphi}_F|\tilde{V}_{[n]} = \big(\langle\tilde{\varphi}_F| \otimes \mathbb{1}_2\big)\tilde{V}_{[n]} = V'_{[n]}M_{[n]}, \tag{4.12}$$

where the 2×2 matrix $V'_{[n]}$ is the left unitary in the SVD and $M_{[n]}$ is the remaining part. The recipe for constructing the isometries is the induction

$$\big(M_{[k]} \otimes \mathbb{1}_2\big)\tilde{V}_{[k-1]} = V'_{[k-1]}M_{[k-1]}, \tag{4.13}$$

where the isometry $V'_{[k-1]}$ is constructed from the SVD of the left hand side, and $M_{[k-1]}$ is always chosen to be the remaining part. After n applications of Eq. (4.13) in Eq. (4.11), from left to right, we set $|\varphi_I\rangle = M_{[1]}|\tilde{\varphi}_I\rangle$, producing

$$|\tilde{\psi}\rangle = V'_{[n]} \dots V'_{[1]}|\varphi_I\rangle. \tag{4.14}$$

Simple rank considerations show that $V'_{[n-k]}$ has dimension $2\min[D, 2^k] \times \min[D, 2^{k+1}]$. In particular, every $V'_{[k]}$ could be embedded into an isometry $V_{[k]}$ of dimension $2D \times D$. Physically, this just means we would have redundant ancillary levels that we need not to use. Finally, decoupling the ancilla in the last step is guaranteed by the fact that, after the application of $V_{[n-1]}$, merely two levels of $\mathcal{H}_\mathcal{A}$ are yet occupied, and can be mapped entirely onto the system $\mathcal{H}_\mathcal{B}$. This is precisely the action of $V_{[n]}$ through its embedded unitary $V'_{[n]}$.

This proves the equivalence of two sets of n-qubit states, which are described either as D-dimensional MPS with open boundary conditions, or as states that are generated sequentially and isometrically via a D-dimensional ancillary system which decouples in the last step.

It is instructive to estimate an upper bound for the number of free parameters available for an n-qubit MPS with D-dimensional bonds. Taking into account that the isometry condition (4.8) does not restrict the set of allowed states and that a transformation of the form

$$V^i \mapsto U_i\, V^i\, U_{i+1}, \tag{4.15}$$

employing D-dimensional unitary matrices U_i and U_{i+1} $(i = 1, \dots, n)$ does not alter the coefficients of the MPS (4.10) we obtain an upper bound of $nD^2/2$. Since the number of free parameters for a general n-qubit state is

given by $2^n - 1$ the dimensionality of a source capable of generating an arbitrary n-qubit state grows exponentially with n. Fortunately many interesting states like for instance GHZ, W, $AKLT$ [55] and cluster states belong to the class of MPS with 2-dimensional bonds [59].

4.2.2 $2D$-dimensional source

Motivated by current cavity QED set-ups, we will now provide a third equivalent characterization, namely, a set of multi-qubit states that are sequentially generated by a source consisting of a $2D$-level atom. In contrast to the first sequential scheme, the latter will not require arbitrary isometries. Consider an atomic system with D states $|a_i\rangle$ and D states $|b_i\rangle$ (see also Fig. 4.4), so

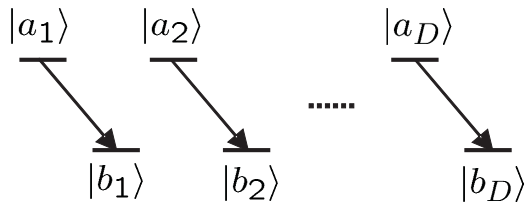

Figure 4.4: D-standard map: Levels $|a_i\rangle$ are mapped on the corresponding levels $|b_i\rangle$ accompanied by the generation of a photon in a certain time-bin. In a cavity-QED set-up the $2D$ atomic levels are considered to be ground states coupled via a Raman transition or an adiabatic passage. Therefore spontaneous decay is suppressed.

that $\mathcal{H}_\mathcal{A} = \mathcal{H}_a \oplus \mathcal{H}_b \simeq \mathbb{C}^D \otimes \mathbb{C}^2$. That is, we will write $|\varphi\rangle|1\rangle$ for a superposition of $|a_i\rangle$ states, whereas $|\varphi\rangle|0\rangle$ corresponds to a superposition of $|b_i\rangle$ states. Since the last qubit marks the atomic state, whether it belongs to the $|a_i\rangle$ or to the $|b_i\rangle$ subspace, we will refer to it as the tag-qubit and write $\mathcal{H}_\mathcal{A} = \mathcal{H}_{\mathcal{A}'} \otimes \mathcal{H}_\mathcal{T}$, with an effective ancilla system $\mathcal{A}'$. Now we consider the atomic transitions from each $|a_i\rangle$ state to its respective $|b_i\rangle$ state accompanied by the generation of a photon in a certain time-bin. This is described by a unitary evolution, since now called "D-standard map", of the form

$$\begin{aligned} T: \ |\varphi\rangle_{\mathcal{A}'}|1\rangle_\mathcal{T}|0\rangle_\mathcal{B} &\mapsto |\varphi\rangle_{\mathcal{A}'}|0\rangle_\mathcal{T}|1\rangle_\mathcal{B} \ , \\ |\varphi\rangle_{\mathcal{A}'}|0\rangle_\mathcal{T}|0\rangle_\mathcal{B} &\mapsto |\varphi\rangle_{\mathcal{A}'}|0\rangle_\mathcal{T}|0\rangle_\mathcal{B} \ . \end{aligned} \tag{4.16}$$

Hence, T effectively interchanges the tag-qubit with the time-bin qubit as illustrated in Fig. 4.5. If, additionally, arbitrary atomic unitaries $U_\mathcal{A}$ are allowed at any time, we can exploit the swap caused by T in order to generate

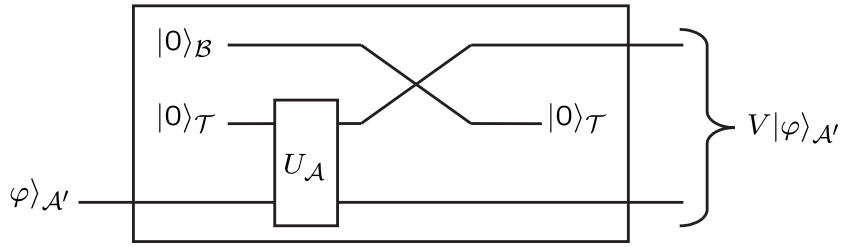

Figure 4.5: The box represents one step of the sequential generation scheme. After the preceding step the atom is in a superposition of ground states, i.e. the tag-qubit is in $|0\rangle_{\mathcal{T}}$. Since after the exchange with the initially empty time-bin qubit it is again in state $|0\rangle_{\mathcal{T}}$, it can be ignored for the sequential generation scheme.

the operation

$$V|\varphi\rangle = \langle 0|_{\mathcal{T}} T\Big(U_{\mathcal{A}}\big(|\varphi\rangle_{\mathcal{A}'}|0\rangle_{\mathcal{T}}\big)|0\rangle_{\mathcal{B}}\Big)\,, \tag{4.17}$$

which is the most general isometry $V : \mathcal{H}_{\mathcal{A}'} \to \mathcal{H}_{\mathcal{A}'} \otimes \mathcal{H}_{\mathcal{B}}$.

Therefore, the so generated n-qubit states include all possible states arising from subsequent applications of $2D \times D$-dimensional isometries. On the other hand, they are a subset of the MPS in Eq. (4.11) with arbitrary $2D \times D$-dimensional maps, assuming that the atom decouples at the end. Hence, these three sets are all equivalent.

4.3 Implementation within cavity QED

Now, we show how these results can be applied in the realm of cavity QED, where an atom is trapped inside a high-Q optical cavity, and we aim at generating multi-photon entangled states. A laser may excite the atom, producing subsequently a photon in the cavity mode, which, after some time, is emitted outside the cavity (see Fig. 4.1). Desirable properties of a cavity QED single-photon source are:

- Deterministic emission time, i.e. the probability for a failure of the source is negligible;
- Control over the temporal profile of the emitted single-photon pulse.

The first point is essential since the time-bin qubits are defined by the absence ($|0\rangle$) and the presence ($|1\rangle$) of a photon in a certain time-interval, i.e. a failure will be misinterpreted as $|0\rangle$. The idea is to control the emission-time

by the laser which excites the atom but spontaneous atomic decay into the background modes reduces the efficiency of the source. In order to suppress these losses one usually employs two meta-stable ground states of the atom and couples them to the cavity mode via a Raman transition or an adiabatic passage. Pulse-shape control is crucial for later use of the emitted pulse. Note in this context, that two single-photon pulses interfere at a beam splitter only if they have identical shapes (see, for instance [98]). A lower limit for the width of the pulse is given by the decay time of the cavity. If the excitation-transfer to the cavity mode takes much longer than this, one can tailor the pulse at will.

We consider two different scenarios, corresponding to the two families of states considered in section 4.2. First, we may have fast and complete access to the atom-cavity system. In consequence, after the implementation of the desired isometry in each step, we should wait until the photon leaks out of the cavity before starting the next step. In this case, according to the analysis in section 4.2.1, we will be able to produce arbitrary D-dimensional MPS with D equal to the number of involved atomic levels. Second, we may have a $2D$-level atom (D $|a_i\rangle$ levels and D $|b_i\rangle$ levels) and two kind of operations: (i) fast arbitrary operations which allow us to manipulate at will all atomic levels; (ii) an operation which maps each $|a_i\rangle$ state to its corresponding $|b_i\rangle$ state while creating a single cavity photon, allowing a tailored output. Here, we will also be able to produce arbitrary D-dimensional MPS (see section 4.2.2).

4.3.1 Arbitrary atom-cavity operations

In this section we will suggest how to implement an arbitrary operation on the atom-cavity system based on present cavity QED experiments [28–30]. We consider a three-level atom coupled to a single cavity mode in the strong-coupling regime. An external laser field drives the transition from level $|a\rangle$ to the excited level $|e\rangle$ with coupling strength Ω, and the cavity mode a drives the transition between $|e\rangle$ and level $|b\rangle$ with coupling strength g, in a typical Λ configuration (see Fig. 4.6(a)). We choose the detuning Δ, with

$$|\Delta| \gg g, \Omega, \tag{4.18}$$

and assume that the cavity decay rate κ is smaller than any other frequency in the problem, so that we can ignore cavity damping during the atom-cavity manipulations.

In an appropriate interaction picture, the Hamiltonian of the system is

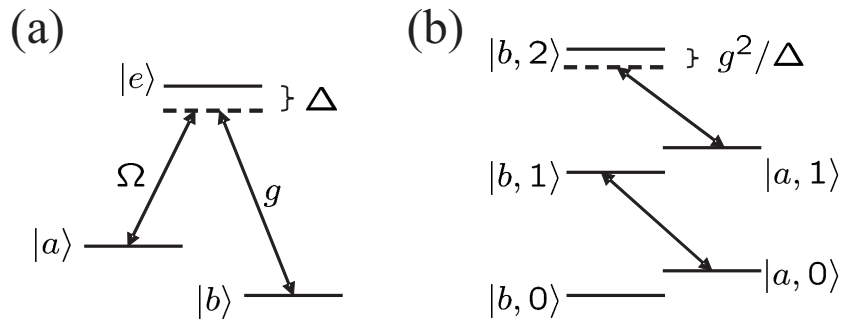

Figure 4.6: (a) Atomic level structure: levels $|a\rangle$ ($|b\rangle$) and $|e\rangle$ are coupled by a laser (cavity mode) off resonance. (b) After adiabatic elimination of the upper state $|e\rangle$, we are left with a Jaynes-Cummings type of Hamiltonian, where states $|a,n\rangle$ and $|b,n+1\rangle$ are coupled. Both, the energy difference of those levels and the corresponding Rabi frequency depends on n. The reason for the first is the ac-Stark shift, whereas the second is due to the Jaynes-Cummings coupling.

then given by

$$H = -\Delta\left(\sigma_{aa} + a^\dagger a\right) + g\big(\sigma_{eb}a + a^\dagger\sigma_{be}\big) + \frac{\Omega}{2}\big(\sigma_{ea} + \sigma_{ae}\big), \tag{4.19}$$

with $\sigma_{kl} = |k\rangle\langle l|$ and $\{k,l\} = \{a,b,e\}$.Using condition (4.18) and that level $|e\rangle$ is initially not populated, we can adiabatically eliminate it. A detailed derivation is given in section 5.1 for the case of N atoms. The Hamiltonian for the effective $D = 2$ atomic system plus cavity mode, in an interaction picture with respect to $-\Delta(\sigma_{aa} + a^\dagger a)$, is then

$$H_{\rm ad} = \frac{\Omega^2}{4\Delta}\,\sigma_{aa} + \frac{g^2}{\Delta}\,a^\dagger a\,\sigma_{bb} + \frac{g\Omega}{2\Delta}\big(\sigma_{ab}a + a^\dagger\sigma_{ba}\big). \tag{4.20}$$

It describes an effective Jaynes-Cummings coupling between the cavity mode and the atomic $|a\rangle \to |b\rangle$ transition with Rabi frequency $g\Omega/2\Delta$. The other terms correspond to ac-Stark shifts (see Fig. 4.6(b)).

We will show how, by controlling the laser frequency and intensity, it is possible to generate arbitrary 2-dimensional MPS. Note that, by allowing the manipulation of D effective atomic levels, it is straightforward to extend these results to the generation of D-dimensional MPS. According to the results presented in section 4.2.1, we just have to show that we can implement any isometry $V : \mathcal{H}_\mathcal{A} \to \mathcal{H}_\mathcal{A} \otimes \mathcal{H}_\mathcal{B}$. In fact, we will show how it is possible to implement arbitrary operations on the atomic qubit and the $\sqrt{SWAP}$ operation on the atom-cavity system, which suffice to generate any isometry

V (since they give rise to a universal set of gates for the two qubit system [5]). The atomic qubit can be manipulated at will using a Raman laser system, as it is normally done with trapped ions [99, 100].

In order to implement the $\sqrt{SWAP}$, we notice that the Hamiltonian (4.20) is block separable in the sub-spaces spanned by $\{|a,n\rangle, |b,n+1\rangle\}$. The energy shift due to the ac-Stark shifts for $n = 0$, δ^0_{ab}, may be compensated by the laser frequency or some external action on the atom (dc-Stark shift). The detunings for the other subspaces are then given by

$$\delta_n = \delta^n_{ab} - \delta^0_{ab} = \frac{ng^2}{\Delta}. \tag{4.21}$$

By choosing the Rabi frequency of the laser small enough, one can ensure that $\delta_n \gg g\Omega/2\Delta$. Then the effective interaction in the remaining subspaces is dispersive and a laser pulse of appropriate duration will implement the unitary operation

$$U = \exp\big[-i\big(|a,0\rangle\langle b,1| + |b,1\rangle\langle a,0|\big)\pi/4\big], \tag{4.22}$$

which corresponds to the desired $\sqrt{SWAP}$ operation. This so-called selective interaction has been employed in a recent experiment [100] and was originally proposed in [101].

In order to generalize this scheme to an arbitrary D-level system, we notice that we can view the atom as a set of M qubits (with $D \leq 2^M$). Thus, if we are able to perform arbitrary atomic operations, together with the $\sqrt{SWAP}$ operation on two specific atomic levels as explained above, we can then implement a universal set of gates and, in consequence, any arbitrary isometry. These operations have to be performed fast compared to the cavity decay time. The temporal profile of the single-photon pulse is then determined by the cavity decay rate.

4.3.2 1-standard map with one additional level

In the following we introduce another method which is closely related to current experiments [28–30] and optimizes our second method for MPS generation (see section 4.2.2).

We consider an atom with three effective levels $\{|a\rangle, |b_1\rangle, |b_2\rangle\}$ trapped inside an optical cavity. With the help of a laser beam, state $|a\rangle$ is mapped to the internal state $|b_1\rangle$, and a photon is generated, whereas the other states remain unchanged. This physical process is described by the map

$$\begin{aligned} M_{\mathcal{AB}}: \ |a\rangle &\mapsto |b_1\rangle \otimes |1\rangle_{\mathcal{B}}\,, \\ |b_1\rangle &\mapsto |b_1\rangle \otimes |0\rangle_{\mathcal{B}}\,, \\ |b_2\rangle &\mapsto |b_2\rangle \otimes |0\rangle_{\mathcal{B}}\,, \end{aligned} \tag{4.23}$$

and can be realized with the techniques used in [28–30]. After the application of this process, an arbitrary operation is applied to the atom, which can be performed by using Raman lasers. The photonic states that are generated after several applications are those MPS where the isometries are given by $V_{[i]} = M_{\mathcal{AB}} U_{\mathcal{A}}^{[i]}$, with $i = 1, \ldots, n$, $U_{\mathcal{A}}^{[i]}$ being arbitrary unitary atomic operators.

One might implement $M_{\mathcal{AB}}$ as a particular case of the Raman scheme presented in the preceding section. Since here we are only interested in a complete transfer of the population from $|a,0\rangle \otimes |0\rangle_{\mathcal{B}}$ to $|b,0\rangle \otimes |1\rangle_{\mathcal{B}}$, it is preferable to operate the system in the bad-cavity regime. Then the temporal profile of the outgoing pulse is controlled by the Rabi frequency Ω of the laser.

Another possibility is to couple the levels $|a\rangle$ and $|b_1\rangle$ via an adiabatic passage. Schemes based on adiabatic passage (see for instance [28, 29]) are usually more insensitive to certain parameter changes as the corresponding Raman schemes. In this section we will therefore focus on this method to implement $M_{\mathcal{AB}}$ and discuss under which circumstances the pulse generation is deterministic. In particular we will estimate the losses due to non-adiabatic contributions in a realistic scenario (with the parameters from [28]). Furthermore we will give a recipe for the sequential generation of W, GHZ, and cluster states within this set-up. Finally we employ the concept of MPDO to take into account a reduced efficiency of the single-photon source and calculate, as an example, the fidelity of the cluster state.

Adiabatic passage

It is convenient to explain the basic idea of the adiabatic passage scheme assuming that the coupling of the cavity mode and the atom to the environment are negligible on the time-scale of the relevant system dynamics.

The Hamiltonian of the system is then given by H from Eq. 4.19 with $\Delta = 0$ and $|b_1\rangle \equiv |b\rangle$. We obtain

$$H' = \frac{\Omega}{2}\big(\sigma_{ea} + \sigma_{ae}\big) + g\big(\sigma_{eb_1} a + a^\dagger \sigma_{b_1 e}\big). \tag{4.24}$$

A laser drives the transition between level $|a\rangle$ and $|e\rangle$ resonantly with Rabi frequency Ω and g is the coupling strength between the cavity mode a and the resonant atomic transition between level $|b_1\rangle$ and $|e\rangle$. In the basis $\{|a,0\rangle, |b_1,1\rangle, |e,0\rangle\}$ the Hamiltonian has the eigenstates

$$\begin{aligned} |D\rangle &= \cos\theta |a,0\rangle - \sin\theta |b,1\rangle, \\ |\xi_\pm\rangle &= \frac{1}{\sqrt{2}}\big(|B\rangle \pm |e,0\rangle\big), \end{aligned} \tag{4.25}$$

where $|D\rangle$ is the so-called dark state with zero eigenvalue,

$$|B\rangle = \sin\theta|a,0\rangle + \cos\theta|b,1\rangle \tag{4.26}$$

is the bright state and the mixing angle is given by $\tan\theta = \Omega/2g$. Initially we have $\Omega(0) = 0$ and the atom prepared in the dark state $|D(0)\rangle = |a,0\rangle$. Then we increase Ω within a time T until $\Omega(T) \gg g$. If the adiabatic following condition (B.9)

$$|\langle\xi_\pm|H|\xi_\pm\rangle - \langle D|H|D\rangle| \gg |\langle\xi_\pm|\dot{D}\rangle|, \tag{4.27}$$

which is derived in appendix B, is fulfilled, the system will remain in the dark state and end up in $|D(\theta = \pi/2)\rangle = |b_1,1\rangle$ without exciting level $|e,0\rangle$. If we increase θ linearly we obtain for right-hand side of (4.27)

$$|\langle\xi_\pm|\dot{D}\rangle| = |\dot{\theta}|/\sqrt{2} = \frac{\pi}{2\sqrt{2}\,T}. \tag{4.28}$$

The frequency gap between the dark state and the other eigenstates is given by

$$|\langle\xi_\pm|H|\xi_\pm\rangle - \langle D|H|D\rangle| = \sqrt{|g|^2 + |\Omega|^2/4} = \delta. \tag{4.29}$$

With (4.28) and (4.29), the adiabatic following condition can then be written as

$$T \gg \frac{\pi}{2\sqrt{2}\,\delta} \tag{4.30}$$

and the probability for non-adiabatic contributions, i.e. the probability to populate the other eigenstates of the system, is given by

$$P_\pm = \frac{\pi^2}{2\delta^2 T^2}. \tag{4.31}$$

Since the frequency gap δ depends on the coupling strength g between the cavity mode and the atom, a significant change of g caused by the motion of the atom might spoil the adiabatic condition. By a sufficiently long operation time T however, we can guarantee that the adiabatic condition is fulfilled.

During the adiabatic passage we neglected the coupling of the cavity mode to the free radiation field. This only justified for $T \ll 1/\kappa$, where κ is the cavity decay rate. After the preparation of $|b_1,1\rangle$ the cavity mode decays and a single-photon pulse builds up in the output-field. In order to fulfill the adiabatic condition (4.30) and to modulate the temporal profile of the outgoing pulse, it is favorable to operate the system in the limit $T \geq 1/\kappa$. Then one has to include the coupling of the cavity mode to the environment from the beginning.

Single-photon pulse generation

In the following we demonstrate how an adiabatic passage between $|a\rangle$ and $|b_1\rangle$, induced by an external laser field and the cavity mode, leads to a single-photon pulse in the output-field of the cavity. Similar methods have been employed in [102, 103].

Fig. 4.7 (a) illustrates the atomic level scheme. We introduce the spontaneous decay rates γ_a and γ_b for the transition from the excited state $|e\rangle$ to the ground states $|a\rangle$ and $|b_1\rangle$ respectively. In Fig. 4.7 (b) the experimental set-up is sketched. The laser drives the atom directly, as a consequence a single-photon pulse builds up in the output-field of the cavity and the atomic decay to levels $|a\rangle$ and $|b_1\rangle$ leads to an excitation of the environment modes $|1\rangle_{\mathcal{E}}$ and $|2\rangle_{\mathcal{E}}$. Here, we are not interested in these modes and describe the

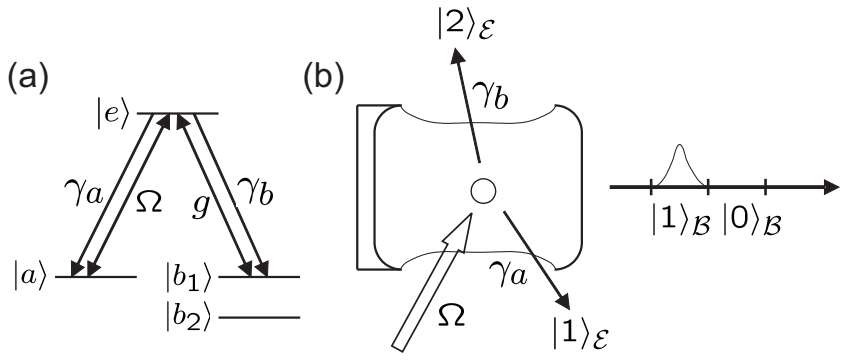

Figure 4.7: (a) Atomic level structure: levels $|a\rangle$ ($|b_1\rangle$) and $|e\rangle$ are driven by a laser with Rabi frequency Ω (cavity mode with coupling strength g) on resonance and couple to the environment. The latter leads to spontaneous emission with decay rate γ_a (γ_b). The ground state $|b_2\rangle$ is not affected. (b) Experimental set-up: An external laser field excites the atom. The cavity mode decays through the right lossy mirror and a single-photon pulse $|1\rangle_{\mathcal{B}}$ builds up in the corresponding time-bin. Spontaneous decay of the atom to level $|a\rangle$ ($|b_1\rangle$) leads to an excitation in the environmental modes $|1\rangle_{\mathcal{E}}$ ($|2\rangle_{\mathcal{E}}$).

evolution of the system by the master equation

$$\frac{d\rho}{dt} = -i\big(H_{\text{eff}}\rho - \rho H_{\text{eff}}^{\dagger}\big) + 2\gamma_a\,\sigma_{ae}\,\rho\,\sigma_{ea} + 2\gamma_b\,\sigma_{b_1e}\,\rho\,\sigma_{eb_1}. \tag{4.32}$$

with the non-Hermitian Hamiltonian H_{eff}. In the rotating-wave approxima-

tion and an appropriate rotating frame it is given by

$$\begin{aligned} H_{\text{eff}} &= \frac{\Omega}{2}\left(\sigma_{ea}+\sigma_{ae}\right)+g\left(\sigma_{eb_1}a+a^\dagger\sigma_{b_1e}\right)-i\gamma\,\sigma_{ee} \\ &\quad + i\sqrt{\frac{\kappa}{2\pi}}\int_{-\omega_b}^{\omega_b}d\omega\left(a^\dagger r(\omega)-ar^\dagger(\omega)\right)+\int_{-\omega_b}^{\omega_b}d\omega\omega r^\dagger(\omega)r(\omega), \end{aligned} \tag{4.33}$$

where the term proportional to $\gamma=\gamma_a+\gamma_b$ accounts for the damping of the excited atomic state $|e\rangle$ due to spontaneous decay. For the free space modes $r(\omega)$ we consider only frequencies within a finite bandwidth ω_b around the cavity resonance frequency ω_c, where the coupling between $r(\omega)$ and the cavity mode a is approximately constant (first Markov approximation). The coupling term is then given by Eq. (2.93) using the condition (2.96). The bandwidth satisfies the condition $\omega_c \gg \omega_b \gg \kappa$.

In the quantum-jump approach (see chapter 2.2) the time-evolution of the wave-function of the system is described by the Schrödinger equation

$$\frac{d|\Psi\rangle}{dt}=-iH_{\text{eff}}|\Psi\rangle \tag{4.34}$$

and subject to quantum jumps at random times. We expand the state of the system into

$$|\Psi(t)\rangle=\left(c_d(t)|D\rangle+c_b(t)|B\rangle+c_e(t)|e,0\rangle\right)\otimes|\text{vac}\rangle+|b_1,0\rangle\otimes|\phi_1(t)\rangle, \tag{4.35}$$

where $|\text{vac}\rangle$ denotes the vacuum state of the free-space modes $r(\omega)$ and

$$|\phi_1(t)\rangle=\int_{-\omega_b}^{\omega_b}d\omega\,c_\omega(t)r^\dagger(\omega)|\text{vac}\rangle \tag{4.36}$$

represents the state of the single-photon output pulse. Substituting (4.35) into the Schrödinger equation (4.34) leads to a system of differential equations for the time-dependent coefficients given by

$$\begin{aligned} \frac{dc_d}{dt} &= -\dot\theta c_b-\sqrt{\frac{\kappa}{2\pi}}\sin\theta\int_{-\omega_b}^{\omega_b}d\omega\,c_\omega \\ \frac{dc_b}{dt} &= \dot\theta c_d+\sqrt{\frac{\kappa}{2\pi}}\cos\theta\int_{-\omega_b}^{\omega_b}d\omega\,c_\omega-i\delta c_e \\ \frac{dc_e}{dt} &= -\gamma c_e-i\delta c_b \\ \frac{dc_\omega}{dt} &= -i\omega c_\omega+\sqrt{\frac{\kappa}{2\pi}}\left(\sin\theta c_d-\cos\theta c_b\right). \end{aligned} \tag{4.37}$$

The coupling between the dark state $|D\rangle$ and the bright state $|B\rangle$ due to a non-adiabatic change of the mixing angle θ is described by the terms proportional to $\dot{\theta}$. Furthermore we have the coupling between the $|b_1, 1\rangle$-contributions of $|D\rangle$ and $|B\rangle$ to the modes of the free radiation field which is proportional to $\sqrt{\kappa/2\pi}\sin\theta$ and $\sqrt{\kappa/2\pi}\cos\theta$ respectively. The excited state $|e, 0\rangle$ couples to $|B\rangle$ with $i\delta$ and decays with a rate γ.

Initially the system is prepared in $|\Psi(0)\rangle = |a, 0\rangle \otimes |\text{vac}\rangle$ and $\Omega(0) = 0$, i.e. $c_b(0) = c_e(0) = c_\omega(0) = 0$ and $c_d(0) = 1$. Here $|D\rangle$ is not eigenstate of the system and in fact it is the aim of the procedure to populate modes of the environment. In the following we will show how this is achieved by slowly increasing $\Omega(t)$ and under which conditions the states $|B\rangle$ and $|e, 0\rangle$ can be adiabatically eliminated. Then losses due to spontaneous atomic decay are suppressed and the excitation is completely transferred to the outgoing pulse. For $T \gg 1/\gamma$ we can set $\dot{c}_e \approx 0$ and obtain for the population of the bright state

$$\frac{dc_b}{dt} = -\frac{\delta^2}{\gamma}\, c_b + \dot{\theta} c_d + \sqrt{\frac{\kappa}{2\pi}}\cos\theta \int_{-\omega_b}^{\omega_b} d\omega\, c_\omega. \tag{4.38}$$

The decay of $|B\rangle$ via the excited state $|e, 0\rangle$ with an effective decay rate δ^2/γ is the reason for the choice of the name "bright" state. Substituting the straight-forward solution

$$c_\omega(t) = \sqrt{\frac{\kappa}{2\pi}} \int_0^t e^{-i\omega(t-\tau)} \big(2\sin\theta(\tau) c_d(\tau) - \cos\theta(\tau) c_b(\tau)\big) d\tau \tag{4.39}$$

for the amplitudes of the environment modes into Eq. (4.38) leads to

$$\begin{aligned} \frac{dc_b}{dt} &= \frac{\kappa\cos\theta}{2\pi} \int_0^t \frac{\sin[\omega_b(t-\tau)]}{t-\tau} \big(\sin\theta(\tau) c_d(\tau) - \cos\theta(\tau) c_b(\tau)\big) d\tau \\ &\quad + \dot{\theta} c_d - \frac{\delta^2 c_b}{\gamma} \\ &\approx \Big(\dot{\theta} + \frac{\kappa\sin 2\theta}{4}\Big) c_d - \Big(\frac{\delta^2}{\gamma} + \frac{\kappa\cos^2\theta}{2}\Big) c_b. \end{aligned} \tag{4.40}$$

In the second line we used the approximations

$$\begin{aligned} c_d(t) &\approx c_d\,(t + 1/\omega_b)\,, \\ c_b(t) &\approx c_b\,(t + 1/\omega_b)\,, \\ \Theta(t) &\approx \Theta\,(t + 1/\omega_b)\,. \end{aligned} \tag{4.41}$$

They are well justified since the system evolves significantly only on the time-scale of the operation time $T \gg 1/\omega_b$. If the bright state decays much faster

than it is populated from the dark state, that is

$$\frac{\delta^2}{\gamma} + \frac{\kappa \cos^2\theta}{2} \gg \dot{\theta} + \frac{\kappa \sin 2\theta}{4}, \tag{4.42}$$

we can adiabatically eliminate it ($c_b \approx 0$). From Eq. (4.29) and $\cos^2\theta \geq 0$ we have g^2/γ as a lower bound for the left-hand side of Eq. (4.42) and with $1 \geq \sin 2\theta$ we obtain the condition

$$\frac{g^2}{\gamma} \gg \dot{\theta} + \frac{\kappa}{4} = \frac{\pi}{2T} + \frac{\kappa}{4}, \tag{4.43}$$

where we assumed again that θ increases linearly from 0 to $\pi/2$. In contrast to the adiabatic following condition (4.30) derived for the simple three-level case considered in the previous section, this condition implies that spontaneous atomic emission can not be suppressed only by increasing the operation time T since at the same time the strong-coupling condition $g^2 \gg \gamma\kappa$ has to be fulfilled, i.e. also the transfer of population to the environment modes should happen slowly. With $c_b \approx 0$ we obtain for the amplitude of the dark state

$$\frac{dc_d}{dt} = -\sqrt{\frac{\kappa}{2\pi}} \sin\theta \int_{-\omega_b}^{\omega_b} d\omega \, c_\omega. \tag{4.44}$$

Substituting the solution for c_ω (4.39) into Eq. (4.44) we end up with

$$\begin{aligned} \frac{dc_d}{dt} &= -\sqrt{\frac{\kappa}{2\pi}} \sin\theta \int_0^t \frac{\sin(\omega_b(t-\tau))}{t-\tau} \, c_d(\tau) \sin\theta(\tau) d\tau \\ &\approx -\frac{\kappa}{2} \, c_d \sin^2\theta. \end{aligned} \tag{4.45}$$

In the second line we used again the conditions from Eq. (4.41). The decay rate of the dark state is proportional to the probability $|\langle b_1, 1|D\rangle|^2 = \sin^2\theta$ for the $|b_1, 1\rangle$ component in the dark state, which couples to the environment. The solution of Eq. (4.45) is given by

$$c_d(t) = \exp\left(-\frac{\kappa}{2} \int_0^t d\tau \sin^2\theta(\tau)\right). \tag{4.46}$$

The temporal profile $\varphi(t)$ of the single-photon pulse $|\phi_1\rangle$ is provided by the Fourier transformation [104]

$$\varphi(t) = \frac{1}{2\pi} \int_{-\omega_b}^{\omega_b} c_\omega(T) e^{-i\omega(t-T)} d\omega. \tag{4.47}$$

Substituting c_ω from (4.39) with $c_b \approx 0$ and c_d from (4.46) we obtain

$$\varphi(t) = \frac{\sqrt{\kappa}}{2} \sin\theta \exp\left(-\frac{\kappa}{2}\int_0^t d\tau \sin^2\theta(\tau)\right). \tag{4.48}$$

The pulse shape is determined by $\theta(t)$ which in turn is completely controlled by the Rabi frequency $\Omega(t)$ of the external laser field given that the coupling strength g between the atom and the cavity mode is known and constant. To guarantee this one has to control the position of the atom in the cavity. Since g is proportional to $\sin(k_c x)$, where the wave-vector k_c corresponds to the optical frequency ω_c of the standing-wave cavity field, it is very sensitive to a variation of the position x of the atom with respect to the cavity-axis. A possibility to overcome these problems is to ensure that the driving pulse and the cavity mode have the same spatial mode structure. This can be accomplished by driving the atom through the cavity mode [102]. Then $\theta(t)$ becomes independent of the random position of the atom and the passage can be controlled by $\Omega(t)$.

If g is not known or changes significantly within the operation time T this reduces not only the controllability of the pulse-shape but also the efficiency of the source. In particular if the atom is close to a node of the cavity field, condition (4.42) may not be satisfied and therefore losses due to atomic spontaneous emissions occur.

Efficiency of the source

For the simple three-level system considered above the adiabatic following condition (4.27) can always be fulfilled by choosing a sufficiently long operation time T. This argument based on level spacing is spoiled by the coupling of the system to the continuum of reservoir modes in the more realistic scenario with $T \geq 1/\kappa$. Here, the condition for the adiabatic elimination of the excited state and the bright state (4.42) also requires the strong coupling regime ($g^2 \gg \gamma\kappa$). If the system is not operated in the adiabatic limit, where $c_e(t) \approx c_b(t) \approx 0$, the population of the excited state $|e,0\rangle$ causes losses.

In the quantum-jump model the probability for a spontaneous emission of the atom in a time-interval $[0,t]$ is given by

$$P_{\text{spont}}(t) = 1 - |c_e(t)|^2 - |c_b(t)|^2 - |c_d(t)|^2 - \int_{-\omega_b}^{\omega_b} |c_\omega(t)|^2 d\omega. \tag{4.49}$$

From (4.37) and (4.40) we obtain with $\dot{c}_e \approx \dot{c}_b \approx 0$ ($T \gg 1/\gamma$) for the

coefficients of the bright state and the excited state

$$\begin{aligned} c_b(t) &\approx A(t)\, c_d(t) \\ c_e(t) &\approx -\frac{i\delta}{\gamma}\, A(t)\, c_d(t) \end{aligned} \tag{4.50}$$

with

$$A(t) = \frac{\dot{\Theta}(t) + \frac{\kappa}{2}\sin\Theta(t)\cos\Theta(t)}{\frac{\delta(t)^2}{\gamma} + \frac{\kappa}{2}\cos^2\Theta(t)}. \tag{4.51}$$

Since here the contribution proportional to c_b in the solution for c_ω (4.39) does not vanish, the differential equation for the dark state amplitude c_d is now given by

$$\frac{dc_d}{dt} = -\frac{\kappa}{2}\sin^2\Theta c_d - \big(\dot{\Theta} - \frac{\kappa}{2}\sin\Theta\cos\Theta\big)c_b, \tag{4.52}$$

where we used again approximations (4.41). Substitution of c_b from Eq. (4.50) leads to

$$\frac{dc_d(t)}{dt} = -R(t)c_d(t), \tag{4.53}$$

with the decay rate

$$R(t) = \frac{\dot{\Theta}(t)^2 + \frac{\kappa\delta(t)^2}{\gamma}\sin^2\Theta(t)}{\frac{\delta(t)^2}{\gamma} + \frac{\kappa}{2}\cos^2\Theta(t)}. \tag{4.54}$$

For the environment modes we obtain with (4.41)

$$\int_{-\omega_b}^{\omega_b} |c_\omega(t)|^2 d\omega = \kappa \int_0^t dt' \big(\sin\Theta(t') - A(t')\cos\Theta(t')\big)^2 |c_d(t)|^2. \tag{4.55}$$

Substituting the results from (4.50) and (4.55) into (4.49) we find

$$\begin{aligned} P_{\text{spont}}(t) &= 1 - \left(1 + A(t)^2 + \frac{\delta(t)^2 A(t)^2}{\gamma^2}\right)|c_d(t)|^2 \\ &\quad - \kappa \int_0^t dt' \big(\sin\Theta(t') - A(t')\cos\Theta(t')\big)|c_d(t')|^2 \end{aligned} \tag{4.56}$$

for the probability of a spontaneous atomic emission. The probability to find the system in the dark state is given by

$$|c_d(t)|^2 = \exp\left(-2\int_0^t R(t')dt'\right). \tag{4.57}$$

The first implementation of a cavity QED single photon source was reported in [28]. In this experiment cold Rubidium 85 atoms were dropped from a magneto-optical trap (MOT) and fall through the cavity. The atom flux is controlled by the loading time of the trap and one can ensure that there is at most one atom in the cavity at the same time. The scheme used for the single photon pulse generation is basically equivalent to the method described above. The states $|a\rangle$ and $|b_1\rangle$ correspond to the $F = 3$ and $F = 2$ hyperfine state of the $5S_{1/2}$ ground state of Rubidium 85. The excited state $|e\rangle$ corresponds to $5P_{3/2}(F = 3)$. The spontaneous emission rate is given by $\gamma \approx 3.0 \times 2\pi\,\mathrm{MHz}$ and the cavity decays with a rate $\kappa \approx 1.25 \times 2\pi\,\mathrm{MHz}$. The initial velocity of the atom is negligible compared to the internal dynamics of the system. On the other hand the axial position x of the atom is not controlled. For the estimation of the losses we consider therefore an average coupling strength $g \approx 2.5 \times 2\pi\,\mathrm{MHz}$. For the adiabatic passage the Rabi frequency of the laser is increased linearly from $\Omega(0) = 0$ to $\Omega(T) = 8.0 \times 2\pi\,\mathrm{MHz}$ within an operation time $T = 15.7/\kappa$. Since a non-zero time-derivative of the function $\Omega(t)$ at $t = 0$ is unphysical we approximate it by

$$\Omega(t) = \sin^2\left(\frac{\pi t}{2T}\right) 8.0 \times 2\pi\,\mathrm{MHz}, \tag{4.58}$$

as depicted in Fig. 4.8 (b). In Fig. 4.8 (a) we plot $P_{\mathrm{spont}}(t)$ (4.56). We observe an increasing probability for a spontaneous emission only in the middle section, where the excited state $|e, 0\rangle$ is populated. The probability for a failure of the source, i.e. a spontaneous atomic emission in the time-interval $[0, T]$, is given by $P_{\mathrm{spont}}(T) = 0.28$.

The control over the position of the atom is considerably improved by employing an additional far off-resonant laser beam as a dipole trap for the atom. In [29] this technique has been applied to built a single-photon source. The parameters of the experiment are given by $\gamma \approx 2.6 \times 2\pi\,\mathrm{MHz}$, $\kappa \approx 4.2 \times 2\pi\,\mathrm{MHz}$, $g \approx 16 \times 2\pi\,\mathrm{MHz}$ and $T = 26.4/\kappa$. For the probability of a spontaneous emission we obtain $P_{\mathrm{spont}}(T) = 0.01$. Note that passive cavity losses reduce the efficiency of the source in this case, while for the previous example [28] the losses are dominated by $P_{\mathrm{spont}}(T)$.

In [30] an ion trap is used to hold a single atom inside the cavity. This approach provides an excellent control over the atom-cavity coupling and as a consequence a precisely defined pulse-shape. On the other hand the ion trap requires a relatively big distance between the cavity mirrors and therefore enhances passive cavity losses, which are the main reason for a single-photon efficiency of 0.08. Unless this problem can be solved, for instance by shrinking the whole apparatus, the set-up is unsuitable for the reliable generation of time-bin qubits.

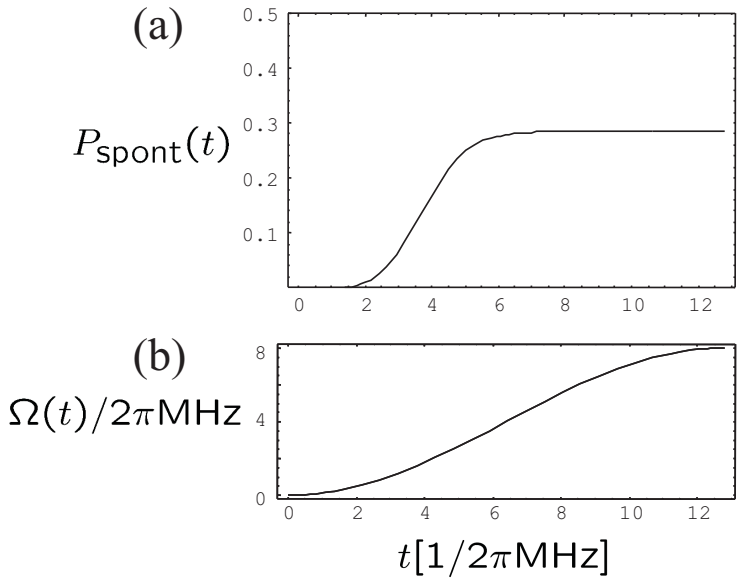

Figure 4.8: In (a) we plot the probability for a spontaneous emission $P_{\mathrm{spont}}(t)$. Figure (b) shows the Rabi frequency $\Omega(t)$ of the laser for the same time-interval $[0, T]$.

A possibility to circumvent the problems caused by a low single-photon efficiency is to use polarization states of the emitted photons as qubits [47,48].

Examples

Let us now provide some simple recipes for the generation of W, GHZ and cluster states by employing the map $M_{\mathcal{AB}}$ (4.23) and arbitrary unitary atomic operators $U_{\mathcal{A}}^{[i]}$. The resulting photonic states are then given by (4.10) with $V_{[i]} = M_{\mathcal{AB}} U_{\mathcal{A}}^{[i]}$. Note, that the states considered here belong to the class of MPS with 2-dimensional bonds. In section 4.2.2 we showed that for their generation we need a 2-standard map. It turns out that the second excited level is not necessary, i.e. a 1-standard map with one additional level is sufficient.

To generate a W-type state of the form

$$\begin{aligned} |\psi_W\rangle \;=\; & e^{i\Phi_1}\sin\Theta_1|0...01\rangle + \cos\Theta_1 e^{i\Phi_2}\sin\Theta_2|0...010\rangle \\ & +... + \cos\Theta_1...\cos\Theta_{n-2}e^{i\Phi_{n-1}}\sin\Theta_{n-1}|010...0\rangle \\ & + \cos\Theta_1...\cos\Theta_{n-1}|10...0\rangle, \end{aligned} \tag{4.59}$$

we choose the initial atomic state $|\varphi_I\rangle = |b_2\rangle$ and operations

$$U_{\mathcal{A}}^{[i]} = U_{ab_2}^{b_1}(\Phi_i, \Theta_i) \; , \tag{4.60}$$

with $i = 1, \ldots, n-1$, where

$$\begin{aligned} U_{kl}^{m}(\Phi_i, \Theta_i) = \; & \cos\Theta_i |k\rangle\langle k| + \cos\Theta_i |l\rangle\langle l| + e^{i\Phi_i} \sin\Theta_i |k\rangle\langle l| \\ & -e^{-i\Phi_i} \sin\Theta_i |l\rangle\langle k| + |m\rangle\langle m| \end{aligned} \tag{4.61}$$

and $\{k, l, m\} = \{a, b_1, b_2\}$. To decouple the atom from the photon state, we choose the last atomic operation as

$$U_{\mathcal{A}}^{[n]} = U_{ab_2}^{b_1}(0, \pi/2) \tag{4.62}$$

and, after the last map $M_{\mathcal{AB}}$, the decoupled atom will be in state $|b_1\rangle$.

To produce a GHZ-type state in a similar way, we choose $|\varphi_I\rangle = |a\rangle$,

$$\begin{aligned} U_{\mathcal{A}}^{[1]} &= U_{ab_2}^{b_1}(\Phi_1, \Theta_1), \\ U_{\mathcal{A}}^{[i]} &= U_{ab_1}^{b_2}(0, \pi/2), \end{aligned} \tag{4.63}$$

with $i = 2, \ldots, n-1$, and finally

$$U_{\mathcal{A}}^{[n]} = U_{b_1 b_2}^{a}(0, \pi/2) U_{ab_1}^{b_2}(0, \pi/2). \tag{4.64}$$

We end up with

$$|\psi_{GHZ}\rangle = \cos\Theta_1 |0...0\rangle + e^{i\Phi_1} \sin\Theta_1 |1...1\rangle. \tag{4.65}$$

For generating cluster states, we choose $|\varphi_I\rangle = |b_2\rangle$ and

$$U_{\mathcal{A}}^{[i]} = U_{ab_2}^{b_1}(\Phi_i, \Theta_i) U_{ab_1}^{b_2}(0, \pi/2) \; , \tag{4.66}$$

with $i = 1, \ldots, n-1$, and for the final step

$$U_{\mathcal{A}}^{[n]} = U_{ab_1}^{b_2}(\Phi_n, \Theta_n) U_{b_1 b_2}^{a}(0, \pi/2) U_{ab_1}^{b_2}(0, \pi/2) \; . \tag{4.67}$$

We obtain

$$|\psi\rangle = \bigotimes_{i=1}^{n} \left(O_{i-1}^{0} |0\rangle_i + O_{i-1}^{1} |1\rangle_i \right) , \tag{4.68}$$

where

$$\begin{aligned} O_{i-1}^{0} &= \cos\Theta_i |0\rangle_{i-1}\langle 0| - e^{-i\Phi_i} \sin\Theta_i |1\rangle_{i-1}\langle 1| \; , \\ O_{i-1}^{1} &= e^{i\Phi_i} \sin\Theta_i |0\rangle_{i-1}\langle 0| + \cos\Theta_i |1\rangle_{i-1}\langle 1| \; , \end{aligned} \tag{4.69}$$

with $i = 2, \ldots, n-1$. Operators O_{i-1}^{0} and O_{i-1}^{1} act on the nearest neighbor-qubit $i-1$ under the assumption $O_0^0 \equiv \cos\Theta_1$ and $O_0^1 \equiv e^{i\Phi_1} \sin\Theta_1$. If one chooses $\Phi_i = 0$ and $\Theta_i = \pi/4$ this leads to the cluster states defined by

$$|\psi_{\rm cl}\rangle = \frac{1}{2^{n/2}} \bigotimes_{i=1}^{n} \left(\sigma_{i-1}^{z} |0\rangle_i + |1\rangle_i \right) \; , \tag{4.70}$$

with $\sigma_0^z \equiv 1$.

Fidelity of the cluster state

In the following we take into account the reduced efficiency of the map $M_{\mathcal{AB}}$ due to non-adiabatic contributions. They cause a population of the excited state $|e\rangle$ and therefore spontaneous atomic emissions with decay rates γ_a and γ_b to levels $|a\rangle$ and $|b_1\rangle$. If there was an emission into the free radiation field, the corresponding time-bin qubit remains empty and counts as $|0\rangle$. We investigate the effect of this "misinterpreted" events on the resulting multi-qubit state.

Until now we described the losses by damping terms in an effective Hamiltonian (4.33). The time-evolution of the system is then described by the master equation (4.32) and leads in general to a mixed state. Here, we include the two modes $|1\rangle_{\mathcal{E}}$ and $|2\rangle_{\mathcal{E}}$ of the free radiation field, which are populated by a spontaneous emission (see Fig. 4.7), in an extended map $M_{\mathcal{A}(\mathcal{BE})}$. This has the advantage that the sequentially generated multi-qubit state can be written as an MPS.

We disregard the environment at the input and introduce $M_{\mathcal{A}(\mathcal{BE})} : \mathcal{H}_{\mathcal{A}} \to \mathcal{H}_{\mathcal{A}} \otimes \mathcal{H}_{\mathcal{B}} \otimes \mathcal{H}_{\mathcal{E}}$, where $\mathcal{H}_{\mathcal{E}} \simeq \mathbb{C}^3$ is the three-dimensional Hilbert space of the environment with three orthogonal states $|1\rangle_{\mathcal{E}}$, $|2\rangle_{\mathcal{E}}$ and the vacuum $|0\rangle_{\mathcal{E}}$. It is defined as

$$\begin{aligned} M_{\mathcal{A}(\mathcal{BE})} : \ |a\rangle &\mapsto \sqrt{1-p_a-p_b}\,|b_1,1\rangle \otimes |0\rangle_{\mathcal{E}} \\ &\quad + \sqrt{p_a}\,|a,0\rangle \otimes |1\rangle_{\mathcal{E}} + \sqrt{p_b}\,|b_1,0\rangle \otimes |2\rangle_{\mathcal{E}}, \\ |b_1\rangle &\mapsto |b_1,0\rangle \otimes |0\rangle_{\mathcal{E}}, \\ |b_2\rangle &\mapsto |b_2,0\rangle \otimes |0\rangle_{\mathcal{E}}, \end{aligned} \tag{4.71}$$

where p_a (p_b) is the probability for a spontaneous decay of the atom to level $|a\rangle$ ($|b_1\rangle$) during one passage. They are given by

$$\begin{aligned} p_a &= \frac{\gamma_a}{\gamma_a+\gamma_b}\, P_{\text{spont}}(T) \\ p_b &= \frac{\gamma_b}{\gamma_a+\gamma_b}\, P_{\text{spont}}(T), \end{aligned} \tag{4.72}$$

where $P_{\text{spont}}(T)$ is the probability for an atomic spontaneous emission during one map.

The isometry $W_{[i]} = M_{\mathcal{A}(\mathcal{BE})} U_{\mathcal{A}}^{[i]}$, which describes step i of the sequential generation scheme, can be written in a basis as

$$W = \sum_{e=0}^{2} \sum_{i=0}^{1} \sum_{\alpha,\beta} W_{\alpha,\beta}^{i,e} |\alpha, i, e\rangle\langle\beta| \tag{4.73}$$

with $\{\alpha,\beta\}=\{a,b_1,b_2\}$. After n steps we obtain the state

$$\begin{aligned}|\Psi_{\rm cle}\rangle &= W_{[n]}\dots W_{[1]}|b_2\rangle \\ &= \sum_{e_n,\dots,e_1=0}^{2}\ \sum_{i_n,\dots,i_1=0}^{1} W_{[n]}^{i_n e_n}\dots W_{[1]}^{i_n e_n}|b_2\rangle|i_n e_n,\dots,i_1 e_1\rangle, \quad (4.74)\end{aligned}$$

where $|b_2\rangle$ is the initial atomic state and

$$W^{i,e}=\sum_{\alpha,\beta} W^{i,e}_{\alpha,\beta}|\alpha\rangle\langle\beta|. \quad (4.75)$$

The intermediate unitary operations $U_{\mathcal{A}}^{[i]}$ on the atom for the generation of a cluster state are given by Eqs. (4.66) and (4.67) with $\Phi_i=0$ and $\Theta_i=\pi/4$. The last unitary operation $U_{\mathcal{A}}^{[n]}$ was chosen such that the atom was left in a superposition of levels $|a\rangle$ and $|b_1\rangle$ before $M_{\mathcal{AB}}$ mapped the atom on the final state $|b_1\rangle$. Here, level $|a\rangle$ is also populated by $M_{\mathcal{A}(\mathcal{BE})}$ with probability p_a and therefore the atom does not decouple after the last step. Since we are only interested in the purely photonic state in the output-field of the cavity we trace over the atomic degrees of freedom and the environment modes. This leads to a MPDO given by

$$\begin{aligned}\rho_{\rm cl} &= {\rm tr}_{\mathcal{E}}\Big[{\rm tr}_{\mathcal{A}}\big(|\psi_{\rm cle}\rangle\langle\psi_{\rm cle}|\big)\Big] \\ &= \sum_{i_1,\dots,i_n=0}^{1}\ \sum_{i'_1,\dots,i'_n=0}^{1} {\rm tr}\big(M_{[n]}^{i_n,i'_n}\dots M_{[1]}^{i_1,i'_1}\widetilde{B}\big)|i_n\dots i_1\rangle\langle i'_n\dots i'_1|,\end{aligned} \quad (4.76)$$

where the coefficients are defined by products of $D^2\times D^2$ matrices $M^{i,i'}$ given by

$$M^{i,i'}=\sum_{e=0}^{2} W^{i,e}\otimes\bar{W}^{i',e} \quad (4.77)$$

and the boundary condition is specified by

$$\widetilde{B}=\sum_{\alpha}|b_2\rangle\langle\alpha|\otimes|b_2\rangle\langle\alpha|. \quad (4.78)$$

The fidelity of the sequential generation of the cluster state is defined as

$$F_{\rm cl}(n)=\sqrt{\langle\psi_{\rm cl}|\rho_{\rm cl}|\psi_{\rm cl}\rangle}. \quad (4.79)$$

For the overlap between the resulting MPDO $\rho_{\rm cl}$ (4.76) and the desired pure cluster state $|\psi_{\rm cl}\rangle$ (4.70) we obtain

$$\langle\psi_{\rm cl}|\rho_{\rm cl}|\psi_{\rm cl}\rangle = \sum_{i_1,\ldots,i_n=0}^{1}\sum_{i_1',\ldots,i_n'=0}^{1} \mathrm{tr}\big(M_{[n]}^{i_n,i_n'}\ldots M_{[1]}^{i_1,i_1'}\widetilde{B}\big)\times \mathrm{tr}\big(V_{[n]}^{i_n'}\otimes\bar{V}_{[n]}^{i_n}\ldots V_{[1]}^{i_1'}\otimes\bar{V}_{[1]}^{i_1}B^{\otimes 2}\big), \tag{4.80}$$

with the isometries $V_{[i]} = M_{\mathcal{AB}}U_{\mathcal{A}}^{[i]}$ and the boundary condition $B = |b_2\rangle\langle b_1|$. In Fig. 4.9 (a) we plot the fidelity $F_{\rm cl}(n)$ for different probabilities $P_{\rm spont}(T)$. Therefore we refer to [28], where $\gamma_a/\gamma_b = 5/4$. The dash-dotted line corre-

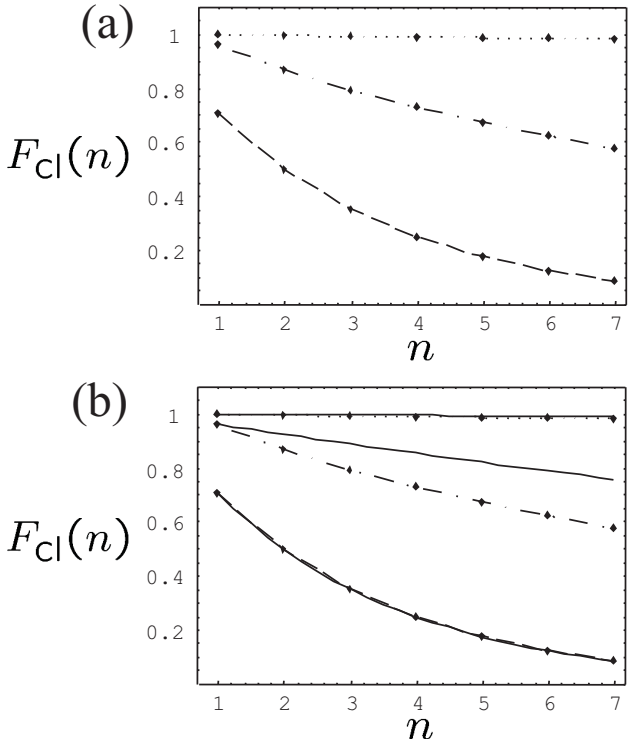

Figure 4.9: (a) The plots show $F_{\rm cl}(n)$ versus the number of qubits n for $P_{\rm spont}(T) = 0.01$ (dotted line), $P_{\rm spont}(T) = 0.28$ (dash-dotted line) and $P_{\rm spont}(T) = 1$ (dashed line). In (b) we compare each $F_{\rm cl}(n)$ with the function $(f_0)^n$, where $f_0 = F_{\rm cl}(1)$ is the respective fidelity for the first qubit.

sponds to the probability for a spontaneous emission of $P_{\rm spont}(T) = 0.28$ as estimated above. For the $n = 7$ qubit cluster state we obtain the disappointing fidelity of $F_{\rm cl}(7) = 0.58$. With the parameters from [29] we estimated

$P_{\text{spont}}(T) = 0.01$. This leads to a satisfactory fidelity of $F_{\text{cl}}(7) = 0.98$. The corresponding function $F_{\text{cl}}(n)$ is depicted by the dotted line. Finally we also considered $P_{\text{spont}}(T) = 1$ (dashed line). In this case all time-bin are left empty and we end up with the product state $|0\rangle^{\otimes n}$.

In Fig. 4.9 (b) we compare $F_{\text{cl}}(n)$ with a function $(f_0)^n$, where $f_0 = F_{\text{cl}}(1)$ is the fidelity obtained for the first step, i.e. the generation of the first qubit of the cluster state. $(f_0)^n$ is then the fidelity for the generation of an n-qubit product state, where the source is initialized in each step and we perform always the same operation. For $P_{\text{spont}}(T) < 1$, $F_{\text{cl}}(n)$ decreases faster than $(f_0)^n$. This is comprehensible since here an error in a certain generation step causes an incorrect initial state of the source for the next step and therefore affects all subsequent steps. If the fidelity for the first step corresponds to $P_{\text{spont}}(T) = 1$, the resulting product state is also $|0\rangle^{\otimes n}$. The coincidence with $F_{\text{cl}}(n)$ for $P_{\text{spont}}(T) = 1$ shows, that in this case the fidelity for the cluster state generation is decreased by a constant factor in each step.

Chapter 5

Collective effects in cavity QED

In this chapter we study collective effects in a system of many atoms coupled to the same mode of an optical cavity. We characterize these effects and point out how they can be employed for the generation of entangled multi-atom states.

In section 5.1 we introduce the model for a suitable configuration of an ensemble of atoms in a cavity. In the bad-cavity limit the system obeys the superradiance master equation. In section 5.2 we calculate the output field of the cavity and in section 5.3 we discuss its properties. It turns out that under certain conditions the system evolves into subradiant states. In section 5.4 we demonstrate that current experimental set-ups [62] are in principle suitable for observing these states.

5.1 An ensemble of atoms in a cavity

We consider a system of N atoms coupled to the same cavity mode as illustrated in Fig. 5.1. For the internal structure of atom i we assume an effective Λ-type three-level system with two ground states $|a\rangle_i$ and $|b\rangle_i$ and one excited state $|e\rangle_i$ with $i = 1, \ldots, N$. The atomic transition $|a\rangle_i \rightarrow |e\rangle_i$ is driven off-resonantly by an external laser field with frequency ω_a and Rabi frequency Ω_a. We will refer to it as the pump laser. The other transition $|b\rangle_i \rightarrow |e\rangle_i$ couples with $r_i g$ to a single off-resonant cavity mode with resonance frequency ω_c. Here, g is the maximal value of the coupling strength and r_i accounts for its position dependence. For the standing-wave cavity field we have $r_i = \sin(k_c x_i)$, where k_c is the wave vector corresponding to the cavity resonance frequency ω_c and x_i denotes the position of atom i. Both transitions couple also directly to the free radiation field and therefore spontaneously decay with rates γ_a and γ_b. Since each atom couples independently

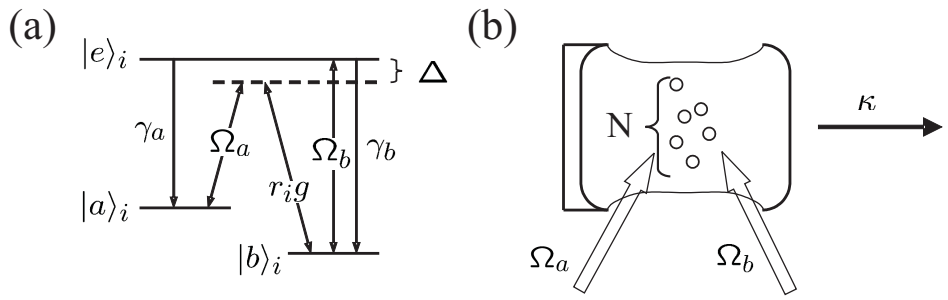

Figure 5.1: (a) Level structure of atom i: the ground states $|a\rangle_i$ ($|b\rangle_i$) and the excited state $|e\rangle_i$ are coupled by an external laser with Rabi frequency Ω_a (the cavity mode with coupling strength $r_i g$) with detuning Δ. The $|b\rangle_i \rightarrow |e\rangle_i$ transition is additionally driven resonantly by a recycling laser with Rabi frequency Ω_b. Level $|e\rangle_i$ spontaneously decays into $|a\rangle_i$ and $|b\rangle_i$ with decay rates γ_a and γ_b. (b) Set-up: N atoms couple to a single cavity mode. The two lasers irradiate the atoms directly and the cavity mode decays mainly through the less reflective mirror with rate κ.

to the environment this may spoil the collective dynamics which relies on the coherent coupling of all atoms to the same cavity mode. In order to avoid population of the excited states $|e\rangle_i$, we choose the same large detuning Δ for pump laser and cavity mode from the respective atomic transition. The direct transitions to $|e\rangle_i$ are then suppressed and we obtain an effective Raman transition between levels $|a\rangle_i$ and $|b\rangle_i$. The coherent population transfer from the atom to the cavity mode is then described by a Jaynes-Cummings interaction of the form

$$\frac{r_i g \Omega_a \sqrt{n}}{\Delta}\big(|a\rangle_i\langle b| \otimes |n-1\rangle\langle n| + |b\rangle_i\langle a| \otimes |n\rangle\langle n-1|\big), \tag{5.1}$$

where n denotes the number of photons in the cavity mode. If the cavity is initially in the vacuum state we obtain Rabi oscillations between $|a\rangle_i \otimes |0\rangle$ and $|b\rangle_i \otimes |1\rangle$. At the same time the coupling to the free radiation field leads to a decay of the cavity mode with rate κ. If the atoms are initially prepared in levels $|a\rangle_i$ and the cavity decay is faster then the Rabi oscillations, the population is gradually transferred to the state $|b\rangle_i \otimes |0\rangle$. In order to repeat the process we have to recycle the atoms back to the initial state $|a\rangle_i$. This is accomplished by an additional recycling laser which drives the $|b\rangle_i \rightarrow |e\rangle_i$ transition resonantly with frequency ω_b and Rabi frequency Ω_b. From level $|e\rangle_i$ the atoms then spontaneously decay back to level $|a\rangle_i$.

The Hamiltonian for a single atom is of the form (2.51). It involves the independent driving of both atomic transitions by the external laser fields

and the coupling between the $|b\rangle_i \rightarrow |e\rangle_i$ transition and the cavity mode. In the following we neglect the dipole-dipole coupling of the atoms. This is justified if the distance between them is bigger than the wavelength of the atomic transitions. The Hamiltonian of the system is then given by the sum of the single-atom Hamiltonians. We obtain

$$\begin{aligned} H &= \omega_c a^\dagger a + (\omega_c - \omega_a) X_{aa} + \omega_b X_{ee} + \frac{\Omega_a}{2}\big(e^{-i\omega_a t} X_{ea} + e^{i\omega_a t} X_{ae}\big) \\ &\quad + \frac{\Omega_b}{2}\big(e^{-i\omega_b t} X_{eb} + e^{i\omega_b t} X_{be}\big) + g\sum_{i=1}^{N} r_i\big(\sigma_{eb}^{(i)} a + a^\dagger \sigma_{be}^{(i)}\big), \end{aligned} \tag{5.2}$$

where a and $a^\dagger$ are the annihilation and creation operator for the cavity mode. The collective operators are defined as

$$X_{kl} = \sum_{i=1}^{N} \sigma_{kl}^{(i)} \tag{5.3}$$

for $\{k, l\} = \{a, b, e\}$ and

$$\sigma_{kl}^{(i)} = |k\rangle_i \langle l|. \tag{5.4}$$

In an interaction picture with respect to

$$H_{01} = \omega_b (a^\dagger a + X_{ee}) + (\omega_b - \omega_a) X_{aa} \tag{5.5}$$

we obtain the time-independent Hamiltonian

$$\begin{aligned} H_I &= \Delta(a^\dagger a + X_{aa}) + \frac{\Omega_a}{2}(X_{ae} + X_{ea}) + \frac{\Omega_b}{2}(X_{be} + X_{eb}) \\ &\quad + g\sum_{i=1}^{N} r_i\big(\sigma_{eb}^{(i)} a + a^\dagger \sigma_{be}^{(i)}\big), \end{aligned} \tag{5.6}$$

where the detuning $\Delta < 0$ is defined as

$$\Delta = \omega_c - \omega_b. \tag{5.7}$$

The master equation of the system can be derived employing the method introduced in section 2.1.2. In the interaction picture with respect to H_{01} it is given by

$$\frac{d\rho_I}{dt} = -i[H_I, \rho_I] + \big(\mathcal{L}_a + \mathcal{L}_b + \mathcal{L}_c\big)\rho_I \tag{5.8}$$

with the density operator

$$\rho_I(t) = e^{iH_{01}t} \rho(t)\ e^{-iH_{01}t}. \tag{5.9}$$

The Lindblad operators

$$\begin{aligned}
\mathcal{L}_a\rho &= 2\gamma_a \sum_{i=1}^{N} \sigma_{ae}^{(i)} \rho \sigma_{ea}^{(i)} - \gamma_a X_{ee}\rho - \gamma_a \rho X_{ee}, \\
\mathcal{L}_b\rho &= 2\gamma_b \sum_{i=1}^{N} \sigma_{be}^{(i)} \rho \sigma_{eb}^{(i)} - \gamma_b X_{ee}\rho - \gamma_b \rho X_{ee}, \\
\mathcal{L}_c\rho &= 2\kappa a \rho a^\dagger - \kappa a^\dagger a \rho - \kappa \rho a^\dagger a,
\end{aligned} \tag{5.10}$$

describe the spontaneous decay of the atomic transitions and the cavity decay. For (5.10) we took the results from Eq. (2.50) assuming that the atoms decay independently, i.e. they do not influence the coupling of another atom to the free radiation field. As above we require that the distance between the atoms is large compared to wave-length of the emitted radiation. Then spatial correlations in the electromagnetic field vanish and one can assume that the atoms couple to statistically independent reservoirs.

Raman transition between the two ground states

The advantage of the atomic Λ configuration is, that there exists the possibility to implement a coherent population transfer to the cavity mode. Therefore we need equal detuning

$$|\Delta| \gg \sqrt{n}g, \Omega_a, \Omega_b, \gamma_a, \gamma_b, \kappa \tag{5.11}$$

for the off-resonant driving of both atomic transitions. In the following we use a method described for instance in [105–107] to derive an effective Hamiltonian for the Raman coupling between the ground states $|a\rangle_i$ and $|b\rangle_i$.

In the limit (5.11) the off-resonant terms proportional to g and Ω_a in the original Hamiltonian H_I (5.6) can be regarded as small perturbations. Therefore the idea is to use perturbation theory with respect to the small parameters g/Δ and Ω_a/Δ. This is accomplished by applying small nonlinear rotations U_1 and U_2 to the original Hamiltonian, such that one can easily identify negligible terms. We define the rotated density operator

$$\widetilde{\rho}(t) = U_2 U_1 \rho_I(t) U_1^\dagger U_2^\dagger \tag{5.12}$$

and obtain the master equation

$$\frac{d\widetilde{\rho}}{dt} = -i[\widetilde{H}, \widetilde{\rho}] + U_2 U_1 \big(\mathcal{L}_a + \mathcal{L}_b + \mathcal{L}_c\big) \rho_I U_1^\dagger U_2^\dagger. \tag{5.13}$$

We will consider the transformation of the Lindblad terms later and concentrate now on the derivation of the effective Hamiltonian $\widetilde{H} = U_2 U_1 H_I U_1^\dagger U_2^\dagger$. The unitary transformations are defined as $U_1 = e^{S_1/\Delta}$ and $U_2 = e^{S_2/\Delta}$ with

$$\begin{aligned} S_1 &= g\sum_{i=1}^{N} r_i\big(\sigma_{be}^{(i)} a^\dagger - a\,\sigma_{eb}^{(i)}\big), \\ S_2 &= \frac{\Omega_a}{2}(X_{ae} - X_{ea}). \end{aligned} \tag{5.14}$$

We employ the Baker-Hausdorff relation

$$e^{S/\Delta} H e^{-S/\Delta} \approx H + \frac{1}{\Delta}[S,H] + \frac{1}{2\Delta^2}[S,[S,H]] \tag{5.15}$$

and – since $|\Delta| \gg \sqrt{n}g, \Omega_a, \Omega_b$ – neglect terms proportional to $1/\Delta^2$. The effective Hamiltonian turns out to be

$$\begin{aligned} \widetilde{H} \;\approx\; & \Delta(a^\dagger a + X_{aa}) + \frac{\Omega_b}{2}(X_{be} + X_{eb}) + \underbrace{\frac{g\Omega_a}{2\Delta}\sum_{i=1}^{N} r_i\big(\sigma_{ab}^{(i)} a + a^\dagger \sigma_{ba}^{(i)}\big)}_{\text{Raman coupling}} \\ & + \underbrace{\frac{\Omega_a\Omega_b}{4\Delta}(X_{ab} + X_{ba})}_{\text{Raman coupling}} + \underbrace{\frac{g\Omega_b}{2\Delta}(a + a^\dagger)\sum_{i=1}^{N} r_i\big(\sigma_{bb}^{(i)} - \sigma_{ee}^{(i)}\big)}_{\text{Scattering of the recycling laser}} \\ & + \underbrace{\frac{\Omega_a^2}{4\Delta}(X_{aa} - X_{ee})}_{\text{Stark shifts}} + \frac{g^2}{\Delta}\sum_{i,j=1}^{N} r_i r_j\big[a^\dagger \sigma_{be}^{(i)}, \sigma_{eb}^{(i)} a\big]. \end{aligned} \tag{5.16}$$

Apart from the desired resonant Raman transition with the effective Rabi frequency $g\Omega_a/2\Delta$, we also obtain an off-resonant Raman transition with an effective Rabi frequency $\Omega_a\Omega_b/4\Delta$. Furthermore we obtain terms which account for the off-resonant scattering of the recycling laser on the cavity mode and the dynamic Stark shifts of levels $|a\rangle_i$ and $|e\rangle_i$ due to the off-resonant driving by the pump laser. The last term in (5.16) can be written as

$$\sum_{i,j=1}^{N} r_i r_j\big[a^\dagger \sigma_{be}^{(i)}, \sigma_{eb}^{(i)} a\big] = \underbrace{\sum_{i} r_i^2\big(a^\dagger a \sigma_{bb}^{(i)} - a a^\dagger \sigma_{ee}^{(i)}\big)}_{\text{Stark shifts}} - \sum_{i\neq j} r_i r_j\, \sigma_{be}^{(i)} \otimes \sigma_{eb}^{(j)}. \tag{5.17}$$

We identify the dynamic Stark shifts of levels $|b\rangle_i$ and $|e\rangle_i$ due to the off-resonant coupling to the cavity mode. The cross-terms describe the excitation exchange between different atoms via the cavity mode, that is the transition $|b\rangle_i \otimes |e\rangle_j \to |e\rangle_i \otimes |b\rangle_j$.

The master equation for $\widetilde{\rho}$ is given by Eq. (5.13). We expand the rotated Lindblad terms in a series with respect to $1/\Delta$ and since $|\Delta| \gg \sqrt{n}g, \Omega_a, \gamma_a, \gamma_b, \kappa$ we can neglect terms of the order $1/\Delta^2$. This leads to an effective master equation

$$\begin{aligned} \frac{d\widetilde{\rho}}{dt} &= -i[\widetilde{H}, \widetilde{\rho}] + U_2 U_1 \big(\mathcal{L}_a + \mathcal{L}_b + \mathcal{L}_c\big)\rho_I U_1^\dagger U_2^\dagger \\ &= -i[\widetilde{H}, \widetilde{\rho}] + \big(\mathcal{L}_a + \mathcal{L}_b + \mathcal{L}_c\big)\widetilde{\rho} + \mathcal{L}_\Delta \widetilde{\rho}. \end{aligned} \tag{5.18}$$

with the additional contributions

$$\begin{aligned} \mathcal{L}_\Delta \widetilde{\rho} &= -\frac{g\kappa}{\Delta} \sum_i r_i \Big(2a\widetilde{\rho}\sigma_{eb}^{(i)} + 2\sigma_{be}^{(i)}\widetilde{\rho}a^\dagger - \Big\{ \sigma_{eb}^{(i)} a + a^\dagger \sigma_{be}^{(i)}, \widetilde{\rho} \Big\} \Big) \\ &\quad + \frac{2\gamma_a}{\Delta} \sum_i \Bigg(\sigma_{ae}^{(i)} \widetilde{\rho} \Big[r_i g a^\dagger \sigma_{ba}^{(i)} + \frac{\Omega_a}{2} \big(\sigma_{aa}^{(i)} - \sigma_{ee}^{(i)} \big) \Big] \\ &\qquad\qquad + \Big[r_i g \sigma_{ab}^{(i)} a + \frac{\Omega_a}{2} \big(\sigma_{aa}^{(i)} - \sigma_{ee}^{(i)} \big) \Big] \widetilde{\rho}\, \sigma_{ea}^{(i)} \Bigg) \\ &\quad + \frac{2\gamma_b}{\Delta} \sum_i \Bigg(\sigma_{be}^{(i)} \widetilde{\rho} \Big[r_i g a^\dagger \big(\sigma_{bb}^{(i)} - \sigma_{ee}^{(i)} \big) + \frac{\Omega_a}{2} \sigma_{ab}^{(i)} \Big] \\ &\qquad\qquad + \Big[r_i g \big(\sigma_{bb}^{(i)} - \sigma_{ee}^{(i)} \big) a + \frac{\Omega_a}{2} \sigma_{ba}^{(i)} \Big] \widetilde{\rho}\, \sigma_{eb}^{(i)} \Bigg) \\ &\quad - \frac{\gamma_a + \gamma_b}{\Delta} \Big\{ \sum_i r_i g \big(\sigma_{eb}^{(i)} a + a^\dagger \sigma_{be}^{(i)} \big) + \frac{\Omega_a}{2} (X_{ae} + X_{ea}), \widetilde{\rho} \Big\}. \end{aligned} \tag{5.19}$$

They describe off-resonant processes.

In an interaction picture with respect to

$$H_{02} = \Delta \left(a^\dagger a + X_{aa} \right) \tag{5.20}$$

the off-resonant terms acquire phase factors $\exp(\pm i\Delta t)$ and can be neglected within the rotating-wave approximation in the limit (5.11). The master equation (5.18) for

$$\rho_{II} = e^{iH_{02}t}\ \widetilde{\rho}\ e^{-iH_{02}t} \tag{5.21}$$

is then given by

$$\frac{d\rho_{II}}{dt} = -i[H_{II}, \rho_{II}] + \big(\mathcal{L}_a + \mathcal{L}_b + \mathcal{L}_c\big)\rho_{II}. \tag{5.22}$$

The Hamiltonian in this interaction picture is

$$\begin{aligned} H_{II} &= \frac{\Omega_b}{2}(X_{be}+X_{eb}) + \widetilde{g}\sum_{i=1}^{N} r_i\big(\sigma_{ab}^{(i)}a + a^\dagger\sigma_{ab}^{(i)}\big) \\ &\quad + \frac{\Omega_a^2}{4\Delta}(X_{aa}-X_{ee}) + \frac{g^2}{\Delta}\sum_{i,j=1}^{N} r_i r_j\big[a^\dagger\sigma_{be}^{(i)}, \sigma_{eb}^{(j)}a\big], \end{aligned} \tag{5.23}$$

where we introduced an effective coupling strength $\widetilde{g} = g\Omega_a/2\Delta$ for the resonant Raman transition. The off-resonant Raman transition and the scattering term were discarded in the rotating-wave approximation. In Fig. 5.2 we illustrate the effective level scheme for atom i.

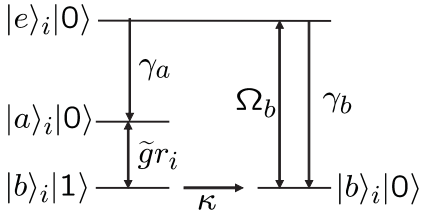

Figure 5.2: Effective level scheme of the atom. The two ground levels $|a\rangle_i$ and $|b\rangle_i$ are coupled via a Raman transition with the effective coupling strength $\widetilde{g}r_i = r_i g\Omega_a/2\Delta$. The recycling laser has the Rabi frequency Ω_b. The spontaneous decay rates of the atomic transitions are given by γ_a and γ_a.

Adiabatic Elimination of the cavity mode

For further investigations we consider a bad-cavity regime, where the condition

$$\kappa \gg \widetilde{g}, \gamma_a, \gamma_b \tag{5.24}$$

holds. In this case the cavity mode decays instantaneously compared to other significant changes and it is basically always in the vacuum state. Then, the master equation of the system (5.22) can be considerably simplified by an adiabatic elimination of the cavity mode. An appropriate strategy to derive the resulting atomic master equation is to transform the original master equation to the so-called dissipation picture [108, 109].

In the bad-cavity limit, the Hamiltonian of the system (5.23) is approximately given by

$$H_{II} \simeq H_a + \widetilde{g}\big(X_+ a + X_- a^\dagger\big) \tag{5.25}$$

with the collective atomic operators

$$\begin{aligned} X_+ &= \sum_i r_i \sigma_{ab}^{(i)}, \\ X_- &= \sum_i r_i \sigma_{ba}^{(i)} \end{aligned} \tag{5.26}$$

and the purely atomic Hamiltonian

$$\begin{aligned} H_a &= \frac{\Omega_b}{2}\big(X_{eb} + X_{be}\big) + \frac{\Omega_a^2}{4\Delta}\big(X_{aa} - X_{ee}\big) - \frac{g^2}{\Delta}\sum_i r_i^2 \sigma_{ee}^{(i)} \\ &\quad - \frac{g^2}{\Delta}\sum_{i\neq j} r_i r_j\, \sigma_{be}^{(i)} \otimes \sigma_{eb}^{(j)}. \end{aligned} \tag{5.27}$$

We introduce the density operator of the system in the dissipation picture as

$$\rho_d(t) = e^{-\mathcal{L}_c t}\rho_{II}(t), \tag{5.28}$$

where $\mathcal{L}_c$ is the Lindblad operator for the cavity decay defined in Eq. (5.10). The master equation is then given by

$$\frac{d\rho_d}{dt} = -i\widetilde{g}\left(e^{-\kappa t}\mathcal{L}_1 + e^{\kappa t}\mathcal{L}_2\right)\rho_d - i[H_a, \rho_d] + (\mathcal{L}_a + \mathcal{L}_b)\rho_d, \tag{5.29}$$

where we defined

$$\begin{aligned} \mathcal{L}_1\rho &= a[X_+, \rho] + [X_-, \rho]a^\dagger, \\ \mathcal{L}_2\rho &= [a, \rho]X_+ + X_-[a^\dagger, \rho], \end{aligned} \tag{5.30}$$

and used the relations

$$\begin{aligned} \mathcal{L}_c\big(a\rho\big) &= a\big(\mathcal{L}_c + \kappa\big)\rho, \\ \mathcal{L}_c\big(\rho a^\dagger\big) &= \big((\mathcal{L}_c + \kappa)\rho\big)a^\dagger, \\ \mathcal{L}_c\big([a, \rho]\big) &= \big[a, (\mathcal{L}_c - \kappa)(\rho)\big], \\ \mathcal{L}_c\big([a^\dagger, \rho]\big) &= \big[a^\dagger, (\mathcal{L}_c - \kappa)(\rho)\big]. \end{aligned} \tag{5.31}$$

Since we are only interested in the atomic observables we trace over the cavity degrees of freedom and define a purely atomic density operator

$$\rho_a(t) = \mathrm{tr}_c\big(\rho_d(t)\big). \tag{5.32}$$

From Eq. (5.29) we obtain

$$\frac{d\rho_a}{dt} = \mathrm{tr}_c\left(\mathcal{L}_1 e^{-\kappa t}\rho_d\right) - i[H_a, \rho_a] + (\mathcal{L}_a + \mathcal{L}_b)\rho_a, \tag{5.33}$$

where $\mathrm{tr}_c(\mathcal{L}_2\rho_d)$ does not contribute since $\mathrm{tr}_c(a\rho_d) = \mathrm{tr}_c(\rho_d a)$. In order to find a master equation for ρ_a we have to eliminate the density operator ρ_d which still appears in (5.33). Therefore we integrate Eq. (5.29) formally. This leads to

$$\begin{aligned} e^{-\kappa t}\rho_d &= e^{-\kappa t}e^{-iH_a t}\rho_d(0)e^{iH_a t} + e^{-\kappa t}(\mathcal{L}_a+\mathcal{L}_b)\rho_d \\ &\quad -i\widetilde{g}e^{-\kappa t}\int_0^t d\tau e^{-\kappa\tau}e^{-iH_a(t-\tau)}\big(\mathcal{L}_1\rho_d(\tau)\big)e^{iH_a(t-\tau)} \\ &\quad -i\widetilde{g}\int_0^t d\tau e^{-\kappa(t-\tau)}e^{-iH_a(t-\tau)}\big(\mathcal{L}_2\rho_d(\tau)\big)e^{iH_a(t-\tau)}. \end{aligned} \tag{5.34}$$

In the limit (5.24), already after a short time $t \gtrsim \kappa^{-1}$ all terms on the right-hand side except the last one are negligible and we have

$$e^{-\kappa t}\rho_d \simeq -i\widetilde{g}\int_0^t d\tau e^{-\kappa\tau}e^{-iH_a\tau}\big(\mathcal{L}_2\rho_d(t-\tau)\big)e^{iH_a\tau}, \tag{5.35}$$

where we substituted τ by $t-\tau$. Here, the factors in the integral give a non-vanishing contribution only for $\tau \lesssim \kappa^{-1}$. In this regime the atom-cavity interaction with coupling strength $\widetilde{g}$ and the spontaneous emission of the atom with decay rates γ_a and γ_b can be neglected (5.24) and therefore the time evolution is determined by the purely atomic part of the Hamiltonian H_a. Then, the master equation for ρ_d (5.29) reduces to

$$\frac{d\rho_d}{dt} \simeq -i[H_a,\rho_d] \tag{5.36}$$

and we substitute the solution

$$\rho_d(t-\tau) \simeq e^{iH_a\tau}\rho_d(t)e^{-iH_a\tau} \tag{5.37}$$

into Eq. (5.35). Since we are only interested in times $t \gtrsim \kappa^{-1}$ we can also extend the upper limit of the integral to infinity. We finally obtain

$$e^{-\kappa t}\rho_d \simeq -i\widetilde{g}\left([a,\rho_d]X_a + X_a^\dagger[a^\dagger,\rho_d]\right), \tag{5.38}$$

where

$$X_a = \int_0^\infty d\tau e^{-\kappa\tau}e^{-iH_a\tau}X_+e^{iH_a\tau}. \tag{5.39}$$

With this result the master equation for ρ_a (5.33) turns out to be

$$\frac{d\rho_a}{dt} = -\widetilde{g}^2\Big([X_+,X_a^\dagger\rho_a] + [\rho_a X_a, X_-]\Big) - i[H_a,\rho_a] + (\mathcal{L}_a+\mathcal{L}_b)\rho_a. \tag{5.40}$$

In the limit

$$\kappa \gg \Omega_b, \frac{\Omega_a^2}{\Delta}, \frac{g^2}{\Delta} \tag{5.41}$$

we obtain $X_a \simeq X_+/\kappa$ and rewrite Eq. (5.40) as

$$\begin{aligned} \frac{d\rho_a}{dt} &= -i[H_a, \rho_a] + (\mathcal{L}_a + \mathcal{L}_b)\rho_a \\ &\quad + \frac{\widetilde{g}^2}{\kappa}\big(2X_-\rho_a X_+ - X_+X_-\rho_a - \rho_a X_+X_-\big). \end{aligned} \tag{5.42}$$

The last term describes the collective decay of the atoms via the cavity mode with an effective decay rate proportional to $\widetilde{g}^2/\kappa$. This collective effect is caused by the fact that all atoms couple to the same radiation field, i.e. the common cavity mode. In free space, the same behavior can be observed if the distance between the atoms is smaller than the wave-length of the emitted light. Then, dipole-dipole interaction and atomic collisions can not be neglected.

5.2 The output-field of the cavity mode

In order to identify collective effects in the output-field of the cavity mode, we need a relation between the internal dynamics of the system and the evolution of the reservoir modes. The aim of this section is to express the output-field operator r_{out} in terms of the collective atomic operators $X_\pm$. Therefore we employ the formalism developed in section 2.4.

For a damped quantum system we found the input-output relation (2.105)

$$r_{\text{out}}(t) = r_{\text{in}}(t) + \sqrt{\kappa}\; a(t). \tag{5.43}$$

Here, the operator a, which couples linearly to the reservoir modes is the cavity mode operator. Then the input-output relation expresses the outgoing field at the mirror as the sum of the incident field plus the field radiated from the cavity. In order to find an expression for the cavity mode operator a in the bad-cavity limit we use the quantum Langevin equation (2.99) and choose the system operator $s \equiv a$. We obtain

$$\frac{da(t)}{dt} = -i[a(t), H_S] - \kappa a(t) + \sqrt{\kappa}\; r_{\text{in}}(t), \tag{5.44}$$

where the system operators $H_S \equiv H_{II}$ is given by Eq. (5.25). Substituting H_{II} into (5.44) leads to

$$\frac{da(t)}{dt} = -\kappa a(t) - i\widetilde{g}X_-(t) - \sqrt{\kappa}\; r_{\text{in}}(t). \tag{5.45}$$

For $\kappa \gg \widetilde{g}$ (bad-cavity limit) we obtain the approximate solution

$$a(t) = -i\widetilde{g}X_-(t)/\kappa - r_{\rm in}(t)/\sqrt{\kappa}. \tag{5.46}$$

For $a^\dagger$ we follow the same strategy and obtain the operator identity

$$a^\dagger = i\widetilde{g}X_+/\kappa - r_{\rm in}/\sqrt{\kappa}. \tag{5.47}$$

Since we consider frequencies in the optical regime at room temperature the input-field is in the vacuum state. Using $r_{\rm in}\rho_{\rm in} = \rho_{\rm in}r_{\rm in}^\dagger = 0$ we find simple relations between the output-field operators and the collective atomic operators given by

$$\begin{aligned} r_{\rm out}(t) &= \sqrt{\kappa}\, a(t) = -i\widetilde{g}X_-(t)/\sqrt{\kappa}, \\ r_{\rm out}^\dagger(t) &= \sqrt{\kappa}\, a^\dagger(t) = i\widetilde{g}X_+(t)/\sqrt{\kappa}. \end{aligned} \tag{5.48}$$

It is straightforward to determine the output emission rate for N atoms

$$I_N(t) = \langle r_{\rm out}^\dagger(t) r_{\rm out}(t)\rangle = \frac{\widetilde{g}^2}{\kappa}\,\langle X_+(t)X_-(t)\rangle = \frac{\widetilde{g}^2}{\kappa}\,{\rm tr}\big(\rho_a(t)X_+X_-\big) \tag{5.49}$$

if the solution $\rho_a(t)$ of the master equation (5.42) is known. In order to calculate the second-order correlation function

$$\begin{aligned} G_{2,N}(t,t+\tau) &= \langle r_{\rm out}^\dagger(t) r_{\rm out}^\dagger(t+\tau) r_{\rm out}(t+\tau) r_{\rm out}(t)\rangle \\ &= \frac{\widetilde{g}^4}{\kappa^2}\,\langle X_+(t)X_+(t+\tau)X_-(t+\tau)X_-(t)\rangle \end{aligned} \tag{5.50}$$

we will employ the quantum regression theorem from section 2.3.

5.3 Collective decay

In the following we assign a characteristic feature of the output emission rate to the well-known superradiance effect. We will introduce the so-called Dicke states and point out the origin of the effect. This leads us to the question whether it is possible to use the set-up for the preparation of the atomic system in certain entangled states. This issue will be discussed in the second part of the section.

5.3.1 Superradiance

Here, we are only interested in the collective atomic decay via the cavity mode and therefore omit the recycling laser ($\Omega_b = 0$). Furthermore we assume that

the excited atomic states $|e\rangle_i$ are initially not populated. The master equation for the atoms (5.42) in an interaction picture with respect to $(\Omega_a^2/4\Delta)X_{aa}$ is then reduced to

$$\frac{d\rho_a}{dt} = \frac{\widetilde{g}^2}{\kappa}\big(2X_-\rho_a X_+ - X_+X_-\rho_a - \rho_a X_+X_-\big). \tag{5.51}$$

In order to identify collective effects in the dynamics described by Eq. (5.51) we compare it with the corresponding master equation for independent atoms. It is given by

$$\frac{d\rho_a^{\rm ind}}{dt} = \frac{\widetilde{g}^2}{\kappa}\big(2\sum_i \sigma_{ba}^{(i)}\rho_a^{\rm ind}\sigma_{ab}^{(i)} - X_{aa}\rho_a^{\rm ind} - \rho_a^{\rm ind}X_{aa}\big), \tag{5.52}$$

where we assumed equal coupling strengths for all atoms ($r_i = 1$ for all i) and introduced the density operator $\rho_a^{\rm ind}$ for the independent atoms. In this case correlations between different atoms vanish and for arbitrary atomic operators we have

$$\langle O_i O_j\rangle = \langle O_i\rangle\langle O_j\rangle \quad \text{for} \quad i \neq j. \tag{5.53}$$

The emission rate (5.49) is then given by

$$\begin{aligned} I_N^{\rm ind}(t) &= \frac{\widetilde{g}^2}{\kappa}\,\langle\sum_{i,j=1}^{N}\sigma_{ab}^{(i)}\sigma_{ba}^{(j)}\rangle \\ &= \frac{\widetilde{g}^2}{\kappa}\,\langle X_{aa}(t)\rangle = \frac{\widetilde{g}^2}{\kappa}\,{\rm tr}\big(\rho_a^{\rm ind}(t)X_{aa}\big). \end{aligned} \tag{5.54}$$

In the second line we omitted the fast oscillating terms $\langle\sigma_{ab}^{(i)}\rangle$ and $\langle\sigma_{ba}^{(j)}\rangle$.

We solved (5.51) and (5.52) for $N = 2$ and $N = 3$ with an initial state

$$\rho_a^{\rm ind}(0) = \rho_a(0) = \bigotimes_{i=1}^{N}|a\rangle_i\langle a|. \tag{5.55}$$

In Fig. 5.3 (a) we compare the resulting emission rates $I_2(t)$ and $I_2^{\rm ind}(t)$ for two atoms. For the collectively decaying atoms we observe an enhanced decay rate for small times. The same effect is even more pronounced for three atoms. In this case, the so-called superradiance peak is apparent.

Enhanced decay of two atoms

To understand the origin of superradiance, it is instructive to consider the case of two excited atoms in the quantum-jump picture. Therefore we rewrite

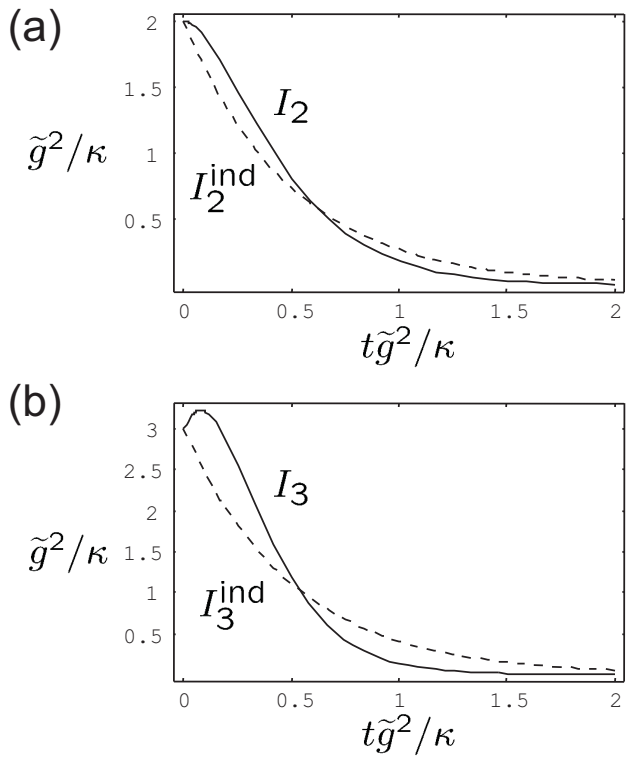

Figure 5.3: In (a) we compare the emission rate $I_2(t)$ for two atoms resulting from the superradiance master equation with the emission rate $I_2^{\rm ind}(t)$ for the case of two independent atoms. In (b) we consider the case of three atoms. $I_3(t)$ and $I_3^{\rm ind}(t)$ are the emission rates for the collective decay and for the case of independent atoms, respectively.

the master equation (5.51) employing an effective Hamiltonian $H_{\rm eff} = -i\widetilde{g}^2 X_+ X_-/\kappa$ and obtain

$$\frac{d\rho_a}{dt} = -i\big(H_{\rm eff}\rho_a - \rho_a H_{\rm eff}^\dagger\big) + 2X_-\rho_a X_+. \tag{5.56}$$

The time-evolution under the condition that no photon is emitted is then described by an effective time-evolution operator

$$\begin{aligned} U_{\rm eff}(t) &= \exp(-iH_{\rm eff}t) = \exp(-\widetilde{g}^2 X_+ X_- t/\kappa) \\ &= e^{-2\widetilde{g}^2 t/\kappa}\big(|a,a\rangle\langle a,a| + |t\rangle\langle t|\big) + |s\rangle\langle s| + |b,b\rangle\langle b,b|, \end{aligned} \tag{5.57}$$

where we assumed equal coupling strengths for both atoms ($r_1 = r_2 = 1$) and introduced singlet and triplet state. They are defined as

$$\begin{aligned} |t\rangle &= \big(|b,a\rangle + |a,b\rangle\big)/\sqrt{2}, \\ |s\rangle &= \big(|b,a\rangle - |a,b\rangle\big)/\sqrt{2}. \end{aligned} \tag{5.58}$$

The probability for no jump in the time interval $(0, t)$ is given by

$$P_0^0(t) = \|U_{\text{eff}}(t)|\Psi_0\rangle\|^2 = e^{-4\tilde{g}^2 t/\kappa}, \tag{5.59}$$

where $|\Psi_0\rangle = |a, a\rangle$ is the initial state. Since the norm of the state decreases, this single trajectory will be subject to a jump and the normalized state after the emission is given by

$$|\Psi_1\rangle = X_-|\Psi_0\rangle/\sqrt{2} = |t\rangle. \tag{5.60}$$

The probability for no jump is again

$$P_0^1(t) = e^{-4\tilde{g}^2 t/\kappa} \tag{5.61}$$

since the triplet state $|t\rangle$ is damped with the same rate as the initial fully excited state.

This shows that the probability for the second emission is the same as for the first one. Compared to the case of two independent emitters, where the probability for the second emission is reduced by $1/2$, the decay is enhanced. The reason for this effect is the constructive interference of the two "decay channels" of the triplet state. On the other hand destructive interference preserves the singlet state from decaying. In the quantum-jump picture this is evident since U_{eff} does not damp the state $|-\rangle$, i.e. the norm is conserved and the probability for an emission is zero. In this case, population is trapped in levels $|a\rangle_i$.

Dicke states

Superradiance was originally studied by Dicke [63] and for the first time observed in [110]. In order to describe the effect for N atoms, the so-called Dicke states [64] $|j, m\rangle$ build a convenient basis. They are the eigenstates of the operator

$$J^2 = J_z^2 + \big(J_+J_- + J_-J_+\big)/2. \tag{5.62}$$

For the atomic system considered here we identify $J_- = X_{ba}$, $J_+ = X_{ab}$ and $J_z = (X_{aa} - X_{bb})/2$. The possible values of j are $N/2, N/2 - 1, \ldots$, the smallest value being 0 if N is even and $1/2$ if N is odd. The index m with $|m| \leq j$ labels the eigenstates of the collective atomic operator J_z, which is proportional to the energy of the system. It is decreased by one under the action of the operator J_-, i.e.

$$J_-|j, m\rangle = \sqrt{j(j+1) - m(m-1)}|j, m-1\rangle. \tag{5.63}$$

If $m = -j$ the result is the zero vector, so the states $|j, -j\rangle$ are the lowest ones of the Dicke ladders. They do not couple to states with lower energies and are therefore called subradiant states. This is a consequence of the indistinguishability of the atoms and the symmetric coupling to the free radiation field via the cavity mode ($r_i = 1$ for all i). Then the symmetry type is preserved and the states $|j, -j\rangle$ have already the lowest energy compatible with their symmetry type.

In the case considered above, the system is initially prepared in the state $|N/2, N/2\rangle = |a, \ldots, a\rangle$. Since the symmetry type is preserved, i.e. $j = N/2$, the collective decay of the atomic system leads down a ladder of $N+1$ equidistant levels from $|N/2, N/2\rangle$ to $|N/2, -N/2\rangle = |b, \ldots, b\rangle$. The intermediate state of the system after $j - m$ emissions is given by

$$|j, m\rangle = \sqrt{\frac{(j+m)!}{N!(j-m)!}}\, X_{ba}^{(j-m)} |a, \ldots, a\rangle. \tag{5.64}$$

and the emission rate (5.49) for equal coupling is

$$\begin{aligned} I_N(j, m) &= \frac{\widetilde{g}^2}{\kappa} \langle X_{ab} X_{ba} \rangle = \frac{\widetilde{g}^2}{\kappa} \langle j, m | J_+ J_- | j, m \rangle \\ &= \frac{\widetilde{g}^2}{\kappa} \big(j(j+1) - m(m-1) \big). \end{aligned} \tag{5.65}$$

It increases from $I_N(N/2, N/2) = N\widetilde{g}^2/\kappa$ for the fully excited state to $I_N(N/2, 0) = N(N/2+1)\widetilde{g}^2/2\kappa$ for the half-deexcited state. This explains that the resulting superradiance peak is more outstanding for a higher number of atoms as observed in Fig. 5.3.

For the case of two atoms, the triplet state $|1, 0\rangle$ and the fully excited state $|1, 1\rangle$ correspond to the same emission rate $I_2(1, 1) = I_2(1, 0) = 2\widetilde{g}^2/\kappa$, while the antisymmetric singlet state $|0, 0\rangle$ does not radiate. Obviously it would be desirable to prepare the system in such a subradiant state but for equal coupling strengths the master equation (5.51) is symmetric under the exchange of two atoms and therefore preserves the symmetry type of the atomic system.

5.3.2 Subradiance

Subradiant states are neither easy to create nor to observe. Although, in principle, all physical systems, where cooperative spontaneous decay is observed, are suitable for this task, the first experimental evidence for subradiance [111] was reported more than twenty years after the first observation of superradiance [110]. In the following we will show, under which conditions

subradiance appears in the cavity set-up and also point out how it can be employed for the probabilistic generation of multi-atom entangled states.

The basic idea is that inhomogeneous coupling between the atoms and the cavity breaks the permutation symmetry and as consequence the initially symmetric state $|N/2, N/2\rangle$ evolves into a mixture of states, which do not belong to the $j = N/2$ symmetry type anymore. In order to validate this assumption, we solve the superradiance master equation (5.51) and the corresponding master equation for independent atoms (5.52) for $N = 2$ and different coupling strengths $r_1 = 1 = 2r_2$. In Fig. 5.4 (a) we compare the population in the atomic states $|a\rangle_i$

$$P_{a,N}^{\mathrm{ind}}(t) = \mathrm{tr}\big(X_{aa}\rho_a^{\mathrm{ind}}(t)\big) \tag{5.66}$$

for independent atoms with

$$P_{a,N}(t) = \mathrm{tr}\big(X_{aa}\rho_a(t)\big) \tag{5.67}$$

for the collectively decaying system. In both cases, the system is initially prepared in $|a, a\rangle$. As expected, in the steady state of the collectively decaying system, population is trapped in levels $|a\rangle_i$ ($P_{a,2}(t \to \infty) \neq 0$). In Fig. 5.4 (b) we solve (5.51) and (5.52) for $N = 3$ and different coupling strengths $r_1 = r_2 = 1 = 2r_3$. Also here, the steady state of the superradiance master equation contains contributions of subradiant states, while the independent atoms loose their "excitation" completely.

This shows, that for inhomogeneous coupling the collectively decaying atoms can be found in a decoherence free subspace with a certain probability.

Inhibited decay of two atoms

In order to understand the underlying mechanism we consider the two-atom case in the quantum-jump picture. Here, the time-evolution of the system under the condition of no photon emission is decribed by

$$U_{\mathrm{eff}} = e^{-r^2\tilde{g}^2 t/\kappa}\big(|a, a\rangle\langle a, a| + |t_r\rangle\langle t_r|\big) + |s_r\rangle\langle s_r| + |b, b\rangle\langle b, b|, \tag{5.68}$$

where $r = \sqrt{r_1^2 + r_2^2}$. We introduced singlet- and triplet-type states

$$\begin{aligned} |t_r\rangle &= \big(r_2|b, a\rangle + r_1|a, b\rangle\big)/r, \\ |s_r\rangle &= \big(r_1|b, a\rangle - r_2|a, b\rangle\big)/r. \end{aligned} \tag{5.69}$$

For an initial state $|\Psi_0\rangle = |a, a\rangle$ the probability of no emission in the time-interval $(0, t)$ is given by

$$P_0^0(t) = e^{-r^2\tilde{g}^2 t/\kappa}. \tag{5.70}$$

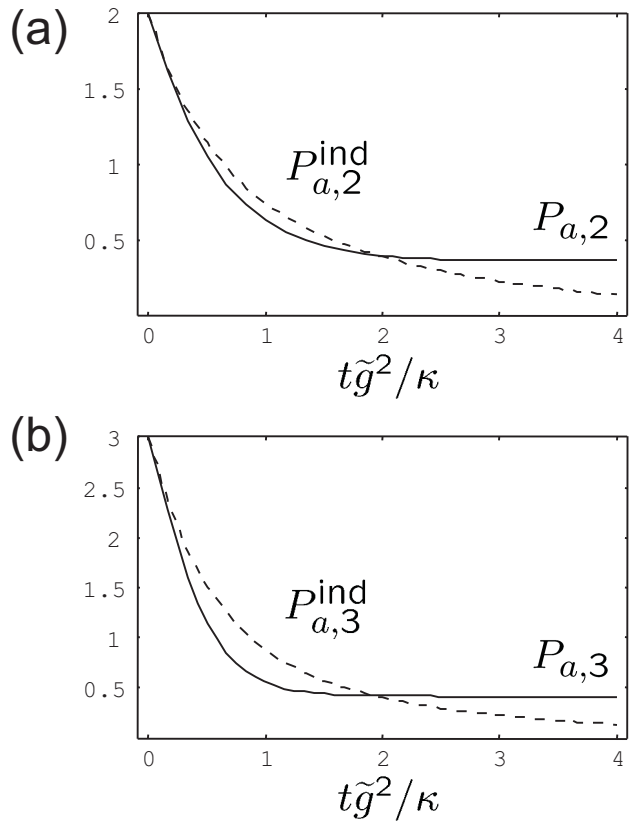

Figure 5.4: In (a) we plot the population of the atomic states $|a\rangle_i$ for two independent atoms $P_{a,2}^{\mathrm{ind}}(t)$ and for two collectively decaying atoms $P_{a,2}(t)$. In (b) we consider the case of three atoms. $P_{a,3}^{\mathrm{ind}}(t)$ and $P_{a,3}(t)$ are the populations of $|a\rangle_i$ for independent and collective decay, respectively.

If we wait long enough this will certainly lead to jump. Here, the normalized state after the emission is

$$\begin{aligned} |\Psi_1\rangle &= X_-|\Psi_0\rangle/r \\ &= \frac{r_1^2 - r_2^2}{r_1^2 + r_2^2}\,|s_r\rangle + \frac{2r_1 r_2}{r_1^2 + r_2^2}\,|t_r\rangle. \end{aligned} \tag{5.71}$$

The probability for no second emission is now given by

$$\begin{aligned} P_0^1(t) &= \|U_{\mathrm{eff}}(t)|\Psi_1\rangle\|^2 \\ &= \frac{(r_1^2 - r_2^2)^2}{(r_1^2 + r_2^2)^2} + e^{-r^2\tilde{g}^2 t/\kappa}\frac{4r_1^2 r_2^2}{(r_1^2 + r_2^2)^2}. \end{aligned} \tag{5.72}$$

It does not vanish for inhomogeneous coupling. This result shows, that with a certain probability

$$P_0^1(t \to \infty) = \frac{(r_1^2 - r_2^2)^2}{(r_1^2 + r_2^2)^2}. \tag{5.73}$$

the system will evolve into the decoherence free singlet-type state $|s_r\rangle$.

For the situation considered in Fig. 5.4 (a), where we assumed $r_1 = 1 = 2r_2$, we prepare the system in the entangled state

$$|s_r\rangle = \big(2|b,a\rangle - |a,b\rangle\big)/\sqrt{5} \tag{5.74}$$

with a probability of $P_0^1(t \to \infty) = 9/25$. This result coincides with the steady state value for the population $P_{a,2}(t \to \infty)$ in Fig. 5.4 (a).

In a conditional scheme the detection of a single photon would indicate the successful preparation of $|s_r\rangle$. The success probability can be maximized by increasing the difference between the coupling constants of the two atoms. In the standing-wave cavity field this can be accomplished by choosing the position of the atoms close to a node and an anti-node. On the other hand, for $r_1 \gg r_2$ the resulting singlet-type state is given by $|s_r\rangle \simeq |b,a\rangle$. This corresponds to the case, where the second atom does not couple at all and the system evolves into a boring product state.

Inhomogeneous Dicke basis

For a system of N atoms, the effect of different coupling strengths can be understood in the Dicke basis. For homogeneous coupling, the state of the system after the first emission of an initially fully excited system is given by $|N/2, N/2-1\rangle$. In order to trap excitation, one has to disturb the system such that the symmetry type is changed, i.e. after one emission the state of the system contains a contribution of $|N/2-1, N/2-1\rangle$. This family of states traps one excitation since it can only decay into the subradiant state ($j = -N/2+1$). If one disturbs the system in each step, the state after $N/2$ emissions would be

$$J_-^{N/2}|N/2, N/2\rangle = \sum_{n=0}^{N/2} c_n |N/2-n, 0\rangle. \tag{5.75}$$

Unfortunately, this is not possible in the configuration considered above.

On the other hand, we have shown, that for inhomogeneous coupling, we obtain states, where excitation is trapped. In order to describe this situation, the homogeneous Dicke basis is not appropriate since $X_-|j,-j\rangle \neq 0$. As has been demonstrated in [112, 113], one has to map it on its inhomogeneous equivalent. In this new basis it turns out, that the inhomogeneous

counterpart of the operator J^2 is not conserved under the action of the inhomogeneous raising and lowering operators X_+ and X_-. The system evolves into a statistical mixture of dark states, defined by

$$X_-|D\rangle = 0. \tag{5.76}$$

In order to prepare a specific entangled state, one has to assign a certain signature in the output-field to it.

In a situation, where the atom-cavity coupling strengths are perfectly controlled, it may be a promising approach to use the inhomogeneous coupling only for a short time-interval in order to disturb the system. After returning to homogeneous coupling, the contributions from states with $j \neq N/2$ would then evolve into subradiant states.

5.3.3 Photon statistics

In order to identify traces of the collective dynamics of the system, it is instructive to investigate also second-order correlations in the output-field of the cavity. Moreover, since the output mode r_{out} and the collective atomic operators X_- are directly related (5.48), correlations between the emitted photons reveal information about the state of the atoms in the cavity and could therefore be employed within a conditional scheme to identify certain entangled states.

In the following we compare intensity correlations in the case of homogeneous and inhomogeneous coupling for $N = 2$ and $N = 3$. Using Eq. (5.49) and (5.50), we calculate

$$\begin{aligned} g_{2,N}(t, t+\tau) &= \frac{G_{2,N}(t, t+\tau)}{I_N(t) I_N(t+\tau)} \\ &= \frac{\langle X_+(t) X_+(t+\tau) X_-(t+\tau) X_-(t)\rangle}{\langle X_+(t) X_-(t)\rangle \langle X_+(t+\tau) X_-(t+\tau)\rangle}, \end{aligned} \tag{5.77}$$

where we normalized the second-order correlation function $G_{2,N}(t, t+\tau)$ with the emission rates at time t and $t+\tau$. We solve the superradiance master equation (5.51) for $r_1 = r_2 = 1$ and $r_1 = 2r_2 = 1$ and employ the quantum regression theorem to obtain $g_{2,2}(t, t+\tau)$ and $g^{\text{inh}}_{2,2}(t, t+\tau)$, respectively. For $N = 3$, we assume $r_1 = r_2 = r_3 = 1$ for $g_{2,3}(t, t+\tau)$ and $r_1 = r_2 = 2r_3 = 1$ for $g^{\text{inh}}_{2,3}(t, t+\tau)$.

In Fig. 5.5 (a) we compare $g_{2,2}(0, \tau)$ and $g^{\text{inh}}_{2,2}(0, \tau)$. Due to superradiance the probability for an emission immediately after an emission at $t = 0$ is equal to the probability for an emission at $t = 0$ in the case of homogeneous

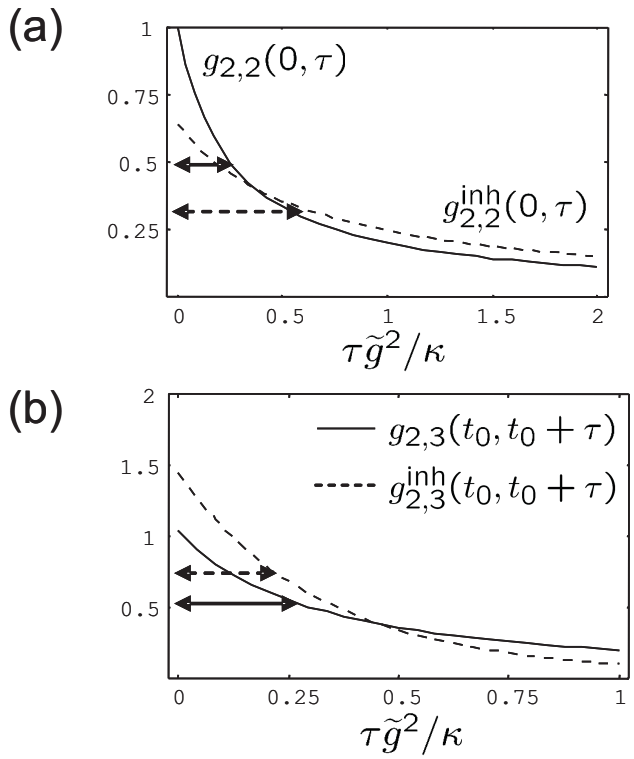

Figure 5.5: In (a) we compare the normalized second-order correlation function $g_{2,2}(0,\tau)$ for two atoms for homogeneous coupling with the case of inhomogeneous coupling $g^{\mathrm{inh}}_{2,2}(0,\tau)$. In (b) we consider the case of three atoms. $g_{2,3}(t_0,t_0\tau)$ and $g^{\mathrm{inh}}_{2,3}(t_0,t_0+\tau)$ are the normalized second-order correlation functions for homogeneous and inhomogeneous coupling, respectively. The correlation lengths is indicated by arrows.

coupling, i.e. $g_{2,2}(0,0) = 1$. On the other hand, for inhomogeneous coupling, $g^{\mathrm{inh}}_{2,2}(0,0) < 1$ since the singlet type contribution $|s_r\rangle$ does not decay at all. This explains also the significantly longer correlation time (indicated by arrows). The case of three atoms is considered in Fig. 5.5 (b). For the time of the first emission we choose $t_0 \approx 0.078\kappa/\widetilde{g}^2$, which corresponds to the maximum of the superradiance peak in the emission rate $I_3(t)$. The resulting normalized correlation functions $g_{2,3}(t_0,t_0+\tau)$ and $g^{\mathrm{inh}}_{2,3}(t_0,t_0+\tau)$ show now a similar behavior. The correlation times are basically equal and since the homogeneous case does not involve any subradiant states, we conclude that after an emission at $t = t_0$ in the inhomogeneous case subradiant states are not yet populated.

Second-order correlations in the output-field are a characteristic feature of collectively decaying systems. For independent atoms the probability for

an emission is not enhanced or delayed by an emission, i.e. the normalized second-order correlation function is flat (as long as no recycling mechanism is involved).

5.4 Experimental conditions

In the preceding section we showed that atoms, coupled to the same cavity mode, decay collectively. Furthermore, we found that a controlled reduction of the symmetry, i.e. inhomogeneous but constant coupling between the atoms and the cavity mode, lead to the interesting phenomenon of subradiance. This effect can be employed to generate entangled multi-atom states. Therefore it would be desirable that the position of the atoms in the standing-wave cavity field is well defined. Excellent control over the atomic position is provided by an ion trap, which holds the atoms at fixed positions inside the cavity. Unfortunately the photon efficiency of current experimental realizations is very bad (0.08 in [30]) due to passive cavity losses. Since any probabilistic scheme would be based on the detection of the output field of the cavity, these set-ups are not appropriate at present.

For the evaluation of the feasibility of our approach, we will therefore refer to another recent experiment, where atoms are dropped through the cavity [62]. As pointed out in section 4.3.2 for a similar set-up [28], the motion of the atoms leads to a significant variation of the atom-cavity coupling strength on time-scales relevant for the internal dynamics. Since the collective behavior of the system is based on interference, it is evident that an unknown and varying atom-cavity coupling will substantially reduce the efficiency of a conditional generation scheme. On the other hand, as long as traces of collectivity can be observed, it is, in principle, possible to implement such a scheme. In the following we will therefore consider the worst case scenario, where the coupling strength randomly changes on a time-scale fast compared to the internal dynamics of the system.

In section 5.3.1, we consider the effect of random coupling strength on the superradiance master equation and compare the resulting time-evolution with the case of independent atoms. The situation of the experiment [62], where the approximations from section 5.1 are not well justified will be investigated numerically in section 5.3.2.

5.4.1 Random coupling

In order to identify traces of collective effects in the superradiance master equation for random coupling we examine the evolution of the system for

small times. Since the width of the Gaussian profile of the cavity mode is much larger than the optical wavelength of the standing wave cavity field, we assume for the position dependent coupling $r_i(x) = \sin(k_c x_i)$, where the wave-vector k_c corresponds to the resonance frequency of the cavity ω_c and x_i denotes the position of the atom with respect to the cavity axis. The effect of the fast and randomly changing atomic positions is considered by averaging over all atomic positions, i.e.

$$\langle \rho_a(t) \rangle_x = \frac{1}{L^N} \int_0^L dx_1 \dots dx_N \rho_a(t), \tag{5.78}$$

where L denotes the length of the cavity.

We write the master equation (5.51) as

$$\frac{d\rho_a(t)}{dt} = \frac{\widetilde{g}^2}{\kappa} \sum_{i,j=1}^{N} r_i r_j \mathcal{L}_{ij} \rho_a(t) \tag{5.79}$$

with

$$\mathcal{L}_{ij}\rho_a = 2\sigma_{ba}^{(i)} \rho_a \sigma_{ab}^{(j)} - \sigma_{ab}^{(i)} \sigma_{ba}^{(j)} \rho_a - \rho_a \sigma_{ab}^{(i)} \sigma_{ba}^{(j)} \tag{5.80}$$

and obtain for the time-evolution of the system

$$\begin{aligned} \langle \rho_a(t) \rangle_x &= \rho_a(0) + \frac{\widetilde{g}^2}{\kappa} \sum_{i,j} \langle r_i r_j \rangle_x \mathcal{L}_{ij} \rho_a(0) t \\ &\quad + \frac{\widetilde{g}^4}{2\kappa^2} \sum_{i,j,k,l} \langle r_i r_j r_k r_l \rangle_x \mathcal{L}_{ij} \mathcal{L}_{kl} \rho_a(0) t^2 + \mathcal{O}(t^3) \\ &= \rho_a(0) + \frac{\widetilde{g}^2}{\kappa} \sum_{i} \langle r_i^2 \rangle_x \mathcal{L}_{ii} \rho_a(0) t \\ &\quad + \frac{\widetilde{g}^4}{2\kappa^2} \sum_{i,j} \langle r_i^2 r_j^2 \rangle_x \big(\mathcal{L}_{ij}\mathcal{L}_{ij} + \mathcal{L}_{ij}\mathcal{L}_{ji} + \mathcal{L}_{ii}\mathcal{L}_{jj} \big) \rho_a(0) t^2 + \mathcal{O}(t^3). \end{aligned} \tag{5.81}$$

Since $L \gg k_c$, only terms proportional to $\sin^2(k_c x_i)$ and $\sin^2(k_c z_i) \sin^2(k_c z_j)$ survived.

Now, we compare this result with the time-evolution for independently decaying atoms. The corresponding master equation (5.52) is given by

$$\frac{d\rho_a^{\mathrm{ind}}(t)}{dt} = \frac{\widetilde{g}^2}{\kappa} \sum_{i=1}^{N} r_i^2 \mathcal{L}_{ii} \rho_a^{\mathrm{ind}}(t). \tag{5.82}$$

For the position averaged atomic density operator we obtain

$$\begin{aligned}\langle\rho_a^{\mathrm{ind}}(t)\rangle_x &= \rho_a(0) + \frac{\widetilde{g}^2}{\kappa}\sum_i \langle r_i^2\rangle_x \mathcal{L}_{ii}\rho_a(0)t \\ &\quad + \frac{\widetilde{g}^4}{2\kappa^2}\sum_{i,j}\langle r_i^2 r_j^2\rangle_x \mathcal{L}_{ii}\mathcal{L}_{jj}\rho_a(0)t^2 + \mathcal{O}(t^3).\end{aligned} \tag{5.83}$$

Since $\langle\rho_a(t)\rangle_x - \langle\rho_a^{\mathrm{ind}}(t)\rangle_x$ does not vanish, we conclude that traces of collective effects will be observed even in the case of random coupling. This result encourages us to investigate the system under realistic experimental conditions.

5.4.2 Numerical results

The aim of the following numerical simulations is to show that the system discussed above is appropriate for the observation of collective effects in setups recently used for cavity QED experiments. In particular, we refer to [62]. There, the conditions (5.11), (5.24) and (5.41) for the Raman transition and the adiabatic elimination of the cavity mode are not fulfilled. As a consequence, photons from the cavity mode may be reabsorbed by the atoms. Worse than that, the excited levels $|e\rangle_i$ are populated and spontaneous atomic emissions into the free radiation field spoil the collective behavior of the atoms.

We will calculate the emission rate

$$I_N(t) = \langle r_{\mathrm{out}}^\dagger(t) r_{\mathrm{out}}(t)\rangle \tag{5.84}$$

and the normalized intensity-correlation function

$$g_{2,N}(\tau) = \frac{\int G_{2,N}(t, t+\tau)dt}{(\int I_N(t)dt)^2}, \tag{5.85}$$

where we average over the time of the first emission. The second-order correlation function is defined as

$$G_{2,N}(t, t+\tau) = \langle r_{\mathrm{out}}^\dagger(t) r_{\mathrm{out}}^\dagger(t+\tau) r_{\mathrm{out}}(t+\tau) r_{\mathrm{out}}(t)\rangle. \tag{5.86}$$

We consider three scenarios:

- The atoms couple to the cavity mode with equal coupling strengths ($r_i = 1$ for i) at all times.

- The atom-cavity coupling strengths change fast on the time-scale of the internal system dynamics. This resembles the situation in [62].
- The atoms evolve independent of each other.

For the simulations, we omit the approximations from section 5.1 and use the original description of the system. The Hamiltonian H_I and the master equation for the density operator $\rho_I(t)$ are given by Eq. (5.6) and (5.8). In the quantum-jump approach, the time-evolution is described by an effective Hamiltonian

$$H_{\text{eff}} = H_I - i\kappa a^\dagger a - i(\gamma_a + \gamma_b) X_{ee} \tag{5.87}$$

as long as no spontaneous photon emission occurs. H_{eff} is derived from the master equation of the system (5.8), which can then be written as

$$\begin{aligned} \frac{d\rho_I}{dt} &= -i\big(H_{\text{eff}}\rho_I - \rho_I H_{\text{eff}}^\dagger\big) + 2\kappa a \rho_I a^\dagger \\ &\quad + 2\gamma_a \sum_{i=1}^{N} \sigma_{ae}^{(i)} \rho_I \sigma_{ea}^{(i)} + 2\gamma_b \sum_{i=1}^{N} \sigma_{be}^{(i)} \rho_I \sigma_{eb}^{(i)}. \end{aligned} \tag{5.88}$$

We identify the jump-operators $\sqrt{2\gamma_a}\,\sigma_{ae}^{(i)}$ and $\sqrt{2\gamma_b}\,\sigma_{be}^{(i)}$. They describe the spontaneous emission of atom i and cause a "jump" in the time-evolution of the system. Analogously we find $\sqrt{2\kappa}\,a$ for the cavity mode. The effect of fast and randomly changing coupling strengths is mimicked by choosing random atomic positions in each trajectory.

The physical system, which corresponds to the case of independent atoms, would contain a separate cavity mode $a_i(t)$ for each atom i, i.e. the atoms do not interact via a common cavity mode. From the relations (5.48) we obtain for the second-order correlation function

$$\begin{aligned} G_{2,N}(t, t+\tau) &= \langle r_{\text{out}}^\dagger(t) r_{\text{out}}^\dagger(t+\tau) r_{\text{out}}(t+\tau) r_{\text{out}}(t) \rangle \\ &= \kappa^2 \langle \sum_{i,j,k,l=1}^{N} a_i^\dagger(t) a_j^\dagger(t+\tau) a_k(t+\tau) a_l(t) \rangle. \end{aligned} \tag{5.89}$$

For independent emitters, relation (5.53) leads to

$$\begin{aligned} G_{2,N}^{\text{ind}}(t, t+\tau) &= N(N-1)\big(|G_{1,1}(t, t+\tau)|^2 + I_1(t) I_1(t+\tau)\big) \\ &\quad + N G_{2,1}(t, t+\tau), \end{aligned} \tag{5.90}$$

where we neglected fast oscillating terms. We introduced the emission rate $I_1(t)$, the first-order correlation function $G_{1,1}(t, t+\tau)$ and the second-order

correlation function for a single atom coupling to the cavity mode $a(t)$. They are defined as

$$\begin{aligned} I_1(t) &= \kappa\langle a^\dagger(t)a(t)\rangle, \\ G_{1,1}(t,t+\tau) &= \kappa\langle a^\dagger(t)a(t+\tau)\rangle, \\ G_{2,1}(t,t+\tau) &= \kappa^2\langle a^\dagger(t)a^\dagger(t+\tau)a(t+\tau)a(t)\rangle. \end{aligned} \tag{5.91}$$

For the emission rate of N independent atoms we obtain analogously

$$I_N^{\mathrm{ind}}(t) = \kappa\langle\sum_{i,j=1}^{N} a_i^\dagger(t)a_j(t)\rangle = NI_1(t). \tag{5.92}$$

We adopt the parameters from [62]. In the level scheme of Rubidium 85 we identify the Λ-system from Fig. 5.1 by $|a\rangle_i = |5S_{1/2}(F=3)\rangle$, $|b\rangle_i = |5S_{1/2}(F=2)\rangle$ and $|e\rangle_i = |5P_{3/2}(F=3)\rangle$ for $i = 1,\ldots,N$. The Rabi frequencies of the laser fields are given by $\Omega_a \approx 7.6\times 2\pi\,\mathrm{MHz}$ and $\Omega_b \approx 3.3\times 2\pi\,\mathrm{MHz}$. The detuning of pump laser and cavity mode from the corresponding atomic transitions is given by $\Delta \approx -20\times 2\pi\,\mathrm{MHz}$. The maximal cavity-atom coupling strength is $g = 2.5\times 2\pi\,\mathrm{MHz}$ and the cavity decay rate $\kappa \approx 1.25\times 2\pi\,\mathrm{MHz}$. The rates for the spontaneous decay of the atoms are $\gamma_a \approx 5/9\gamma$ and $\gamma_b \approx 4/9\gamma$, where $\gamma = 3\times 2\pi\,\mathrm{MHz}$. For all simulations we assume that the atoms are initially prepared in levels $|a\rangle_i$.

For $N = 1$ we solved the master equation directly using the method described in appendix C. $G_{1,1}(t,t+\tau)$ and $G_{2,1}(t,t+\tau)$ are then calculated with the quantum regression theorem. These results were used in Eq. (5.91) to treat the case of independent atoms. For $N = 2$ and $N = 3$ we employed the quantum-jump approach.

Continuous recycling

In Fig. 5.6 we plotted the emission rates $I_1(t)$ for a single atom, $I_2(t)$ for two atoms and $I_2^{\mathrm{ind}}(t)$ for two independent atoms. Since the cavity mode is initially in the vacuum state, the emission rates vanish at $t = 0$. Before they reach their steady state values, we observe small oscillations. They can be dedicated to first order atomic transitions between level $|a\rangle_i$ and $|e\rangle_i$ due to the off-resonant coupling to the laser with Rabi frequency Ω_a and to the cavity mode with coupling strength $\sqrt{n}\,g$. If one increases the detuning Δ to fulfil the condition (5.11), the oscillations vanish. Since we do not observe any significant differences between $I_2(t)$ and $I_2^{\mathrm{ind}}(t)$ we conclude that the emission rate is not appropriate to provide evidence for collective effects in the output-field of the cavity.

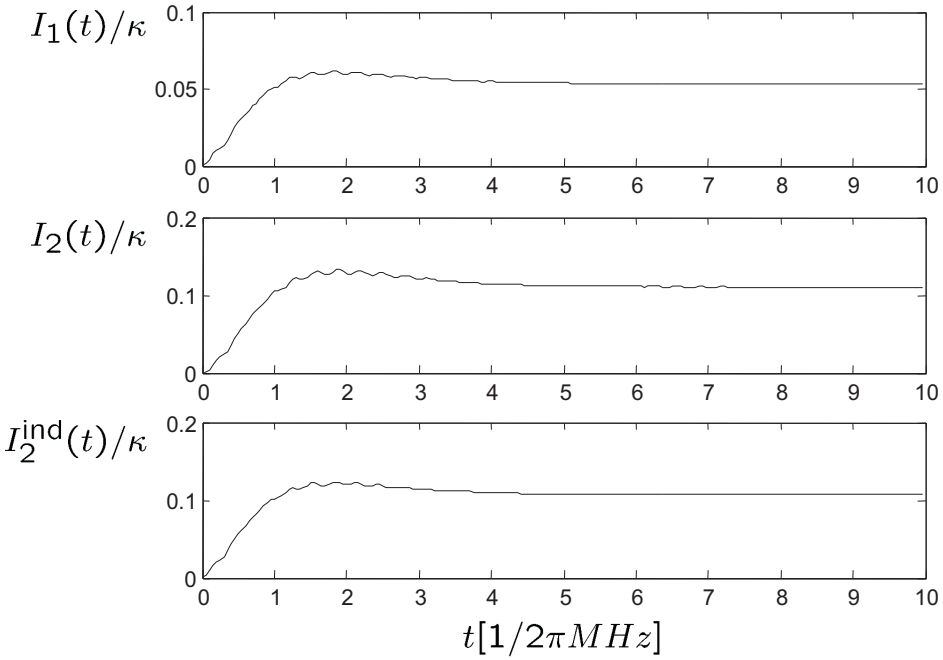

Figure 5.6: Emission rates $I_1(t)$ for one atom, $I_2(t)$ for two atoms and $I_2^{\mathrm{ind}}(t)$ for two independent atoms.

We will therefore concentrate on intensity-correlations and consider in Fig. 5.7 $g_{2,1}(\tau)$ for a single atom, $g_{2,2}(\tau)$ for two atoms, $g_{2,2}^{\mathrm{rand}}(\tau)$ for two atoms with random coupling and $g_{2,2}^{\mathrm{ind}}(\tau)$ for two independent atoms. In Fig. 5.8 we plot the normalized second-order correlation function $g_{2,3}(\tau)$ for three atoms, $g_{2,3}^{\mathrm{rand}}(\tau)$ for three atoms with random coupling and $g_{2,3}^{\mathrm{ind}}(\tau)$ for three independent atoms. Apart from the small oscillations, which correspond to the small oscillations in the emission rate, we observe anti-bunching in the single-atom case, i.e. $g_{2,1}(0) < g_{2,1}(\tau)$. This is not surprising since the atom has to be initialized in the state $|a\rangle$. Here, this is accomplished by the recycling mechanism via the excited state $|e\rangle$ (see Fig. 5.2). The reason for $g_{2,1}(\tau = 0) \neq 0$ is that we observe the behavior of the atom via the cavity mode, which is not necessarily empty after a photon emission.

For two atoms, coupled homogeneously to the same cavity mode, the second-order correlation function indicates bunching for small times ($g_{2,2}(0) > g_{2,2}(\tau)$). This effect is well understood for the case of independent emitters. A comparison of $g_{2,1}(\tau)$, $g_{2,2}^{\mathrm{ind}}(\tau)$ and $g_{2,3}^{\mathrm{ind}}(\tau)$ reveals a transition from anti-bunching to bunching, where the bunching peak develops inside the anti-bunching minimum at $\tau = 0$. In Eq. (5.90) the bunching peak can be assigned to the term proportional to $|G_{1,1}|^2$ which results from the beating

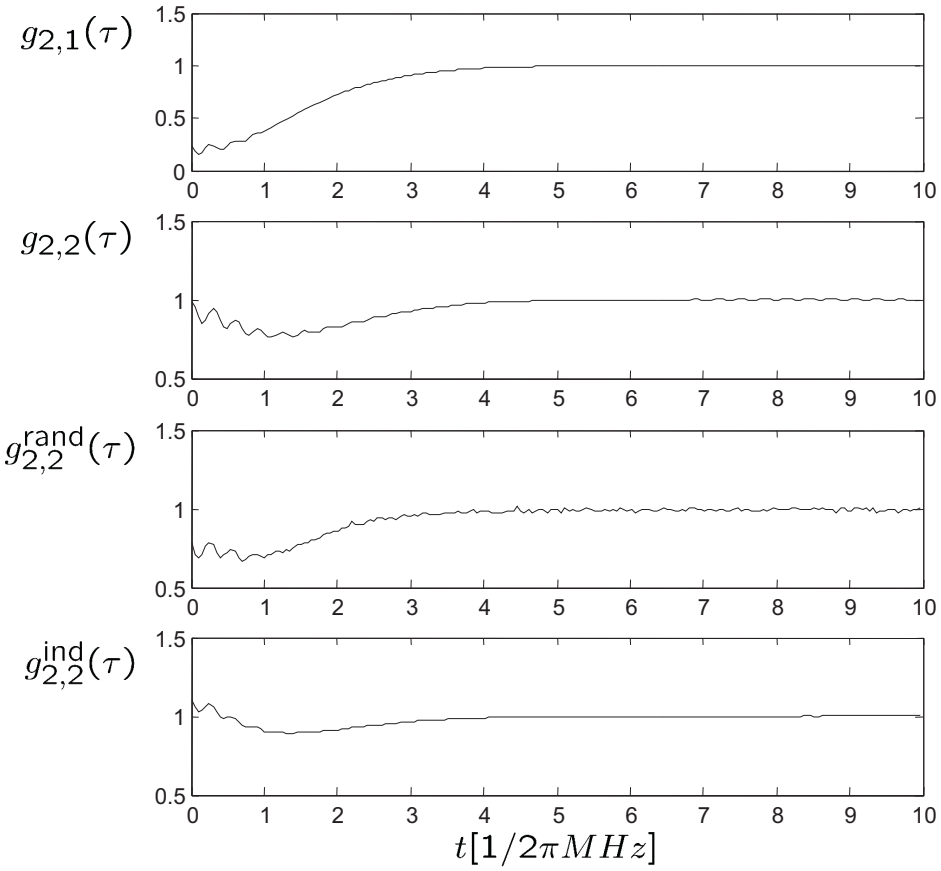

Figure 5.7: Normalized second-order correlation function $g_{2,1}(\tau)$ for a single atom, $g_{2,2}(\tau)$ for two atoms, $g_{2,2}^{\mathrm{rand}}(\tau)$ for two atoms with random coupling and $g_{2,2}^{\mathrm{ind}}(\tau)$ for two independent atoms.

of light emitted by different atoms. The effect is confirmed by $g_{2,3}(\tau)$ for three collectively evolving atoms and was first reported in [62]. Despite this agreement, we observe a considerably different behavior than in the case of independent atoms. This manifests in a less distinctive bunching peak (in particular for N=3) and in more pronounced oscillations near $\tau = 0$. Both must be attributed to the interaction of the atoms via the common cavity mode. For random coupling, the amplitude of the oscillations is comparable to the one for independent atoms but, in particular for $g_{2,2}^{\mathrm{rand}}(\tau)$, the bunching peak is reduced. This single-atom like behavior can be traced back to situations where one atom couples only weakly to the cavity mode. This explains also that the effect is stronger for $N = 2$.

Even though a comparison of $g_{2,2}^{\mathrm{rand}}(\tau)$ with $g_{2,2}^{\mathrm{ind}}(\tau)$ and $g_{2,3}^{\mathrm{rand}}(\tau)$ with $g_{2,3}^{\mathrm{ind}}(\tau)$ clearly evidences collective effects in the system for random coupling,

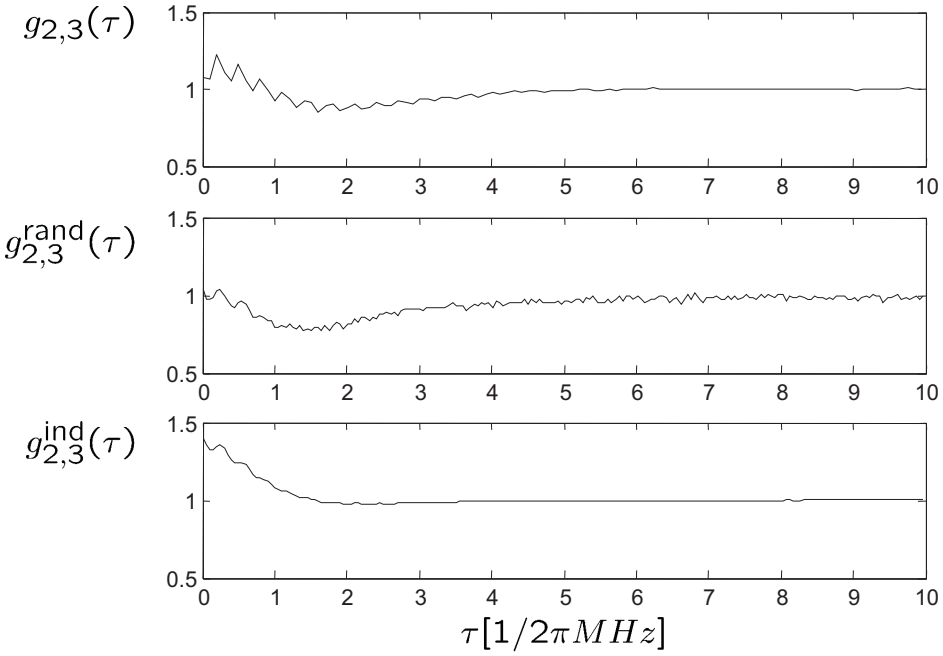

Figure 5.8: Normalized second-order correlation function $g_{2,3}(\tau)$ for three atoms, $g^{\mathrm{rand}}_{2,3}(\tau)$ for three atoms with random coupling and $g^{\mathrm{ind}}_{2,3}(\tau)$ for three independent atoms.

we could not assign them to the collective decay considered above, i.e. superradiance or subradiance. Since the continuous recycling of the system via the excited state involves a spontaneous emission into the free radiation field it is likely that these effects are indeed suppressed. We found qualitative agreement with the experimental results from [62]. In order to reproduce them exactly one needs to take into account that the atoms are dropped through the cavity and the resulting fluctuations in the number of atoms.

No recycling

We will now focus on the collective decay via the cavity mode and omit the recycling laser ($\Omega_b = 0$). In Fig. 5.9 we plotted the emission rate for homogeneous coupling $I_2(t)$, random coupling $I_2^{\mathrm{rand}}(t)$ and for two independent atoms $I_2^{\mathrm{ind}}(t)$. The enhanced decay rate for small times in the case of collectively decaying atoms with respect to the case of independent atoms evidences superradiance. For random coupling the peak is shifted towards smaller times and it is even more pronounced. We conclude that even for randomly changing atom-cavity coupling collective decay is observed in the output-field.

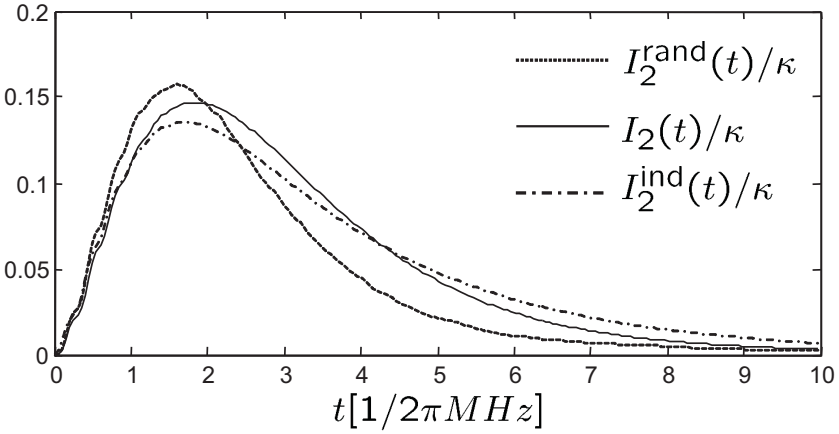

Figure 5.9: $I_2(t)$ is the emission rate for two atoms and homogeneous coupling. We plotted also the emission rate $I_2^{\mathrm{ind}}(t)$ for independent atoms and $I_2^{\mathrm{rand}}(t)$ for randomly changing coupling strengths.

In order to identify subradiance we choose $r_1 = 2r_2 = 1$ and determine the population $P_{a,2}(t)$ of the atomic levels $|a\rangle_i$. For the parameters from [62] we obtain the dotted line in Fig. 5.10. In this case, subradiance is not evident since the population of the states $|a\rangle_i$ vanishes. This is a consequence of the spontaneous decay of the atoms via the excited levels $|e\rangle_i$ which disturbs the collective decay.

For the derivation of the effective master equation (5.18) in section 5.1 we neglected terms proportional to $\gamma g^2/\Delta^2$, $\gamma\Omega_a^2/\Delta^2$ and $\gamma g\Omega_a/\Delta^2$ They account for the spontaneous decay and compete with the collective decay rate of $N\widetilde{g}^2/\kappa = N\Omega_a^2 g^2/(\kappa\Delta^2)$. In order to observe collective effects one has to operate the system in the regime

$$\begin{aligned} \Omega_a^2 &\gg \kappa\gamma, \\ Ng^2 &\gg \kappa\gamma. \end{aligned} \tag{5.93}$$

This can be accomplished – without violating the conditions (5.11), (5.24) and (5.41) – by assuming smaller values for γ_a and γ_b. The solid line in Fig. 5.10 shows $P_{a,2}(t)$ for $\widetilde{\gamma}_a = \gamma_a/10$ and $\widetilde{\gamma}_b = \gamma_b/10$. Albeit we did not change the other parameters from [62], i.e. they still violate the conditions (5.11), (5.24) and (5.41), the result could be considerably improved. For small times the system decays mainly collectively and with a certain probability it evolves into the singlet-type state $|s_r\rangle = (2|b,a\rangle - |a,b\rangle)/\sqrt{5}$.

In Fig. 5.10 we plot also the population $P_{a,2}^{\mathrm{rand}}(t)$ of the atomic levels $|a\rangle_i$ for random atom-cavity coupling. We observe a similar behavior as for $P_{a,2}(t)$, i.e. with a non-vanishing probability the levels $|a\rangle_i$ remain populated.

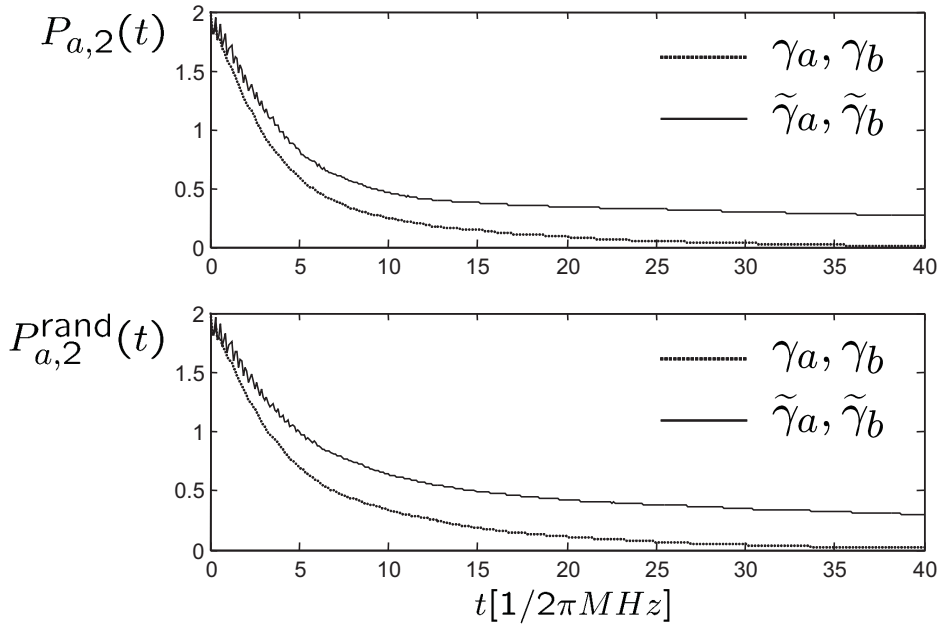

Figure 5.10: Population of atomic levels $|a\rangle_i$ for $N = 2$: For $P_{a,2}(t)$ we chose $r_1 = 2r_2 = 1$. For random coupling we obtain $P_{a,2}^{\mathrm{rand}}(t)$. The dotted lines correspond to the original values for γ_a and γ_b from [62]. For the solid lines we assumed $\widetilde{\gamma}_a = \gamma_a/10$ and $\widetilde{\gamma}_b = \gamma_b/10$.

Unfortunately we do not know the atomic state in this case. Contributions with $r_1 \gg r_2$ and $r_1 \ll r_2$, where one atom is basically decoupled, lead to the product states $|b, a\rangle$ and $|a, b\rangle$. In order to prepare a certain entangled state, it is therefore essential to control the position of the atoms. In contrast to other proposals [68–70], we do not require individual addressing of the atoms.

In Fig. 5.11 we consider $N = 3$ and show plots of the population $P_{a,3}(t)$ in levels $|a\rangle_i$ for $r_1 = r_2 = 2r_3 = 1$ and $P_{a,3}^{\mathrm{rand}}(t)$ for random coupling. As above, the dotted lines correspond to the original values for γ_a and γ_b from [62], while the solid lines indicate $\widetilde{\gamma}_a = \gamma_a/10$ and $\widetilde{\gamma}_b = \gamma_b/10$. The results resemble basically the case of two atoms.

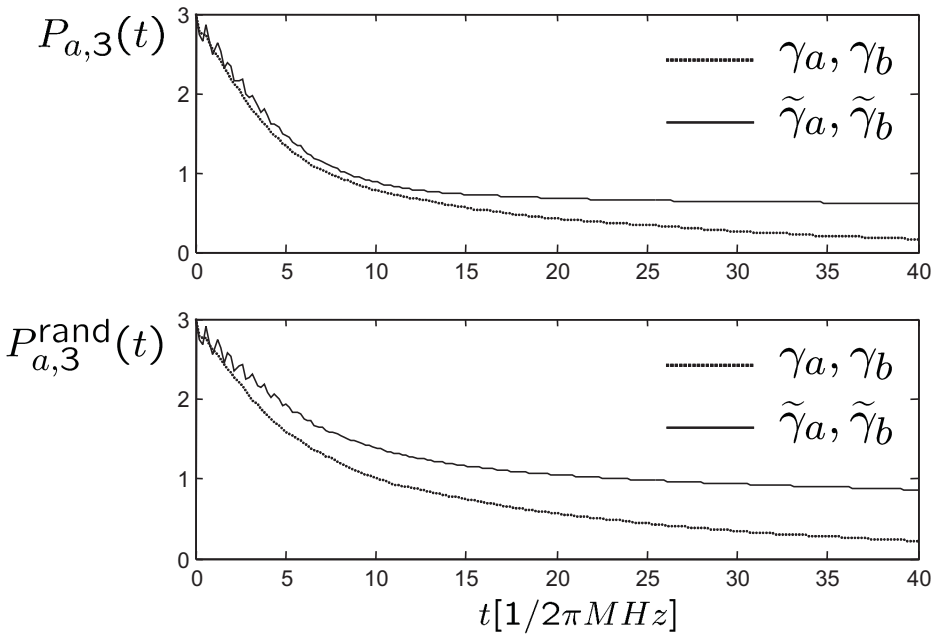

Figure 5.11: Population of atomic levels $|a\rangle_i$ for $N = 3$: For $P_{a,3}(t)$ we chose $r_1 = r_2 = 2r_3 = 1$. For random coupling we obtain $P_{a,3}^{\mathrm{rand}}(t)$. The dotted lines correspond to the original values for γ_a and γ_b from [62]. For the solid lines we assumed $\widetilde{\gamma}_a = \gamma_a/10$ and $\widetilde{\gamma}_b = \gamma_b/10$.

Chapter 6

Conclusions

Trapping atoms in the vacuum field of a cavity

In chapter 3 we showed that it is possible to trap an atom in the vacuum field of a high-Q cavity. To do this we need a weak laser which couples directly to the atom in the cavity. It induces a position dependent ac-Stark shift to the ground state of the cavity-atom system. We use this energy shift as a trapping potential and as we showed by an analytic estimation and a numerical simulation it is deep enough to trap an atom with a realistic initial momentum.

The advantage of this approach is the low effective decay rate due to the little amount of excitation in the system. This requires to cool the atom to a lower kinetic energy than the potential depth. In order to obtain a long life time it would be good to have an initial kinetic energy of the order of one photon recoil. This is still difficult to achieve, even though it is possible to cool an atom below one photon recoil with the method of velocity-selective coherent population trapping [114] or Raman-cooling [115]. Another possibility would be a cavity assisted cooling method [34–36].

The trapping time we can achieve in the optical regime with our approach is of the same order or even lower as observed already in experiments [38–41]. The benefit of this method is that the time after which the first jump occurs is longer because there is only very little excitation in the system. As mentioned before this decay time is very important for any kind of quantum information application since the jump destroys the coherence in the atomic state. In the microwave regime the trapping times can be much longer. Note that in the case studied in many references [34, 35, 40, 41] the trapping force may be velocity dependent since they are also interested in laser cooling, whereas for us this is not the case. In this sense it will be difficult to exactly compare the results of both approaches.

Sequential generation of entangled multi-qubit states

In chapter 4 we characterized all multi-qubit states achievable within a general sequential generation scheme, where an ancillary system is coupled in turn to a number of initially uncorrelated qubits, in terms of matrix-product states [53, 54]. Furthermore we provided a recipe for the generation on demand of any multi-qubit state within a sequential generation scheme.

In particular we considered a scenario where the role of the ancillary system is assigned to a single-photon source [28–30] and the generated qubits are time-bin qubits defined by the absence and presence of a photon. The formalism presented here is also valid for other types of single-photon sources, in the context of cavity QED or quantum dots. For example, it could be extended to characterize the polarization-entangled multi-qubit photon states generated by an analogous cavity QED photon source [48]. In fact, the presented ideas and proofs apply to any multi-qudit state with $\mathcal{H}_{\mathcal{B}} \simeq \mathbb{C}^d$ that is generated sequentially by a D-dimensional source.

In a wider scope, we have established a formalism describing a general sequential quantum factory, where the source is able to perform arbitrary unitary source-qudit operations before each qudit leaves. Apart from the multiphoton states, the present formalism applies also to many other physical scenarios: (a) to coherent microwave cavity QED experiments [116], where atoms sequentially cross a cavity, and thus the outcoming atoms end up in a MPS with the dimensions given by the effective number of states used in the cavity mode; (b) a light pulse crossing several atomic ensembles [117], which will be left in a matrix product Gaussian state [118]; (c) trapped ion experiments where each ion interacts sequentially with a collective mode of the motion [99, 100, 119].

Furthermore we showed that current experimental set-ups [28–30] are suitable for the generation of W, GHZ and cluster states. Here, the employed adiabatic passage leads to considerable losses due to spontaneous atomic emissions. We calculated the fidelity of the cluster state with parameters from [28, 29]. We included the dissipation in the present formalism, by replacing MPS by matrix-product density operators [54, 97]. This description applies also, for example, to the micromaser set-up [120] and other realistic scenarios.

Collective effects in cavity QED

In chapter 5 we investigated collective effects in a cavity QED set-up with an ensemble of atoms coupled to the same cavity mode. We considered a Λ-type level scheme for the atoms and employed a Raman transition to couple them to the cavity mode to avoid spontaneous atomic emissions. For

homogeneous atom-cavity coupling and in the bad-cavity limit the system then obeys the superradiance master equation. Compared to a collectively decaying ensemble of atoms in free space the cavity configuration has the advantage that dipole-dipole interaction and atomic collisions, who attenuate the collective dynamics, can be neglected.

We showed that for inhomogeneous atom-cavity coupling the system evolves into subradiant states with a certain probability. Within a conditional scheme such a scenario can be employed to prepare the atoms in certain entangled states. Recent cavity QED experiments [28–30, 62] are in principle suitable for the implementation of these ideas. In particular we investigated the situation in [62], where the atoms are dropped through the cavity and the position of the atoms is not controlled. It turned out that even for randomly changing atomic positions, traces of collective effects can be observed in the output-field of the cavity mode.

On the other hand it would be desirable to employ a set-up where the position of the atoms is well-controlled. Then, the success rate of any conditional preparation scheme based on the presented ideas will be considerably improved. Excellent control over the position of the atoms is provided by an ion trap [30] placed inside a cavity. At present passive cavity losses reduce the photon efficiency of this set-up substantially but scaling down the whole apparatus promises an improvement. New techniques, like additional far-off resonant dipole traps [42–44] and cavity-induced cooling [34–36] raise hope that the control over the coupling-strength will improve considerably in the future.

Appendix A

MPS representation of an arbitrary state

In section 4.2 we gave a recipe for the sequential generation of any MPS. Here we show that any n-qudit state

$$|\psi\rangle = \sum_{i_1,\ldots,i_n=0}^{d} c_{i_n,\ldots,i_1}|i_n,\ldots,i_1\rangle \tag{A.1}$$

has an MPS representation. Similar to the proof in section 4.2.1 we subsequently construct the involved matrices by singular value decompositions (SVD). Therefore we write the state $|\psi\rangle$ as a $d \times d^{n-1}$ matrix

$$C_{[n]} = \sum_{i_n,\ldots,i_1=1}^{d} c_{i_n,(i_{n-1},\ldots,i_1)}|i_n\rangle\langle i_{n-1},\ldots,i_1|. \tag{A.2}$$

This matrix can be decomposed into

$$\begin{aligned} C_{[n]} &= \sum_{i_n,k_n=1}^{d} U_{k_n}^{i_n}|i_n\rangle\langle k_n| \sum_{k_n,i_{n-1},\ldots,i_1=1}^{d} M_{i_{n-1},\ldots,i_1}^{k_n}|k_n\rangle\langle i_{n-1},\ldots,i_1| \\ &= U_{[n]}M_{[n]}\ , \end{aligned} \tag{A.3}$$

where the $d \times d$ matrix $U_{[n]}$ is the left unitary in the SVD and $M_{[n]}$ is the remaining part with dimension $d \times d^{n-1}$. In the second step we write $M_{[n]}$ as a $d^2 \times d^{n-2}$ matrix

$$C_{[n-1]} = \sum_{k_n,i_{n-1},\ldots,i_1=1}^{d} M_{i_{n-1},(i_{n-2},\ldots,i_1)}|k_n,i_{n-1}\rangle\langle i_{n-2},\ldots,i_1| \tag{A.4}$$

and perform another SVD. For step m we obtain

$$\begin{aligned} C_{[n-m]} &= \sum_{k_{n-m+1}=1}^{d^m} \sum_{i_{n-m},\ldots,i_1=1}^{d} M^{k_{n-m+1}}_{i_{n-m},(i_{n-m-1},\ldots,i_1)} |k_{n-m+1}, i_{n-m}\rangle\langle i_{n-m-1},\ldots,i_1| \\ &= U_{[n-m]} M_{[n-m]} \ , \end{aligned} \tag{A.5}$$

where the $d^{m+1} \times d^{m+1}$ unitary matrix $U_{[n-m]}$ and the $d^{m+1} \times d^{n-(m+1)}$ rest matrix $M_{[n-m]}$ are defined as

$$U_{[n-m]} = \sum_{k_{n-m+1}=1}^{d^m} \sum_{i_{n-m}=1}^{d} \sum_{k_{n-m}}^{d^{m+1}} U^{i_{n-m}}_{k_{n-m+1},k_{n-m}} |k_{n-m+1}, i_{n-m}\rangle\langle k_{n-m}| \tag{A.6}$$

and

$$M_{[n-m]} = \sum_{k_{n-m}}^{d^{m+1}} \sum_{i_{n-m-1},\ldots,i_1=1}^{d} M^{k_{n-m}}_{i_{n-m-1},\ldots,i_1} |k_{n-m}\rangle\langle i_{n-m-1},\ldots,i_1|. \tag{A.7}$$

In the last step we write the $d^{n-1} \times d$ matrix $M_{[2]}$ as a d^n dimensional vector

$$C_{[1]} = \sum_{k_2=1}^{d^{n-1}} \sum_{i_1=1}^{d} M^{k_2}_{i_1} |k_2, i_1\rangle \ . \tag{A.8}$$

Since in every step the number of singular values is equal to the rank of $C_{[n-m]}$ the superfluous dimensions disappear naturally. This is crucial for the application of the method since the dimension of the matrices correspond to the dimension of the source for the sequential generation.

The original n qudit state can finally be written as

$$\begin{aligned} |\psi\rangle &= U_{[n]} U_{[n-1]} \ldots U_{[2]} C_{[1]} \\ &= \sum_{i_n,\ldots,i_1} \left(U^{i_n}_{[n]} U^{i_{n-1}}_{[n-1]} \ldots U^{i_2}_{[2]} C^{i_1}_{[1]} \right) |i_n,\ldots,i_1\rangle. \end{aligned} \tag{A.9}$$

In the second line we introduced $d^m \times d^{m+1}$ matrices

$$U^{i_{n-m}}_{[n-m]} = \sum_{k_{n-m+1}=1}^{d^m} \sum_{k_{n-m}=1}^{d^{m+1}} U^{i_{n-m}}_{k_{n-m+1},k_{n-m}} |k_{n-m+1}\rangle\langle k_{n-m}|. \tag{A.10}$$

The $1 \times d$ matrix $U^{i_n}_{[n]}$ and the $d^{n-1} \times 1$ matrix $C^{i_1}_{[1]}$ are defined as

$$\begin{aligned} U^{i_n}_{[n]} &= \sum_{k_n=1}^{d} U^{i_n}_{k_n} \langle k_n| \ , \\ C^{i_1}_{[1]} &= \sum_{k_2=1}^{d^{n-1}} M^{k_2}_{i_1} |k_2\rangle \end{aligned} \tag{A.11}$$

and can be interpreted as the initial and final state of the source. Since after the application of $U_{[n-1]}$ at most d levels of the source are populated, one can always map its state onto the physical system. This is performed by $U_{[n]}$ and therefore the source decouples from the state $|\psi\rangle$.

Appendix B

Adiabatic following condition

If the Hamiltonian $H(t)$ of a system is time-dependent, this leads in general to time-dependent eigenstates $|\psi_i(t)\rangle$ and time-dependent eigenvalues $\lambda_i(t)$. The state of the system is then given by

$$|\Psi(t)\rangle = \sum_i c_i(t) \exp\Big(- i \int_0^t \lambda_i(\tau) d\tau \Big) |\psi_i(t)\rangle. \tag{B.1}$$

If the amplitudes c_i are constant, one speaks of adiabatic following or an adiabatic passage. In this case, a system initially (at time t_0) prepared in a certain eigenstate $|\psi_0(t_0)\rangle$ (e.g. a dark state) will always remain in $|\psi_0(t)\rangle$. We will now estimate the error probability and find under which condition the assumption of constant c_i's is valid. An extensive analysis can be found in [121].

Non-adiabatic contributions to the time-evolution result in a non-vanishing probability to find the system in an eigenstate $|\psi_k(t_1)\rangle$ with $k \neq 0$ at a time $t_1 > t_0$. It is given by

$$P_k(t_1) = |c_k(t_1)|^2. \tag{B.2}$$

In order to determine $c_k(t)$ we use the Schrödinger equation

$$\langle \tilde{\psi}_k(t)| \frac{d}{dt} |\Psi(t)\rangle = -i \langle \tilde{\psi}_k(t)| H(t) |\Psi(t)\rangle \tag{B.3}$$

with

$$|\tilde{\psi}_k(t)\rangle = \exp\Big(- i \int_0^t \lambda_k(\tau) d\tau \Big) |\psi_k(t)\rangle. \tag{B.4}$$

Substituting (B.1) into Eq. (B.3) leads to

$$\frac{dc_k(t)}{dt} = - \sum_i c_i(t) \exp\Big(- i \int_{t_0}^t [\lambda_i(\tau) - \lambda_k(\tau)] d\tau \Big) \langle \psi_k(t)| \frac{d}{dt} |\psi_i(t)\rangle. \tag{B.5}$$

Assuming that the non-adiabatic corrections are small, we use $c_0(t) \approx 1$ and $c_i(t) \approx 0$ for $i \neq 0$ and end up with

$$c_k(t_1) = -\int_{t_0}^{t_1} dt \exp\Big(-i\int_{t_0}^{t}[\lambda_0(\tau)-\lambda_k(\tau)]d\tau\Big)\langle\psi_k(t)|\frac{d}{dt}|\psi_0(t)\rangle. \quad \text{(B.6)}$$

In a sufficiently small time-interval (t_0, t_1) the expressions $\lambda_0(\tau) - \lambda_k(\tau)$ and $\langle\psi_k(t)|\frac{d}{dt}|\psi_0\rangle$ are approximately constant and we obtain

$$|c_k(t_1)|^2 = 2\left|\frac{\langle\psi_k|\frac{d}{dt}|\psi_0\rangle}{\lambda_k-\lambda_0}\right|^2\big(1-\cos[(\lambda_k-\lambda_0)(t_1-t_0)]\big). \quad \text{(B.7)}$$

The probability to find the system in $|\psi_k(t)\rangle$ is therefore bound by

$$P_k(t_1) = |c_k(t_1)|^2 \leq 4\left|\frac{\langle\psi_k|\frac{d}{dt}|\psi_0\rangle}{\lambda_k-\lambda_0}\right|^2. \quad \text{(B.8)}$$

If during the whole time evolution the adiabatic following condition

$$|\lambda_k - \lambda_0| \gg |\langle\psi_k|\frac{d}{dt}|\psi_0\rangle| \quad \text{(B.9)}$$

for $k \neq 0$ is fulfilled, non-adiabatic corrections can be neglected.

Appendix C

Solution of the master equation

For low-dimensional Hilbert spaces, it is more efficient to solve the master equation directly instead of using the quantum-jump approach. An elegant way to solve the master equation for the d dimensional density operator $\rho(t)$ is to rewrite it as a vector differential equation for the d^2 dimensional vector $\vec{\rho}(t)$ and diagonalize its formal solution. A master equation

$$\frac{d\rho(t)}{dt} = \sum_{i=1}^{d} A_i \rho(t) B_i \tag{C.1}$$

can always be written in the form

$$\frac{d\vec{\rho}(t)}{dt} = \underbrace{\sum_{i=1}^{d} A_i \otimes B_i^T}_{M} \ \vec{\rho}(t), \tag{C.2}$$

where M is the d^2 dimensional evolution matrix. If M is time-independent, the formal solution of Eq. (C.2) is given by

$$\vec{\rho}(t) = e^{Mt}\vec{\rho}(0). \tag{C.3}$$

If M has non-degenerate eigenvalues its eigen decomposition is given by

$$M = PDP^{-1}, \tag{C.4}$$

where the matrix P is composed of the eigenvectors and D is the diagonal matrix with the eigenvalues on its diagonal. Since the relation

$$M^n = PD^nP^{-1} \tag{C.5}$$

holds for any positive integer n we obtain

$$e^{Mt} = Pe^{Dt}P^{-1}. \tag{C.6}$$

With this result it is also straightforward to employ the quantum-regression theorem (2.83) and calculate two-time expectation values. For two arbitrary system operators we obtain

$$\begin{aligned} \langle O_1(t)O_2(t+\tau)\rangle &= \mathrm{tr}_S\Big(O_2(0)e^{\mathcal{L}\tau}[\rho(t)O_1(0)]\Big) \\ &= \mathrm{tr}_S\Big(O_2(0)\otimes \mathbb{1}_d\, e^{M\tau}[\vec{\rho}(t)O_1(0)\otimes \mathbb{1}_d]\Big). \end{aligned} \tag{C.7}$$

Bibliography

[1] P. Benioff, J. Stat. Phys. **22**, 563 (1980).

[2] R. Feynman, J. Theoret. Phys. **21**, 467 (1982).

[3] D. Deutsch, Proc. Roy. Soc. A **400**, 96 (1985).

[4] R. Feynman, Found. Phys. **16**, 507 (1986).

[5] M. Nielsen and I. Chuang, *Quantum computation and quantum information*, Cambridge Univ. Press (2000).

[6] A. Ekert and R. Josza, Rev. Mod. Phys. **68**, 733 (1996).

[7] P. W. Shor, quant-ph/9706033.

[8] P. W. Shor, SIAM J. Comp. **26**, 1484 (1997).

[9] L. Grover, Phys. Rev. Lett. **79**, 325 (1997).

[10] N. Gisin, G. Ribordy, W. Tittel, and H. Zbinden, Rev. Mod. Phys. **74**, 145 (2002).

[11] http://www.idquantique.com; http://www.magitech.com

[12] C. H. Bennett and G. Brassard, *Proc. IEEE International Conference on Computers, Systems and Signal Processing* 175, IEEE Press (1984).

[13] H. J. Briegel, W. Dür, J. I. Cirac, and P. Zoller, Phys. Rev. Lett. **81**, 5932 (1998).

[14] W. Dür, H. J. Briegel, J. I. Cirac, and P. Zoller, Phys. Rev. A **59**, 169 (1999).

[15] J. I. Cirac, P. Zoller, H. J. Kimble, H. Mabuchi, Phys. Rev. Lett. **78**, 3221 (1997).

[16] S. van Enk, J. I. Cirac , and P. Zoller, Science **279**, 205 (1998).

[17] T. Pellizzari, Phys. Rev. Lett. **79**, 5242 (1997).

[18] S. J. van Enk, J. I. Cirac, and P. Zoller, Phys. Rev. Lett. **79**, 5178 (1997).

[19] T. Pellizzari, J. I. Cirac, S. A. Gardiner and P. Zoller, Phys. Rev. Lett. **75**, 3788 (1995).

[20] C. W. Gardiner, J. Ye, H. C. Nagerl, and H. J. Kimble, Phys. Rev. A **61**, 045801 (2000).

[21] S. J. van Enk, J. McKeever, H. J. Kimble, and J. Ye, Phys. Rev. A **64**, 013407 (2001).

[22] P. Münstermann, T. Fischer, P. Maunz, P. W. H. Pinkse, and G. Rempe, Phys. Rev. Lett. **82**, 3791 (1999).

[23] P. Horak, H. Ritsch, T. Fischer, P. Maunz, T. Puppe, P. W. H. Pinkse, and G. Rempe, Phys. Rev. Lett. **88**, 043601 (2002).

[24] M. S. Feld, and K. An, Scientific American **279** (1), 56 (1998).

[25] G. R. Guthöhrlein, M. Keller, K. Hayasaka, W. Lange, and H. Walther, Nature **414**, 49 (2001).

[26] A. B. Mundt, A. Kreuter, C. Becher, D. Leibfried, J. Eschner, F. Schmidt-Kaler, and R. Blatt, Phys. Rev. Lett. **89**, 103001 (2002).

[27] A. Boca, R. Miller, K. M. Birnbaum, A. D. Boozer, J. McKeever, and H. J. Kimble, Phys. Rev. Lett. **93**, 233603 (2004).

[28] A. Kuhn, M. Hennrich, and G. Rempe, Phys. Rev. Lett. **89**, 067901 (2002).

[29] J. McKeever, A. Boca, A. D. Boozer, R. Miller, J. R. Buck, A. Kuzmich, and H. J. Kimble, Science **303**, 1992 (2004).

[30] M. Keller, B. Lange, K. Hayasaka, W. Lange, and H. Walther, Nature **431**, 1075 (2004).

[31] S. Brattke, B. T. H. Varcoe, and H. Walther, Phys. Rev. Lett. **86**, 3534 (2001).

[32] P. Bertet, S. Osnaghi, P. Milman, A. Auffeves, P. Maioli, M. Brune, J. M. Raimond, and S. Haroche, Phys. Rev. Lett. **88**, 143601 (2002).

[33] S. Haroche, M. Brune, and J. M. Raimond, Europhys. Lett. **14** (1), 19 (1991).

[34] P. Horak, G. Hechenblaikner, K. M. Gheri, H. Stecher, and H. Ritsch, Phys. Rev. Lett. **79**, 4974 (1997).

[35] G. Hechenblaikner, M. Gangl, P. Horak, and H. Ritsch, Phys. Rev. A **58**, 3030 (1998).

[36] P. Maunz, T. Puppe, I. Schuster, N. Syassen, P. W. H. Pinkse, and G. Rempe, Nature **428**, 50 (2004).

[37] A. C. Doherty, T. W. Lynn, C. J. Hood, and H. J. Kimble, Phys. Rev. A **63**, 013401 (2001).

[38] J. Ye, C. J. Hood, T. Lynn, H. Mabuchi, D. W. Vernooy, and H. J. Kimble, IEEE Trans. on Instrum. Meas. **48**, 608 (1999).

[39] C. J. Hood, T. W. Lynn, A. C. Doherty, A. S. Parkins, and H. J. Kimble, Science **287**, 1447 (2000).

[40] P. W. H. Pinkse, T. Fischer, P. Maunz and G. Rempe, Nature **404**, 365 (2000).

[41] P. W. H. Pinkse, T. Fischer, P. Maunz, T. Puppe and G. Rempe, J. Mod. Opt. **47**, 2769 (2000).

[42] J. Ye, D. W. Vernooy, and H. J. Kimble, Phys. Rev. Lett. **83**, 4987 (1999).

[43] J. McKeever, J. R. Buck, A. D. Boozer, A. Kuzmich, H.-C. Naegerl, D. M. Stamper-Kurn, and H. J. Kimble, quant-ph/0211013 (2002).

[44] S. Nußmann, K. Murr, M. Hijlkema, B. Weber, A. Kuhn, and G. Rempe, quant-ph/0506067 (2005).

[45] J. A. Sauer, M. D. Barrett, and M. S. Chapman, Phys. Rev. Lett. **87**, 270401 (2001).

[46] C. K. Law and H. J. Kimble, J. Mod. Opt. **44**, 2067-2074 (1997).

[47] K.M. Gheri, C. Saavedra, P. Törm, J. I.. Cirac and P. Zoller, Phys. Rev. A **58**, R2627 (1998);

[48] C. Saavedra, K. M. Gheri, P. Törmä, J. I. Cirac, and P. Zoller, Phys. Rev. A **61**, 062311 (2000).

[49] L. G. Grover, quant-ph/9704012.

[50] J. I. Cirac, A. K. Ekert, S. F. Huelga, and C. Macchiavello, Phys. Rev. A **59**, 4249 (1999).

[51] A. K. Ekert, Phys. Rev. Lett. **67**, 661 (1991).

[52] R. Cleve, D. Gottesmann, and H.-K. Lo, Phys. Rev. Lett. **83**, 648 (1999).

[53] A. Klümper, A. Schadschneider, and J. Zittartz, J. Phys. A **24**, L955 (1991); Z. Phys. B **87**, 281 (1992); Europhys. Lett. **24**, 293 (1993).

[54] M. Fannes, B. Nachtergaele, and R. F. Werner, Comm. Math. Phys. **144**, 443 (1992).

[55] I. Affleck *et al.*, Commun. Math. Phys. **115**, 477 (1988).

[56] S. Östlund and S. Rommer, Phys. Rev. Lett. **75**, 3537 (1995).

[57] H. J. Briegel and R. Raussendorf, Phys. Rev. Lett. **86**, 910 (2001).

[58] D. M. Greenberger, M. Horne, and A. Zeilinger, in *Bell's Theorem, Quantum Theory, and Conceptions of the Universe*, M. Kafatos, Ed. (Kluwer, Dordrecht 1989) pp. 69-72.

[59] F. Verstraete and J. I. Cirac, Phys. Rev. A 70, 060302 (2004)

[60] T. Yoshie, A. Scherer, J. Hendrickson, G. Khitrova, H. M. Gibbs, G. Rupper, C. Ell, O. B. Shchekin, and D. G. Deppe, Nature **432**, 200 (2004).

[61] J. P. Reithmaier, G. Sek, A. Loffler, C. Hofmann, S. Kuhn, S. Reitzenstein, L. V. Keldysh, V. D. Kulakovskii, T. L. Reinecke, and A. Forchel, Nature **432**, 197 (2004).

[62] M. Hennrich, A. Kuhn, and G. Rempe, Phys. Rev. Lett. **94**, 053604 (2005).

[63] R. Dicke, Phys. Rev. **93**, 99 (1954).

[64] F. Arecchi, E. Courtens, R. Gilmore, and H. Thomas, Phys. Rev. A **6**, 2221 (1972).

[65] G. M. Palma, K. A. Suominen, and A. K. Ekert, Proc. R. Soc. A **452**, 567 (1996).

[66] P. Zanardi and M. Rasetti, Phys. Rev. Lett. **79**, 3306 (1997).

[67] D. A. Lidar, I. L. Chuang, and K. B. Whaley, Phys. Rev. Lett. **81**, 2594 (1998).

[68] P. Földi, M. G. Benedict, and A. Czirjak, Phys. Rev. A **65**, 021802(R) (2002).

[69] M. B. Plenio, S. F. Huelga, A. Beige, and P. L. Knight, Phys. Rev. A **59**, 2468 (1998).

[70] A. Beige, D. Braun, and P. L. Knight, New J. Phys. **2**, 22 (2000).

[71] E. T. Jaynes, and F. W. Cummings, Proc. IEEE **51**, 89 (1963).

[72] S. M. Barnett, and P. M. Radmore, *Methods in Theoretical Quantum Optics*, Clarendon Press, Oxford (1997).

[73] H. Haken, *Handbuch der Physik*, Vol. XXV/2c, ed. by L. Genzel, Springer, Berlin (1970).

[74] W. H. Louisell, *Quantum Statistical Properties of Radiation*, Wiley, New York (1973).

[75] H. Carmichael, *Statistical Methods in Quantum Optics 1*, Springer, (1999).

[76] D. Kleppner, Phys. Rev. Lett. **47**, 233 (1981).

[77] E. M. Pourcel, Phys. Rev. **69**, 681 (1946).

[78] J. Dalibard, Y. Castin, and K. Mølmer, Phys. Rev. Lett. **68**, 580 (1992).

[79] R. Dum, P. Zoller, H. Ritsch, Phys. Rev. A **45**, 4879, (1992).

[80] H. Carmichael, *An Open Systems Approach to Quantum Optics*, Lecture Notes in Physics **18**, Springer (1993).

[81] G. C. Hegerfeldt and T. S. Wilser, in *Classical and Quantum Systems*, Proceedings of the Second International Wigner Symposium, July 1991, edited by H. D. Doebner, W. Scherer, and F. Schroeck (World Scientific, Singapore, 1992), p. 104.

[82] M. Lax, Phys. Rev., **129**, 2342 (1963).

[83] M. Lax, Phys. Rev., **157**, 213 (1967).

[84] H. Haken, *Laser Theory* (Springer, Berlin, 1984).

[85] M. Lax, Phys. Rev., **145**, 110 (1966).

[86] C. W. Gardiner and M. J. Collett, Phys. Rev. A **31**, 3761 (1984).

[87] C. W. Gardiner *Quantum Noise*, (Springer, Berlin, 1991).

[88] A. S. Parkins, P. Zoller, and H. J. Carmichael, Phys. Rev. A **48**, 758 (1993).

[89] A. S. Parkins, and H. J. Kimble, Journal Opt. B: Quantum Semiclass. Opt. 1, 496 (1999).

[90] A. Galindo, and P. Pascual, Quantum Mechanics I, Springer-Verlag Berlin Heidelberg (1990).

[91] L. Davidovich, M. Brune, J. M. Raimond, and S. Haroche, Phys. Rev. A **53**, 1295 (1996).

[92] C. W. Gardiner, and P. Zoller, *Quantum Noise: A Handbook of Markovian and Non-Markovian Quantum Stochastic Methods with Applications to Quantum Optics*, Springer Verlag (1999).

[93] W. Dür, G. Vidal, and J. I. Cirac, Phys. Rev. A 62, 062314 (2000).

[94] F. Verstraete and J. I. Cirac, quant-ph/0311130.

[95] F. Verstraete, D. Porras, J. I. Cirac, cond-mat/0404706.

[96] F. Verstraete, M. A. Martin–Delgado, and J. I. Cirac, Phys. Rev. Lett. **92**, 087201 (2004).

[97] F. Verstraete, J. J. Garcia-Ripoll, and J. I. Cirac, Phys. Rev. Lett. **93**, 207204 (2004); M. Zwolak and G. Vidal, *ibid*, 207208 (2004) .

[98] T. Legero, T. Wilk, M. Hennrich, G. Rempe, and A. Kuhn, Phys. Rev. Lett. **93**, 070503 (2004).

[99] D. Kielpinski, C. Monroe, and D. J. Wineland, Nature (London) **417**, 709 (2002).

[100] S. Gulde, M. Riebe, G. P. T. Lancaster, C. Becher, J. Eschner, H. Häffner, F. Schmidt-Kaler, I. L. Chuang, and R. Blatt, Nature (London) **421**, 48 (2003).

[101] M. França Santos, E. Solano, and R. L. de Matos Filho, Phys. Rev. Lett. **87**, 093601 (2001).

[102] L.-M. Duan, A. Kuzmich, and H. J. Kimble, Phys. Rev. A **67**, 032305 (2003).

[103] M. Fleischhauer, S. F. Yelin, and M. D. Lukin, Opt. Comm. **179**, 395 (2000).

[104] D. F. Walls and G. J. Milburn, *Quantum Optics*, Springer, Berlin (1994).

[105] C. Cohen-Tannoudji, B. Diu, F. Laloe, *Quantum Mechanics*, Wiley (1977).

[106] A. B. Klimov, L. L. Sanchez-Soto, A. Navarro and E. C. Yustas, J. Mod. Opt **49**, 2211 (2002).

[107] A. B. Klimov, J. L. Romero, J. Delgado, L. L. Sanchez-Soto, J. Opt. B: Quantum Semiclass. Opt. **5**, 34 (2003).

[108] S. M. Barnett and P. L. Knight, Phys. Rev. A **33**, 2444 (1986).

[109] J. I. Cirac, Phys. Rev. A **46**, 4354 (1992).

[110] N. Skribanowitz, I. P. Herman, J. C. McGillivray, and M. S. Feld, Phys. Rev. Lett. **30**, 309 (1973).

[111] D. Pavolini, A. Crubellier, P. Pillet, L. Cabaret, and S. Liberman, Phys. Rev. Lett. **54**, 1917 (1985).

[112] A. Imamoglu, E. Knill, L. Tian, and P. Zoller, Phys. Rev. Lett. **91**, 017402-1 (2003).

[113] J. M. Taylor, A. Imamoglu, and M. D. Lukin, cond-mat/0308459.

[114] A. Aspect, E. Arimondo, R. Kaiser, N. Vansteenkiste, and C. Cohen-Tannoudji, Phys. Rev. Lett. **61**, 826 (1988).

[115] M. Kasevich, and S. Chu, Phys. Rev. Lett. **69**, 1741 (1992).

[116] A. Rauschenbeutel, G. Nogues, S. Osnaghi, P. Bertet, M. Brune, J.-M. Raimond, and S. Haroche, Science **288**, 2024 (2000).

[117] B. Julsgaard, C. Schori, J.L. Sørensen, E.S. Polzik., Quant. Inform. and Comp., spec. issue **3**, 518 (2003).

[118] N. Schuch, M. Wolf, F. Verstraete, and J.I. Cirac (in preparation).

[119] J. I. Cirac and P. Zoller, Phys. Rev. Lett. **74**, 4091 (1995).

[120] S. Brattke, B. T. H. Varcoe, and H. Walther, Phys. Rev. Lett. **86**, 3534 (2001).

[121] A. Messiah, sl Quantum Mechanics Vol. 2, Wiley, New York (1978).

Acknowledgements

With great pleasure I take the opportunity to thank the people who supported me during my time in the theory group at the MPQ.

My first thanks go to Prof. Ignacio Cirac for suggesting the projects on which this thesis is based. His guidance and encouragement were essential for this work. Moreover, I want to thank him for the challenging, stimulating and international environment for doing research.

I thank Enrique Solano for many fruitful and joyful discussions. I also want to thank him and Michael Wolf for the rewarding collaboration on important parts of this thesis.

I am very grateful to Barbara Kraus and Klemens Hammerer for many interesting and stimulating discussions.

I want to thank my roommates Markus Popp and Henning Christ for the pleasant and enriching time together.

Many thanks to Markus Hennrich, Axel Kuhn and Prof. Gerhard Rempe, who inspired our work by their fascinating cavity-QED experiments.

Special thanks to Prof. Manfred Kleber for his support during all the time I studied at the TUM.